Phil. Trans. R. Soc. Lond. B **313**, 251–270 (1986) [251]
Printed in Great Britain

EYE STRUCTURE AND OPTICS IN THE PELAGIC SHRIMP *ACETES SIBOGAE* (DECAPODA, NATANTIA, SERGESTIDAE) IN RELATION TO LIGHT–DARK ADAPTATION AND NATURAL HISTORY

By E. E. BALL, L. C. KAO, R. C. STONE and M. F. LAND, F.R.S.†
Department of Neurobiology, Research School of Biological Sciences, Australian National University, P.O. Box 475, *Canberra City, A.C.T.* 2601, *Australia*

(*Received* 7 *March* 1985)

[Plates 1–8]

CONTENTS

† Present address: School of Biological Sciences, University of Sussex, Brighton BN1 9QG, U.K.

 [Published 24 September 1986

The structure and optics of the compound eyes of the neritic sergestid shrimp, *Acetes sibogae*, are described. The eyes are nearly spherical and heavily pigmented. The facets are square, indicating that the eye operates by the recently recognized mechanism of reflecting superposition.

The most distal portion of each ommatidium is the corneal lens, which is secreted by two underlying corneagenous cells. These two cells surround the crystalline cone and cone stalk and the four cells of which they are composed and extend proximally at least as far as the distal rhabdom. Near the base of the cone stalk the extensions of the corneagenous cells swell and enclose spheres which bear on their surfaces small particles similar to ribosomes in appearance.

Beneath the corneagenous cells lie four crystalline cone cells, parts of which differentiate to form the crystalline cone and cone stalk. The latter structures are compound, one quarter of each being contributed by each crystalline cone cell. Distally the crystalline cone cells send a small projection, which is surrounded by the corneagenous cells, to the cornea. Proximal extensions of each of the four parts of the cone stalk extend between the retinula cells and meet within the basement membrane.

Between the base of the cone stalk and the regularly layered rhabdom lies the distal rhabdom. It is surrounded by a cell that we have termed retinula cell eight (R8), by analogy with other crustacean systems, and consists of unordered microvilli projecting from the cell membrane into the extracellular space above the layered rhabdom.

In addition to R8, which contributes only to the distal rhabdom, seven other retinula cells contribute to the proximal rhabdom, which consists of alternating ordered layers of orthogonally arranged microvilli. Four of these retinula cells are arranged orthogonally and extend far distally along the crystalline tract. The other three do not extend as far distally and alternate with the first four in their position around the axis of the ommatidium. R8 is located still further proximally at the level of the distal rhabdom. All seven of the retinula cells which contribute to the proximal rhabdom contain proximal pigment and extend through the basement membrane.

The basement membrane consists of a meshwork grid with each intersection supporting a rhabdom so at this point the retinula cell axons project into different squares of the meshwork. Tapetal pigment cells are present in the vicinity of the basement membrane and extend downward to the lamina. The granules of tapetal pigment are covered or exposed by movements of the proximal pigment and also change their intracellular distribution depending on illumination.

In addition to the proximal (retinula cell) pigment and the tapetal pigment the eye contains four types of distal pigment. Moving inward from the cornea these are the distal yellow pigment (DYP) which surrounds the entire eye; the distal reflecting pigment (DRP), which forms a thin layer and is continuous with the tapetal pigment at the edge of the eye; and the black distal pigment and the mirror pigment (MP) both contained within distal pigment cells (DPC).

In the light-adapted state the proximal pigment moves distally, surrounding the rhabdoms, and the tapetal pigment granules move proximally so that they are mainly found beneath the basement membrane. Movements of the distal pigments are less clearcut, but they all appear to move somewhat proximally in the light-adapted state. Multivesicular bodies are more abundant in the retinula cells shortly after dawn, and are possibly related to membrane turnover.

Interommatidial angle, as measured on both fixed and fresh material, varied from 2.8 to 3.8° in different parts of the eye. The crystalline cones were found to have a uniform refractive index radially, which, combined with their square shape, indicates that they function by reflecting superposition. Total internal reflection from the sides of the cones is adequate to explain the maximum diameter of the eyeshine from the dark-adapted eye at night without the need for additional mirrors. Nevertheless, from its organization and appearance the mirror pigment could act as a reflector in the

dark-adapted eye. Also, the size of the glow patch indicates that there would be a gain of nearly two log units in image brightness in going from the light-adapted to the dark-adapted state. Each corneal facet was found to act as a weak converging lens, with a focal length of approximately 300 μm.

The eye structure of *Acetes* is discussed in relation to that of other shrimp and to the natural history of *Acetes*.

1. Introduction

Different species of pelagic shrimp belonging to the family Sergestidae occupy differing depths and migrate vertically to varying extents (Omori 1975). Because of this the light levels they experience, their food and their predators all differ. Their sensory systems, especially the eyes and antennae, also show anatomical, and presumably functional, differences, probably as a result of differing selective pressures (Chun 1896; Foxton 1969; Welsh & Chace 1938). We are interested in understanding these sensory specializations in the light of the natural history of the species possessing them. However, since representatives of many of the most interesting species are rarely captured in good condition and are difficult to keep alive in an environment anything like their own, we decided to study first the small neritic sergestid, *Acetes sibogae australis* Colefax (originally named *Acetes australis* Colefax, 1940 but then made a subspecies of *Acetes sibogae* Hansen, 1919 by Omori (1975)). All further references to *Acetes* in this paper refer to this species unless otherwise noted. It occurs in shallow water saline lakes and inshore areas and its wide environmental tolerances allow it to survive for long periods in the laboratory. We could thus hope to characterize the environmental stimuli to which it responds and since it has the same basic sensory systems as its deep water relatives their sensory systems could later be examined as variations on a theme. We have therefore begun an anatomical survey of the sensory systems of *Acetes* (antennal sensilla: Ball & Cowan (1977) and papers in preparation on the antennular sensilla and the statocyst) as well as laboratory and field studies on *Acetes* behaviour.

The present paper discusses the structure and function of the eyes and the changes that occur related to time of day and ambient light conditions. In recent years there has been a renewed interest in the structure and function of the eyes of pelagic Crustacea, owing to the advent of techniques such as electron microscopy, to advances in understanding of the relation between the structure and function of compound eyes and to a better understanding of the natural history of the pelagic community (see, for example, Ball 1977; Denys *et al.* 1982, 1983; Elofssen & Hallberg 1977; Hallberg 1977; Hallberg *et al.* 1980; Land 1976, 1980; Land *et al.* 1979; Meyer-Rochow 1978; Meyer-Rochow & Walsh 1977, 1978; Nilsson 1982). However, to date the only papers with more than a brief mention of sergestid eye structure are those of Chun (1896), Hanstrom (1933, 1934) and Welsh & Chace (1938). Although these authors made many interesting observations none of them present a detailed study of the structure of the eye. Such a study is particularly timely because of the recent recognition by Vogt (1975) and Land (1976) that most crustacean eyes with square facets, including those of shrimp, operate by the previously unrecognized principle of reflecting superposition. We therefore examined the eye of *Acetes* with the additional goal of understanding the structural basis of this newly recognized mechanism. As we were completing this study a paper appeared by Doughtie & Rao (1984) on the ultrastructure of the eyes of the grass shrimp, *Palaemonetes pugio*, thus providing many interesting comparisons to the results presented here.

2. Materials and methods

Specimens of *Acetes sibogae* were collected by dip-netting and light-trapping in Sydney Harbour and the Tuggerah Lakes of New South Wales, Australia, at various times from 1975 to 1984. As there are no gross sexual differences in eye morphology eyes from both sexes were used. Best fixation was obtained by using a mixture of 2.5% glutaraldehyde (by volume), 20.0 g l^{-1} paraformaldehyde and 10.0 g l^{-1} glucose in Millonig's phosphate buffer, pH 7.4 (Ribi 1976). Eyes were cut off into this fixative and, after being allowed to harden somewhat, some were split in half to promote fixative penetration. The tissue remained in fixative overnight at 5 °C. It was then rinsed repeatedly in buffer, the osmolarity of which had been adjusted with glucose to that of the primary fixative. Secondary fixation was in 20.0 g l^{-1} OsO_4 for 1–2 h with osmolarity adjusted with glucose to that of the primary fixative. The tissue was then dehydrated through an ethanol series, passed through two changes of propylene oxide, rotated overnight in a propylene oxide–Araldite mixture, put through two changes of Araldite and embedded.

For light microscopy, material was sectioned at 0.5 or 1.0 μm and stained with toluidine blue. For transmission electron microscopy thin sections were cut on glass or diamond knives, stained with uranyl acetate and lead citrate and examined and photographed on a Jeol 100 C or a Hitachi H500 electron microscope.

In initial experiments light-adapted eyes were fixed under artificial light in the late afternoon and early evening. Dark-adapted eyes were fixed at night under red light. A more detailed study was then made as follows. On a day with sunrise at 06h40 and sunset at 17h34 animals were fixed under natural light conditions at 06h10, 08h10, 12h25, 17h10, 19h10, and 24h00. Several animals were also placed in boiling water at each of these times to check for pigment movements during fixation. Boiling stops these movements, where conventional fixation often fails.

The eyeshine of dark-adapted *Acetes* fades very rapidly (see Results), and boiling, which has been used by previous authors to stop the retinal pigments in place, results in shrivelling of the eye with consequent loss of the eyeshine. However, we found that by thrusting the shrimp into liquid nitrogen and then returning them to sea water we were able to stop pigment movements and retain the eyeshine. By using this discovery we studied the process of light adaptation at night. *Acetes* were fully dark-adapted and were then exposed to tungsten light of 100–200 lx for the following intervals before being placed in liquid nitrogen: 0, 0.5, 1, 2, 6, 15 and 60 min. After 1–2 min in liquid nitrogen each shrimp was moved to seawater at room temperature. One eye was then used for photography of the eyeshine and frozen sections were taken of the other to study pigment position in relation to eyeshine.

For methods used in studying the optics of the *Acetes* eye see the 'Optics' section.

Description of plate 2

Plate 2. Summary of ommatidial structure in a moderately light adapted eye.

Figure 4. Light micrograph of an eye sectioned along the axis of the eyestalk. Scale bar 10 μm.

Figure 5. Schematic drawing summarizing the organization of a single ommatidium. Boundaries are not shown for the various distal pigment cells due to uncertainty concerning their exact shape (see text). BM, basement membrane; CC, crystalline cone; CCC, crystalline cone cell; Co, cornea; CoC, corneagenous cell; CS, cone stalk; DPC, distal pigment cell; DRh, distal rhabdom; DRP, distal reflecting pigment; DYP, distal yellow pigment; N, nucleus; PP, proximal pigment; R, retinula cell; R8, retinula cell 8; RCA, retinula cell axon; Rh, rhabdom; TP, tapetal pigment; V, vesicle, presumably filled with fluid in the living animal.

1

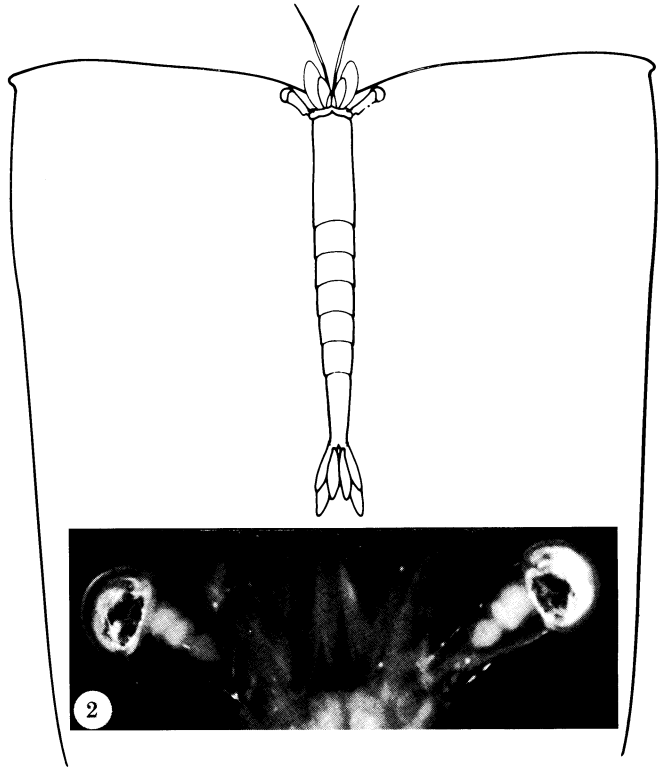

2

3

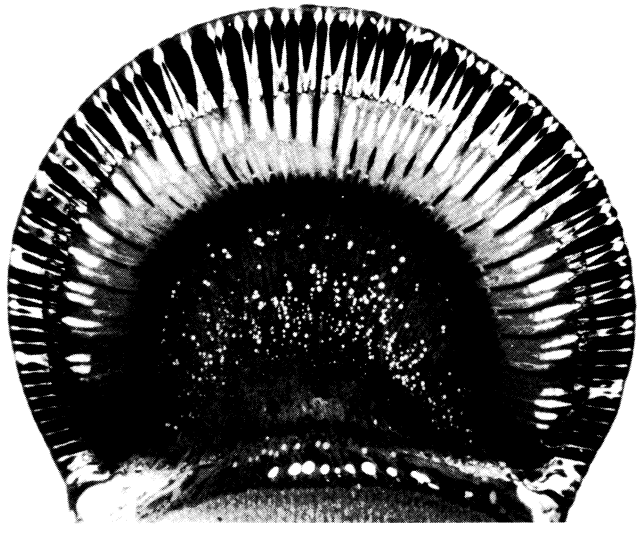

PLATE 1. *Acetes* and the gross morphology of its visual system.

FIGURE 1. Schematic drawing of a swimming *Acetes* with the long antennae trailing back parallel to the body from the elbow. Magn. × 2.5.

FIGURE 2. The stalked eyes of *Acetes* as seen in the living animal. The optic ganglia are visible through each of the transparent eyestalks. Scale bar 500 μm.

FIGURE 3. Section through the eye of *Acetes* to show its overall organization. The eye is nearly spherical and has an obvious clear zone. Scale bar 100 μm.

(*Facing p.* 254)

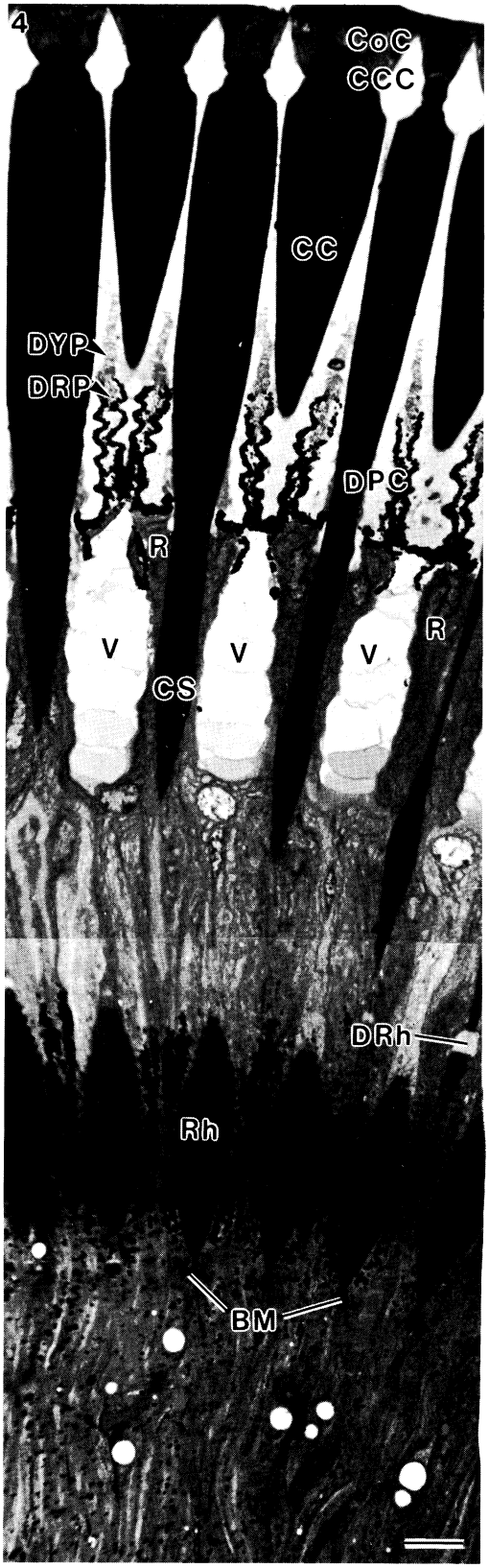

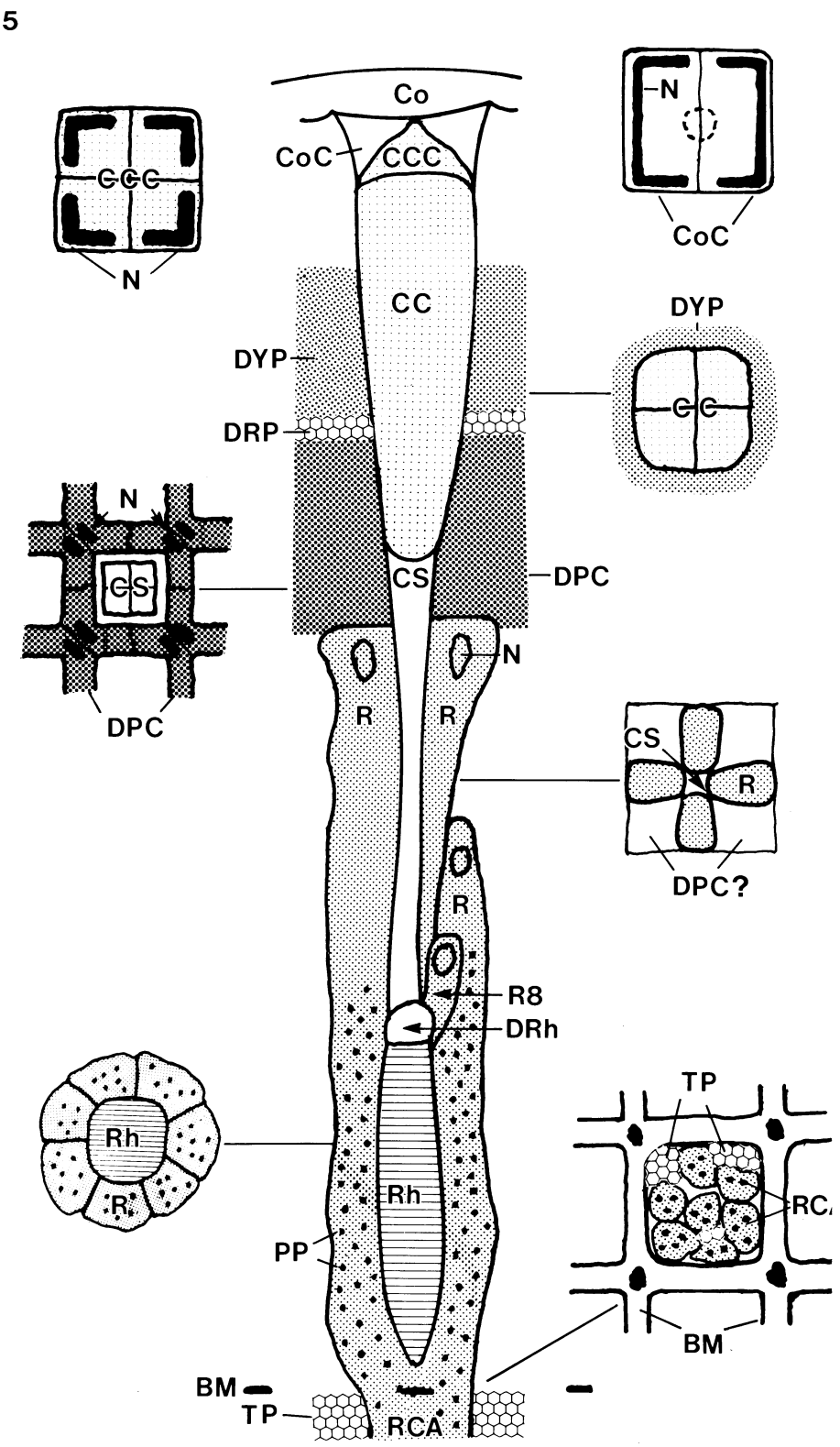

FIGURES 4 AND 5. For description see p. 254.

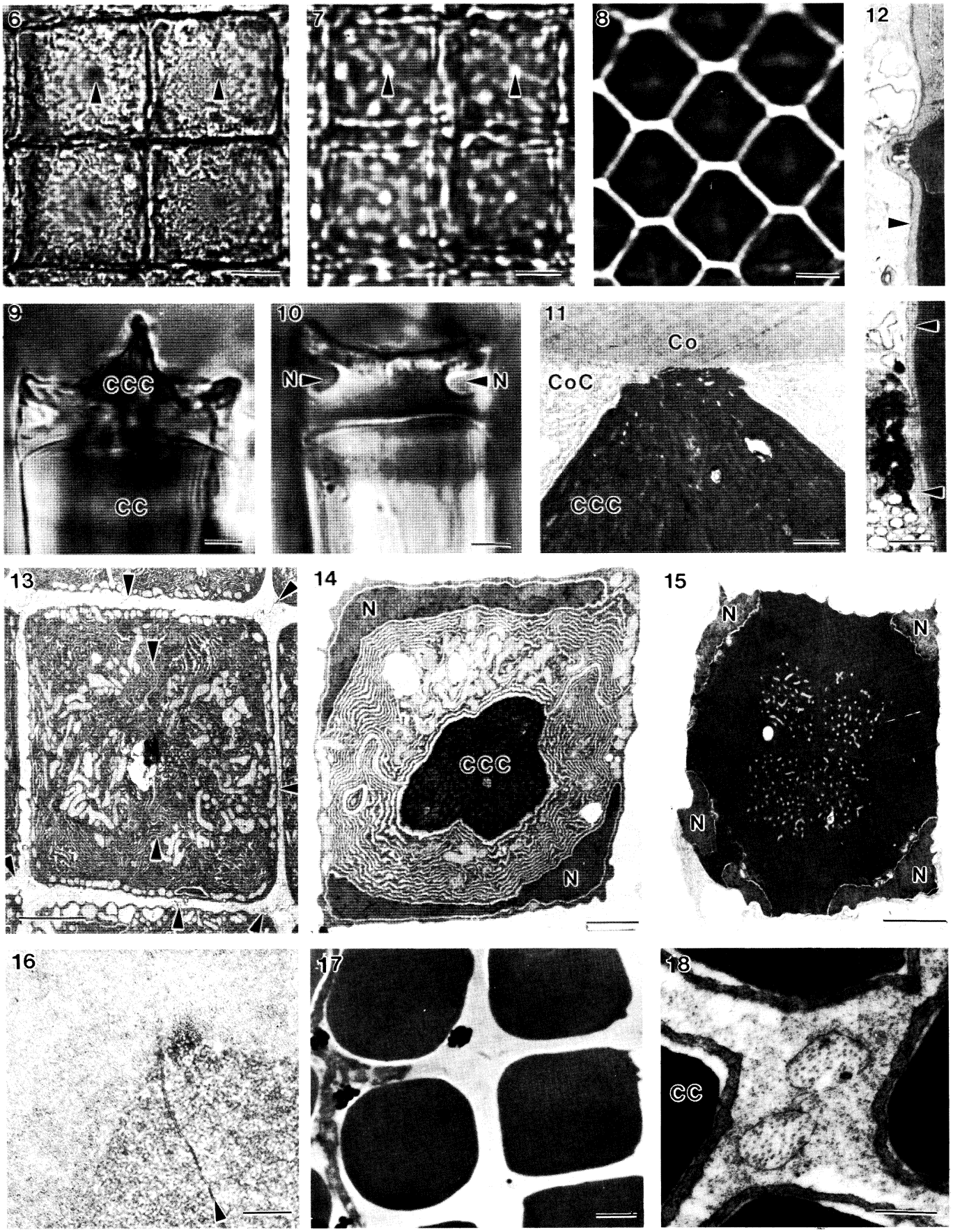

FIGURES 6–18. For description see p. 255.

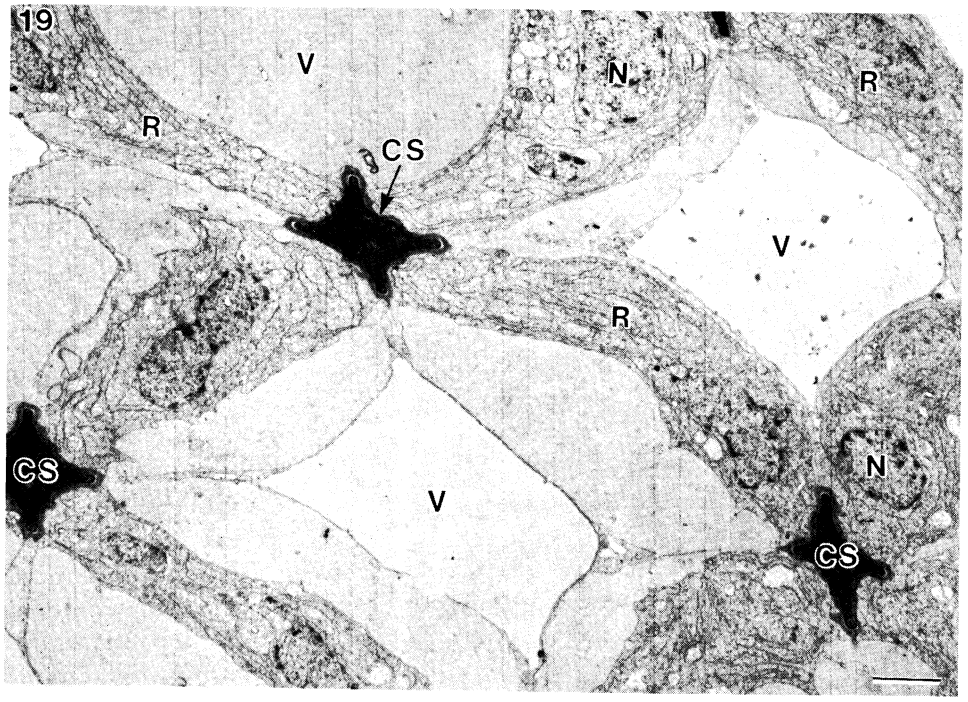

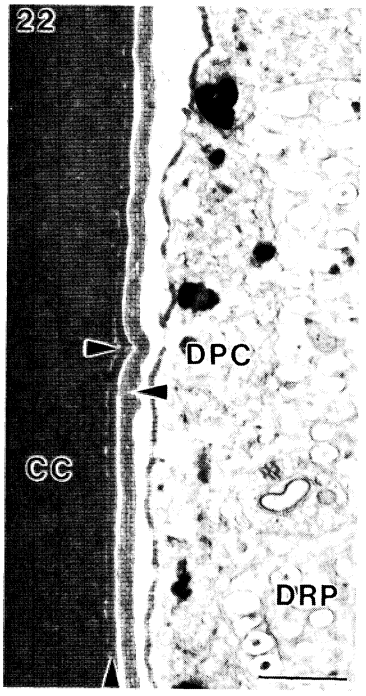

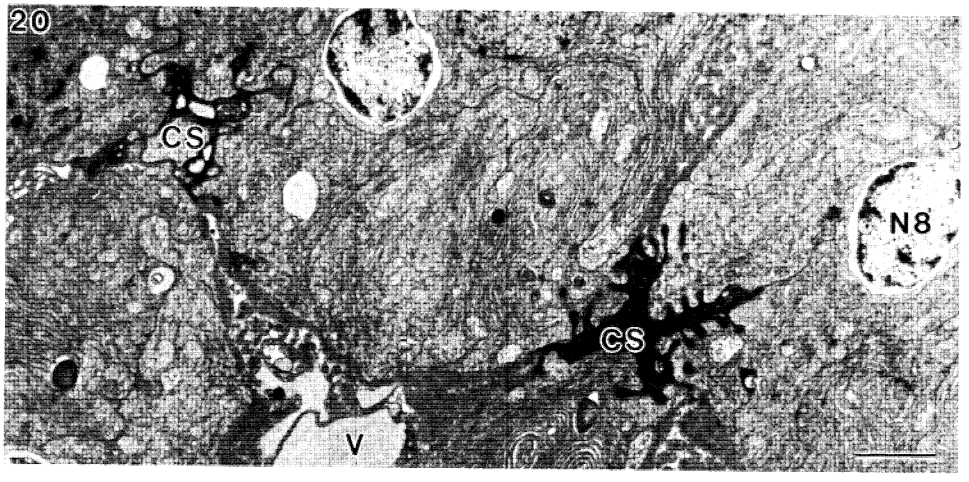

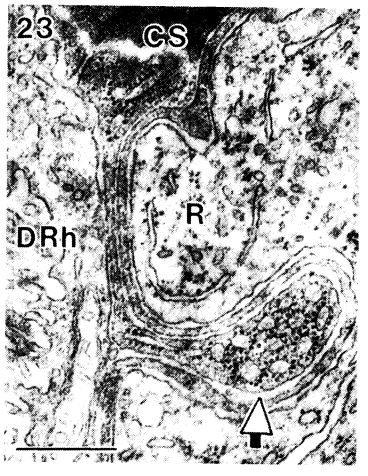

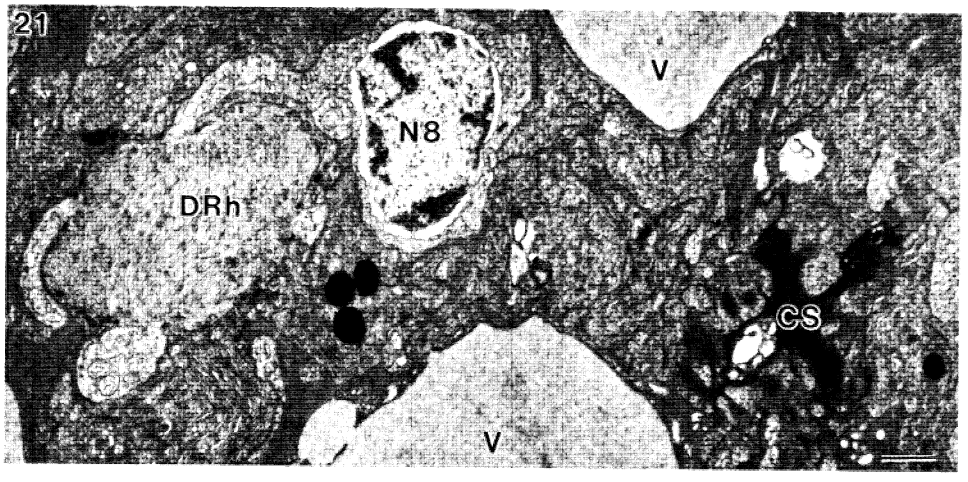

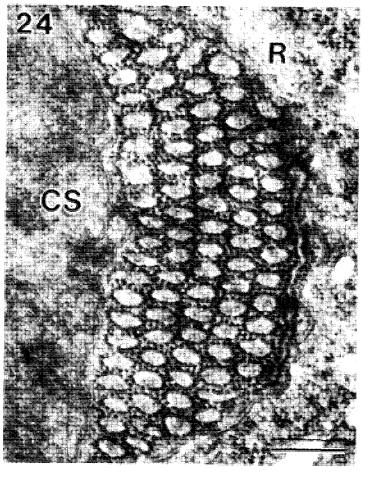

FIGURES 19–24. For description see opposite.

Description of plate 3

Plate 3. Organization of the distal part of the ommatidium.

Figures 6 and 7. Stripped cornea showing large square facets at distal end of eyestalk. Figure 6 is focused to show the central cavity between the corneagenous cells through which the projection of the cone cells reaches the cornea while figure 7 is defocused to show the central light spot (arrows) in each facet caused by light shining through this cavity. Scale bar 10 μm.

Figure 8. Corneal facets from near the edge of the eye are smaller and almost hexagonal. Scale bar 10 μm.

Figure 9. Crystalline cone cells (CCC) and the crystalline cone (CC) into which they differentiate. Scale bar 5 μm.

Figure 10. Similar to figure 9 but focused to show the nuclei (N) of two of the crystalline cone cells. Scale bar 5 μm.

Figure 11. Electron micrograph showing the point of contact of two of the crystalline cone cells (CCC) with the cornea (Co). The paler areas within the crystalline cone cells are mitochondria. The corneagenous cells (CoC), which produce the cornea, surround the crystalline cone cells. Scale bar 1 μm.

Figure 12. A thin layer of the cytoplasm of the corneagenous cell extends proximally (arrows) surrounding the crystalline cone cells. Scale bar 1 μm.

Figure 13. Corneagenous cells just beneath the cornea. There are two corneagenous cells (meeting at the arrows) that are filled with mitochondria. The tips of the crystalline cone cells can be seen in the centre of the field. Membranes of the cells surrounding the corneagenous cells (distal pigment cells? –arrowheads) are also apparent between ommatidia. Scale bar 4 μm.

Figure 14. A slightly more proximal section than that shown in figure 13. Here the elongate nuclei (N) of the two corneagenous cells, which are filled with abundant mitochondria and endoplasmic reticulum, are visible. The contribution of each of the four crystalline cone cells is also clearly apparent at this level. Scale bar 2 μm.

Figure 15. Still further proximally the four crystalline cone cells fill the entire cross section of the ommatidium. The central portion of each is packed with mitochondria and the nuclei (N) are found in the corners of the cells. Note the thin rind of tissue of the corneagenous cells surrounding the entire ommatidium. Scale bar 4 μm.

Figure 16. The periphery of the crystalline cones has a finer grain than the centre. Note the junction between the two crystalline cone cells (arrow). Scale bar 0.5 μm.

Figure 17. Proximally from the cornea (lower left) the crystalline cones become smaller and their corners are more rounded. Also visible are the distal yellow pigment (grey) and the projections of the distal pigment cells (black). Scale bar 5 μm.

Figure 18. Two microtubule-filled projections of the distal pigment cells are present at the intersections of each group of four crystalline cones (CC). Note the thin layer of corneagenous cell cytoplasm surrounding each crystalline cone. Scale bar 0.5 μm.

Description of plate 4

Plate 4. The region from the base of the cone to the distal rhabdom.

Figure 19. Below the pigment-containing portion of the distal pigment cells membranes apparently belonging to these cells extend proximally, partitioning the space. The area between the arms of the cross formed by the four retinula cells (R) associated with each cone stalk (CS) is divided by membranes into a series of compartments or vesicles (V) which are presumably fluid-filled in the living animal. Some of these spaces are clearly intracellular, but others appear to be extracellular. Scale bar 2 μm.

Figure 20. Approaching the distal rhabdom the cone stalks (CS) become cross-shaped, with the arms of the cross frequently bearing irregular protrusions. The nuclei (N8) of R8 stand out at this level owing to their light colour. Scale bar 2 μm.

Figure 21. Slightly deeper into the eye the relation between cell R8, which is clearly recognizable by its light-coloured cytoplasm, and the distal rhabdom (DRh), which it secretes, is clearly apparent. CS, cone stalk; V, vesicle. Scale bar 1 μm.

Figure 22. Cross section of the crystalline cone showing the lack of correlation between the junction of two of its component cells (left-hand arrow) and the junction of the two corneagenous cells that surround it (right-hand arrow). The vertical arrow marks the cytoplasm of the crystalline cone cells. At the right is the distal pigment cell (DPC) surrounding distal reflecting pigment (DRP). Scale bar 1 μm.

Figure 23. Longitudinal section of an ommatidium at the level of the distal rhabdom showing a protrusion of the cytoplasm of a corneagenous cell which contains spheres covered with particles that look like ribosomes (arrow). CS, cone stalk; DRh, distal rhabdom; R, retinula cell. Scale bar 0.5 μm.

Figure 24. Transverse section of an ommatidium showing a similar area containing particle-covered spheres within the cytoplasm of a corneagenous cell near the base of the cone stalk (CS). R, retinula cell. Scale bar 0.3 μm.

3. Body and eyestalk and position during normal swimming

Acetes normally swim in an approximately horizontal position with the eyestalks held laterally at 55–65° to the long axis of the body (figures 1 and 2, plate 1). The eyestalks are held approximately horizontal during level swimming, but are raised when an animal dives.

4. Structure of the ommatidium

Figures 3 and 4 show sections through a light-adapted eye of *Acetes* along the axis of the eyestalk. The structure of a single ommatidium is shown in figure 5, plate 2. The ultrastructure of the parts of an ommatidium will be discussed sequentially working inward from the periphery.

(*a*) *The cornea*

The facets of the eye of *Acetes* are square (figures 6 and 7, plate 3) over most of the eye and are largest (up to 30 μm) at the centre of the eye, gradually reducing in size toward the margins of the eye to as little as half the maximum diameter. In addition to the reduction in size, facets near the edge of the eye are frequently no longer perfect squares, but tend toward hexagons (figure 8). Each facet consists of a biconvex lens which overlies, and is secreted by, two corneagenous cells (figures 5, 11, 13 and 14) each of which contains an elongated U-shaped nucleus (figure 14). Endoplasmic reticulum and mitochondria are abundant, the latter especially along the margins of the cells (figures 13 and 14). These cells extend proximally in a thin layer which surrounds the crystalline cone cells and the crystalline cone and cone stalk into which portions of the latter are differentiated (figure 12). The junctions between the two corneagenous cells are out of register with the junctions between the crystalline cone cells (figure 22, plate 4). Near the base of the cone stalk, just above the distal rhabdom, the extensions of the corneagenous cells swell to enclose spheres which bear on their surface ribosome-like particles (figures 23 and 24). The extensions of the corneagenous cells continue beyond the junction of the cone stalk and the distal rhabdom and at least halfway down the latter (figure 23).

(*b*) *The crystalline cone and cone stalk*

A fused projection of the four crystalline cone cells (figures 6, 7, 9 and 11), which is surrounded by the corneagenous cells, extends distally up the axis of the ommatidium and attaches centrally to the underside of the corneal facet (figure 11). Each crystalline cone cell has a very electron-dense cytoplasm containing abundant mitochondria and an L-shaped nucleus at the distal periphery (figures 5 and 15). Differentiated parts of these four cells contribute to the crystalline cone and its proximal continuation the cone stalk, both of which show the same four-part structure in transverse section (figures 14 and 15). The cones, which are approximately 70 μm long (figures 4 and 5) are not homogeneous but instead usually have a peripheral fine-grained layer and a coarser-grained inner layer (figure 16). Distally the cones are nearly square with a diameter approximately three-quarters that of their overlying facets. The cones become gradually smaller proximally and their corners become progressively more rounded (figure 17) so that at their proximal end they are nearly circular and have shrunk to two-thirds of their maximum diameter. The proximal end of each cone is rounded and is

surrounded by the calyx-shaped end of the cone stalk (figures 5 and 36). Distally the cone stalk is nearly square but proximally the corners of the square become more and more elongate until just above the distal rhabdom a transverse section has the appearance of a cross with elaborate arms (figures 19, 20 and 21). Extensions of the cone stalk project proximally (figures 25 and 31, plate 5) and meet in the basement membrane at the base of each rhabdom (figures 30, 31 and 32).

(*c*) *The rhabdom and retinula cells*

The retinula cells differ considerably from each other in their basic morphology. Four of them reach far distally, almost to the level of the crystalline cone (figures 4, 5 and 19) and their nuclei lie at their distal ends (figures 4 and 5) just proximal to the distal pigment cells. In transverse section at this level the retinula cells have the form of a cross (figures 5 and 19). The nuclei of the three other 'typical' retinula cells lie 30–45 μm further proximally. Desmosomes are present where the retinula cells contact each other adjacent to the rhabdom (figure 28). Along the upper and central portions of the rhabdom the retinula cells are very tightly packed (figure 27). Toward the basement membrane the tapetal cells penetrate between them and the rhabdoms become smaller (figure 28), before ending just above the basement membrane. Mitochondria, multivesicular bodies and rough endoplasmic reticulum are found throughout the retinula cells but are especially abundant just above the basement membrane. Many granules of black proximal pigment approximately 0.4 μm in diameter (figures 4, 5, 25, 27 and 30–32, plate 6) are also present in the retinula cells. In the light-adapted eye this pigment is most abundant between the rhabdoms (figures 4, 27 and 44–46) while in the dark-adapted eye it is found further proximally (as seen in figure 43, which shows an eye still largely dark-adapted). At the basement membrane the four projections of each cone stalk come together, surrounding the base of the rhabdom. At this point the retinula cell axons must project into different squares of the meshwork formed by the basement membrane. We have not established the exact pattern of this projection but in all decapods where this has been carefully investigated the retinula cell axons project into four different squares of the grid (see Stowe (1977) and previous references given there). There is little difference between the appearance of the retinula cells distal to the basement membrane and proximal to it. Bundles of typical axons containing microtubules are first encountered near the lamina several hundred micrometres further proximal. These bundles contain eight axons (or multiples of eight) (figures 33 and 34).

R8 (so named by analogy to other crustacean systems) has the most proximal retinula cell nucleus (figures 5, 20 and 21). The cytoplasm of R8 is paler and has a more empty appearance than that of the other retinula cells (figure 21). It also differs from them in lacking proximal pigment granules. Four lobes of R8 surround and produce the entire distal rhabdom (figures 21 and 25), which varies from 6–11 μm long and 6–10 μm wide. The distal rhabdom, which lies in the light path between the crystalline tract and the regularly layered proximal rhabdom (figures 21 and 25), consists of loosely packed microvilli projecting without apparent order into extracellular space. The microvilli originate from the walls of R8 which surround the extracellular space and consequently at all angles to each other. Within a preparation they may vary in diameter from the same as the microvilli of the main rhabdom to more than twice as large.

The rhabdom itself is a typical decapod rhabdom consisting of alternate layers of orthogonal

microvilli (figure 26). The microvilli arise in groups from larger projections from the walls of the retinula cells (figure 29). There is frequently some disorganization in the otherwise orderly pattern of microvilli where the rhabdom and distal rhabdom meet. A single retinula cell may produce up to 20 layers of microvilli. The rhabdoms are spindle-shaped (figure 4) and come quite close together where they are widest (figures 4 and 27). Their maximum length and width are approximately 75 μm and 14 μm, respectively.

(*d*) *The basement membrane region*

The basement membrane, which forms a meshwork grid with each intersection supporting the base of a rhabdom (figures 30–32), consists of an extracellular basal lamina and the four extensions of each cone stalk (that is, one from each of the crystalline cone cells) which come together embedded in the basal lamina at the base of each rhabdom. The basal lamina contains fibrillar material with a banding periodicity of 56 nm. Haemocytes are frequent in this region. Numerous featureless globules (possibly lipids) are present in the retinula cell axons (figure 32). The area beneath the basement membrane also contains many blood vessels (figures 3, 4 and 32).

Description of plate 5

PLATE 5. The rhabdom.

FIGURE 25. The distal rhabdom (DRh), which is produced by R8, contains loosely packed unordered microvilli in contrast to the tightly packed layered microvilli of the rest of the rhabdom (Rh). The nature of the dense body (*) just above the rhabdom is uncertain. It may be a protrusion of retinula cell cytoplasm. Note the projection of the cone stalk at the level of the rhabdom (arrow) and the black proximal pigment (PP) within the cytoplasm of the retinula cell (R). Scale bar 1 μm.

FIGURE 26. More proximally the rhabdom (Rh) is highly ordered, consisting of alternating, orthogonally arranged layers of microvilli. Scale bar 0.5 μm.

FIGURE 27. Typical rhabdom spacing approximately halfway down the retina. Black proximal pigment is abundant within the retinula cells between the rhabdoms. Scale bar 5 μm.

FIGURE 28. Near the basement membrane the number of retinula cells contributing to the rhabdom can be determined more easily than elsewhere. Desmosomes are found where two retinula cells meet (arrows) and indicate that at this level seven retinula cells contribute to the rhabdom. Tapetal pigment (TP) cells are abundant here between the retinula cells. Scale bar 0.5 μm.

FIGURE 29. High magnification view showing how the rhabdom microvilli arise from a retinula cell (R). Scale bar 0.1 μm.

Description of plate 6

PLATE 6. The basement membrane and below.

FIGURE 30. Section tangential to the basement membrane showing that it is laid out in the form of a grid. A rhabdom arises from each of the intersection points of this grid. Black proximal pigment granules are within the retinula cell axons, which are interspersed with areas of tapetal pigment (TP). Scale bar 2 μm.

FIGURE 31. Section perpendicular to the basement membrane showing how the projections of the cone stalk (CS), which pass around the rhabdom, come together embedded in the basal lamina (BL) at one of the intersection points of the grid. Scale bar 1 μm.

FIGURE 32. Another section perpendicular to the basement membrane showing the complexity of this region. Bases of the cone stalks (CS) are embedded in the basal lamina (BL) with rhabdoms (Rh) extending upward from each of the intersection points of the basement membrane. The arrows mark cells which may be involved in secreting the basal lamina. Note also the large globules (G) of what may be lipid within the retinula cell axons. Tapetal pigment cells (TP) are interspersed among the retinula cells (R) both above and below the basement membrane. BV, blood vessel. Scale bar 2 μm.

FIGURE 33. Eight retinula cell axons are present in each of these axon bundles beneath the basement membrane. Scale bar 1 μm.

FIGURE 34. Another bundle of eight retinula cell axons near the lamina; here surrounded by the proximal portion of the screen of distal yellow pigment (DYP). Scale bar 1 μm.

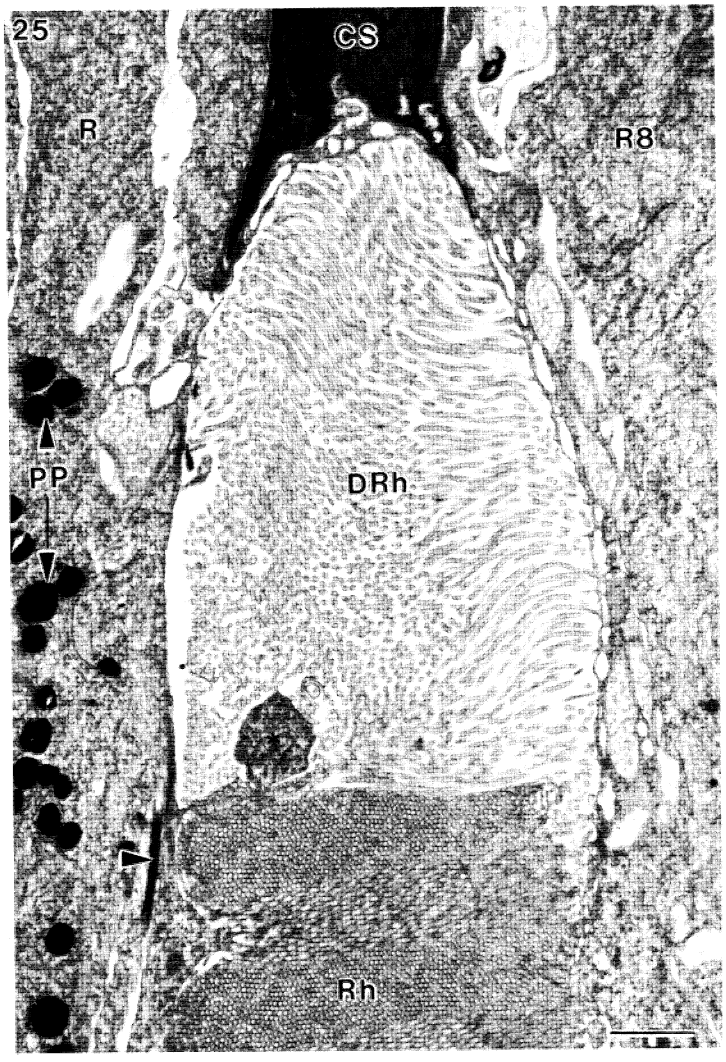

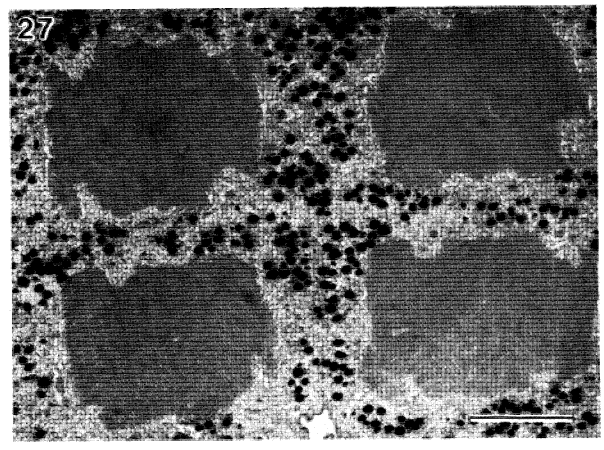

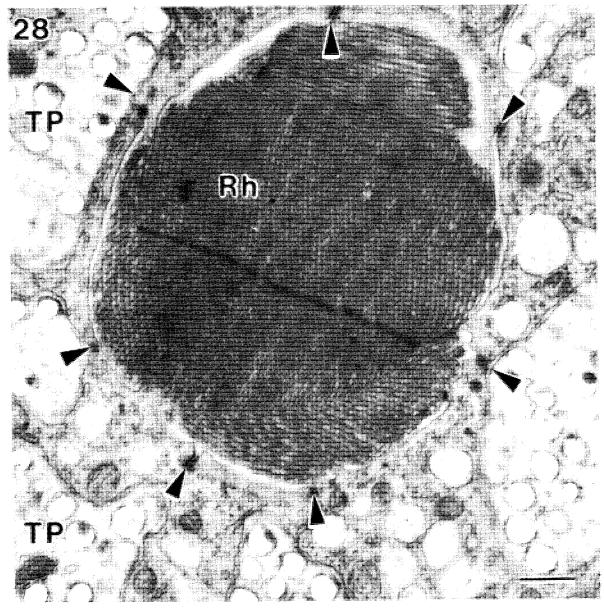

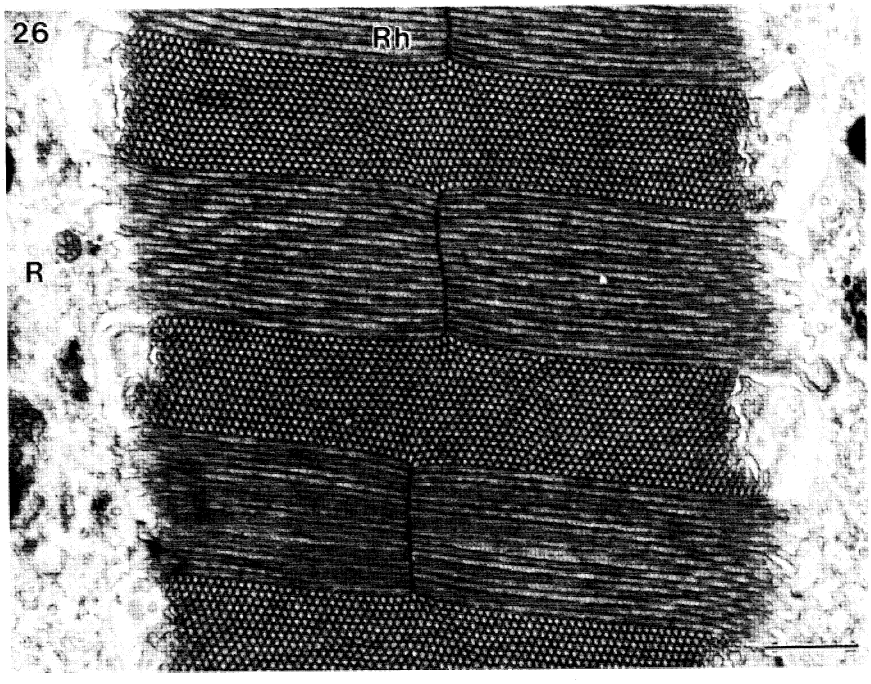

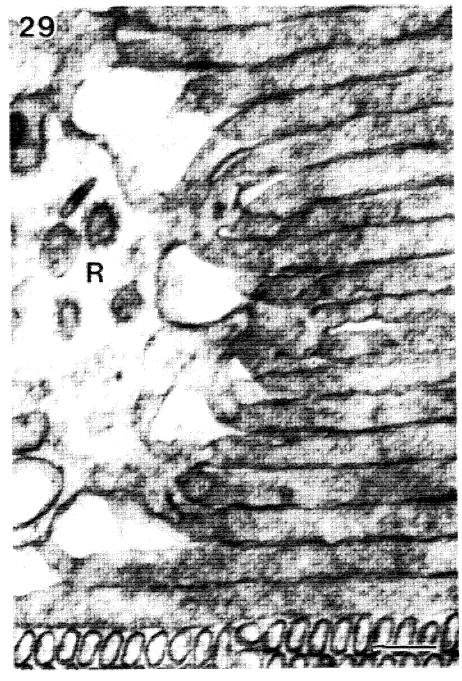

FIGURES 25–29. For description see opposite.

(*Facing p.* 258)

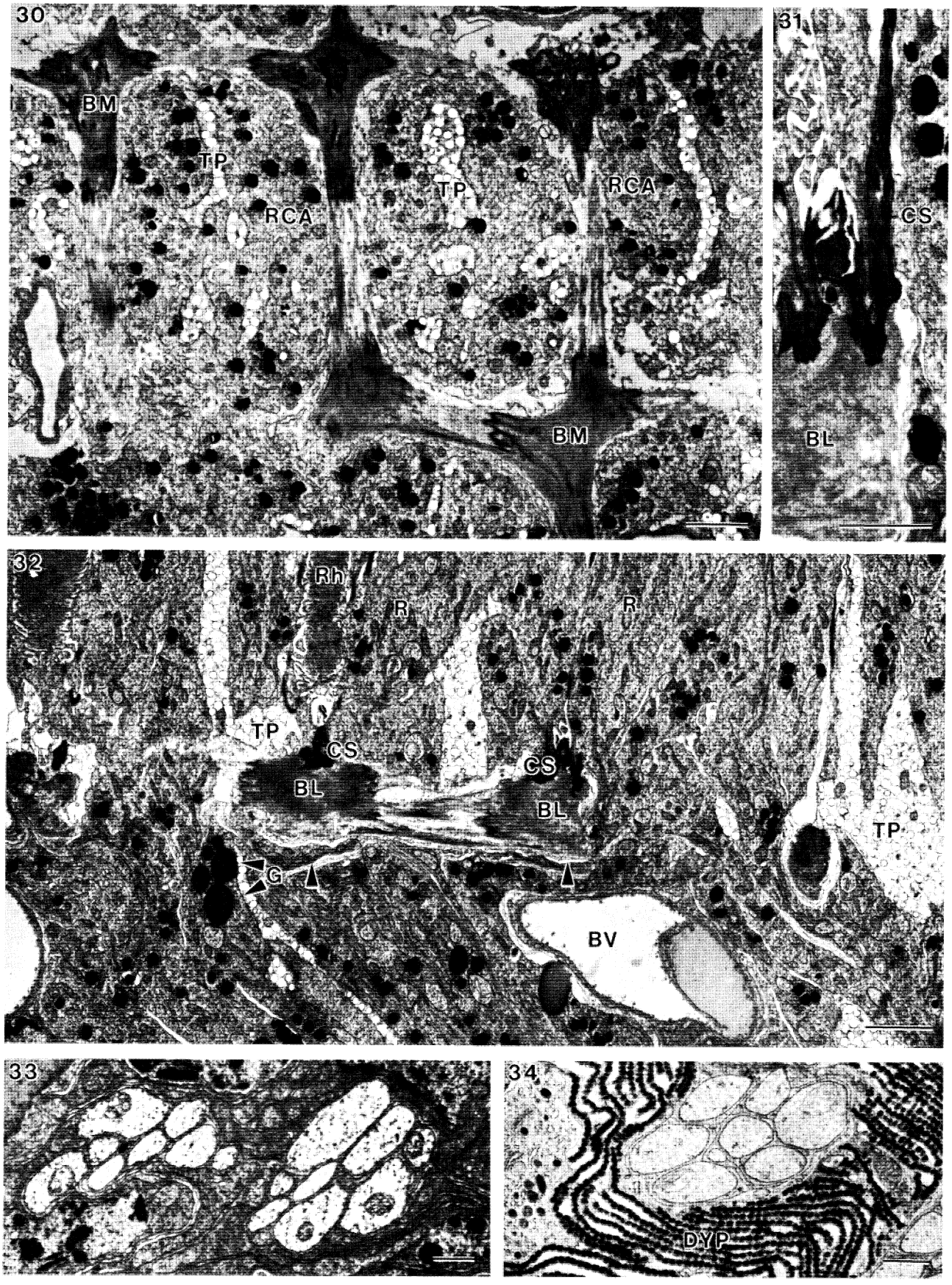

FIGURES 30–34. For description see p. 258.

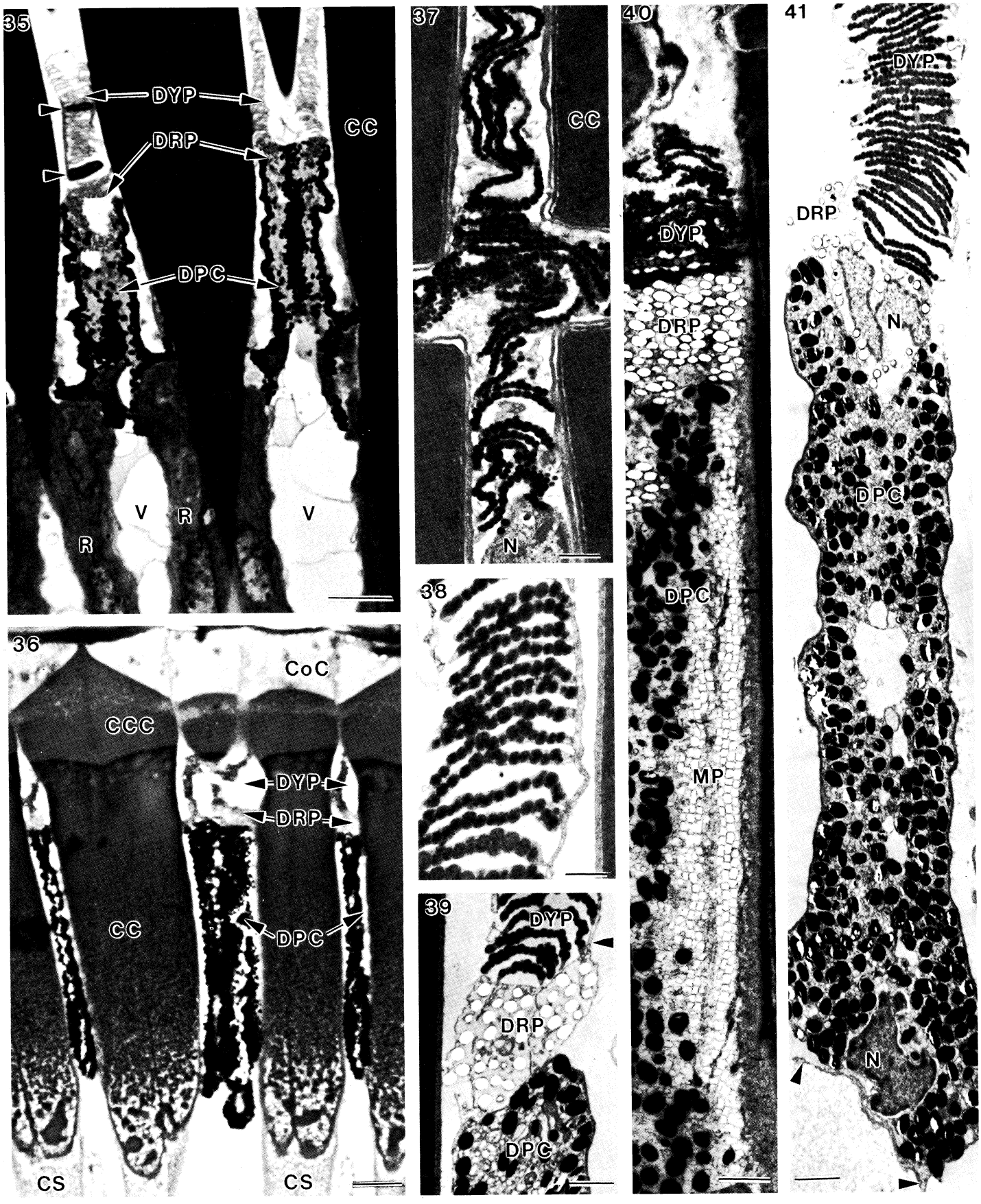

FIGURES 35–41. For description see p. 259.

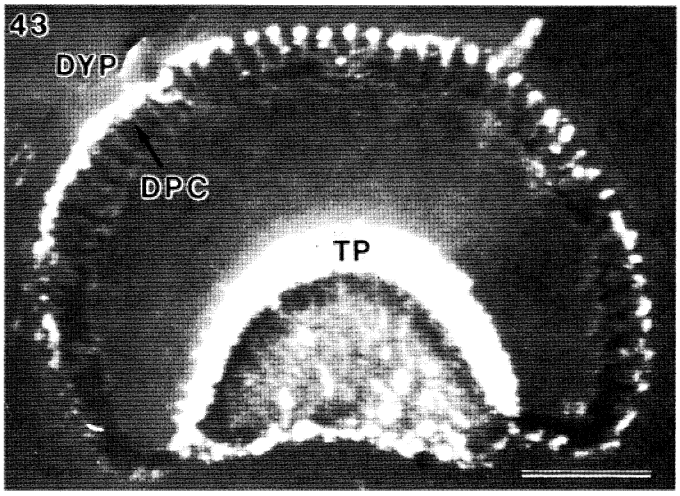

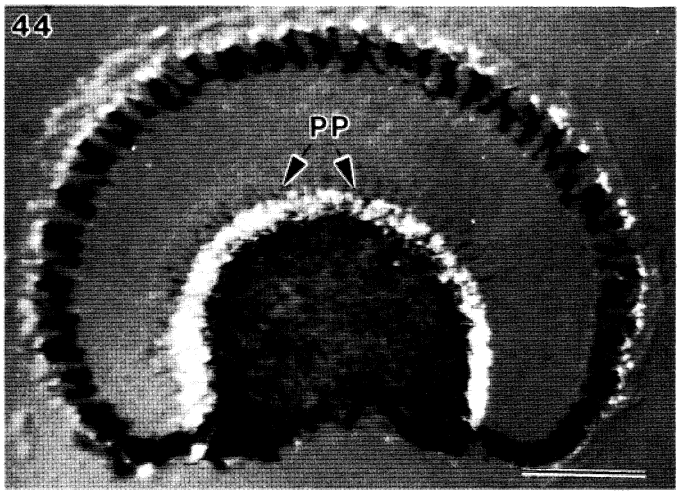

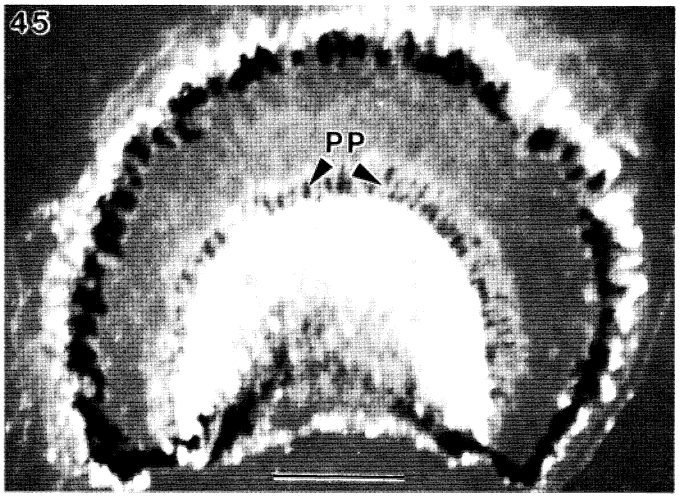

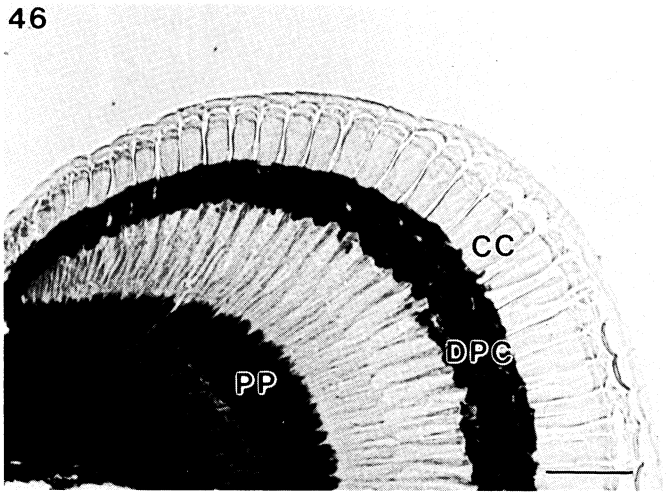

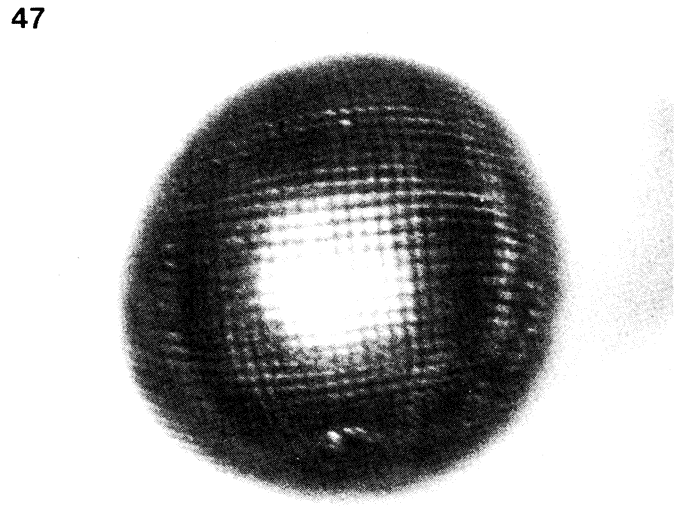

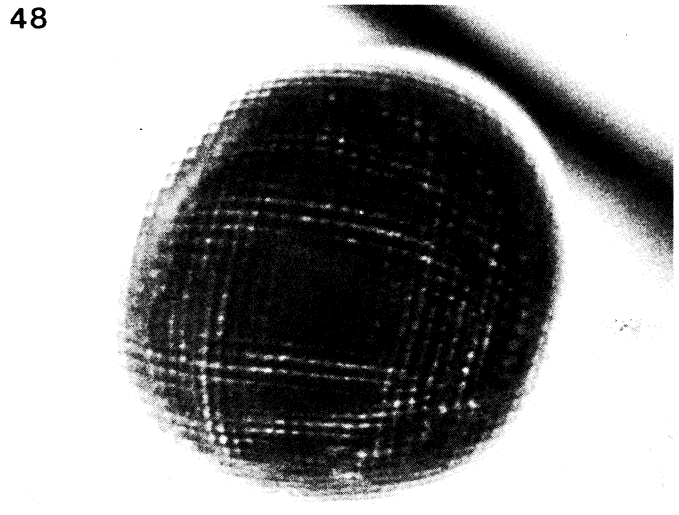

FIGURES 43–48. For description see opposite.

5. The pigment systems of the eye

In addition to the previously discussed proximal pigment within the retinula cells there are five other pigments with potentially distinct functional roles. These are the distal yellow pigment, the distal reflecting pigment, the distal black pigment and the mirror pigment (both in the distal pigment cells) and the proximally located tapetal pigment.

The distal yellow pigment (DYP) forms a continuous outer screen around the entire distal part of the eyestalk (figure 2), crossing it internally just proximal to the lamina (figures 2 and 3). This pigment appears yellow in reflected light in fresh material and frozen sections but grey in toluidine blue-stained material viewed by transmitted light. The retinal portion of this screen appears to expand and contract during light–dark adaptation. We are uncertain as to the shape of the cells containing the DYP. The pigment granules, which have a mean size of 0.20 μm, are arranged in single rows within membranous sacs, which in turn arise from other sacs not containing pigment (figures 35–41). Nuclei are present among these sacs (figures 35 and 37, plate 7), but do not seem to show a consistent pattern of distribution. Figure 39 shows sacs of distal yellow pigment closely associated with a cell containing distal reflecting pigment, so it is possible, but unlikely, that a single cell produces both types of pigment. The sacs of DYP are most commonly arranged parallel to each other and perpendicular to the sides of the cone.

Description of plate 7

Plate 7. The distal pigment complex and its changes during light and dark adaptation.

Figure 35. Section of a light-adapted eye showing the arrangement of the various distal pigments. Note nuclei (arrows) surrounded by the distal yellow pigment (DYP). CC, crystalline cone; DPC, distal pigment cell; DRP, distal reflecting pigment; R, retinula cell; V, vesicles which are presumably filled with fluid in the living animal. Scale bar 10 μm.

Figure 36. Section of a boiled, dark-adapted eye. All pigments are much higher up the side of the cones than in the light adapted state. CoC, corneagenous cell; abbreviations otherwise as in figure 35. Scale bar 10 μm.

Figure 37. Transverse section of a group of ommatidia at the level of the DYP to show how it is arranged in long chains of granules. The nucleus (N) may belong to the DYP. Scale bar 1 μm.

Figure 38. Longitudinal section showing DYP granules lined up within sacs of membrane which are all connected at one end. Scale bar 0.5 μm.

Figure 39. Three types of distal pigment. From this micrograph it appears that the DRP is enclosed in two overlapping cells. The DYP also appears to be intimately associated with a projection arising from the DRP (arrow) and may even be part of the same cell. Scale bar 1 μm.

Figure 40. The arrangement of four types of distal pigment in a dark-adapted eye. Note the brick-like pattern of holes along the side of the cone which may act as a mirror (MP). Other abbreviations as in previous figures. Scale bar 1 μm.

Figure 41. Three types of distal pigment in a light adapted eye. Note the nuclei (N) enclosed by the DRP and DPC and the apparent association of the latter with the membranes extending downward between the retinula cells (unlabelled arrows). Scale bar 1 μm.

Description of plate 8

Plate 8. Dark–light adaptation in the eye of *Acetes*.

Figures 43–45. Changes in pigment position during the course of light adaptation at 30 s (figure 43), 2 min (figure 44) and 15 min (figure 45) following exposure to light. Abbreviations as above. Scale bar 100 μm.

Figure 46. Light-adapted eye fixed in hot Bouin's fluid, showing the black pigment within the DPCs withdrawn to the base of the cones. Scale bar 50 μm.

Figure 47. The maximal patch of eyeshine that was seen in eyes dark-adapted at night. Scale bar 200 μm.

Figure 48. In the light-adapted eye the eyeshine is replaced by an almost square black pseudopupil. Scale bar 200 μm.

The distal reflecting pigment lies beneath the distal yellow pigment. In life it is white by reflected light, while in toluidine-blue-stained sections it appears orange. It is the only one of the distal pigments to glow under crossed polaroids. In material processed for electron microscopy this layer always appears to consist of empty holes ranging in size from 0.08 to 0.60 μm (mean 0.32 μm). Parts of this layer may be surrounded by the underlying distal pigment cells (figures 35, 40 and 41). The nuclei of the cells composing this layer (figure 41) do not seem to show a regular pattern in their distribution except that they are found at the corners of the cones rather than along their sides.

The distal pigment cells (figures 4, 5, 22, 35, 36, 39, 40 and 41) are L-shaped in transverse section, as shown in figure 5, and are elongated along the ommatidial axis. They are arranged so that the two diagonally placed DPCs each surround one corner of a crystalline cone while four other DPCs contribute one arm each to surround the remaining corners. The nucleus is located at the junction of the two arms of the 'L' (figure 5) and just above the most distal retinula cells. In addition to the main body of the cell which lies along the basal part of the crystalline cone or the distal part of the crystalline tract each cell sends a microtubule-filled extension distally to the cornea (figures 17 and 18). Just beneath the cornea, at the level of the corneagenous cells, the distal projections appear to expand again and resume the arrangement that they showed more proximally (figure 13). Under this interpretation the cells containing the DYP and DRP fill the interstices between the crystalline cones and the overarching DPCs. The distal extensions of the DPCs are sometimes made apparent by the black pigment which they contain (for example, in figure 17). The membranes of the DPCs also appear to extend proximally but the cellular geometry is very complex here since membranes also periodically extend laterally to form separate chambers, which are presumably fluid-filled in the living animal, between the retinula cells (figures 4 and 19). We have been able to follow this membrane system as far as the distal portion of the rhabdom, but cannot say for certain that it reaches the basement membrane, although this seems likely.

The black pigment granules within the distal pigment cells range from 0.17 to 0.83 μm in diameter with a mean of 0.50 μm. In addition to the black pigment some electron micrographs of these cells in dark-adapted eyes show apparently empty rectangles arranged in rows against the cone (figure 40). Crystals presumably filled these rectangles in the living animal. We have called this presumed pigment the 'mirror pigment' (MP). Both MP granules and black pigment granules can alter their distribution within the DPCs.

The fifth pigment type is the tapetal pigment which is located in the vicinity of the basement membrane. This pigment is identical to the distal reflecting pigment and is, in fact, continuous with it at the edges of the eye. However, since this type of pigment forms two separate screens in relation to most ommatidia we have here treated it as two separate pigments. As would be expected, the two pigments have the same appearance; white by reflected light and bright orange in toluidine-blue-stained sections viewed by transmitted light. In a few places a dense core can be seen within the otherwise empty holes formerly occupied by pigment granules (for example, figures 28 and 30). This pigment is found from the lamina to between the retinula cells above the basement membrane. However, because of the complexity of the cells we are unable to describe their morphology in detail or to say whether individual cells extend this entire distance.

6. Changes in the eye during light–dark adaptation

Pigment position in a fully light-adapted and a fully dark-adapted eye are shown in figure 42. The large and obvious changes in pigment distribution are in the proximal portion of the eye where the proximal pigment moves distally to surround the rhabdom in the light-adapted state. This movement screens the tapetal pigment. There is also some proximal movement of the tapetal pigment, but we have been unable to establish the extent of this due to the

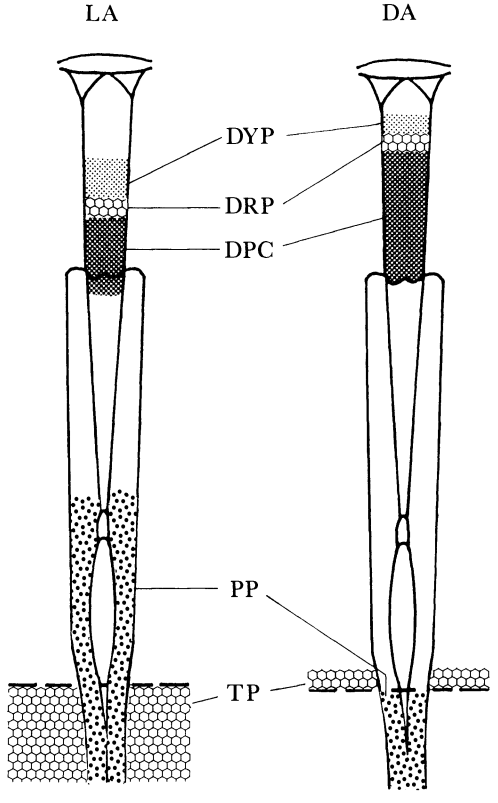

Figure 42. Schematic diagram summarizing pigment positions in an LA and a DA ommatidium. The greatest difference between the two states is in the position of the proximal pigment. The tapetal pigment changes its distribution between the two states, shifting proximally in the light-adapted eye. However, it may never be completely absent on either side of the basement membrane, as shown diagrammatically here. The movements of the distal pigments are both less consistent and less extreme than those of the proximal pigment. The changes shown here may be more extreme than is typical. DPC, distal pigment cell; DRP, distal reflecting pigment; DYP, distal yellow pigment; PP, proximal pigment; TP, tapetal pigment.

simultaneous and much greater movement of the proximal pigment (see, for example, figures 43–45, plate 8). The situation with regard to distal pigment movement is equivocal due to inconsistencies between preparations. However, what appears to happen with these pigments is that in the dark the DPCs expand upward compressing the DYP while in the light the total zone occupied by DPCs contracts and the DYP increases its share of the total. In addition it appears that the distal pigments move proximally relative to the crystalline cone and cone stalk in the light-adapted eye (figures 42 and 46).

We found that in spite of exposing dark-adapted eyes to dim red light only long enough to

remove them and then maintaining them in darkness the retinal pigments moved toward the light-adapted position. Therefore, the only material to reflect adequately the true position of the various pigments was that which was either frozen in liquid nitrogen or boiled with consequent destruction of much structural detail.

The most satisfactory results for relating pigment position to state of light adaptation were obtained by using paired eyes in which pigment position, as seen in cryotome sections, could be matched to the state of the eyeshine. Representative sections from this experiment are shown in figures 43 (0.5 min of light), 44 (2 min) and 45 (15 min). By 2 min the eyeshine had become quite pale, and, as can be seen in figure 44, by this time the proximal pigment had begun to move distally across the zone of tapetal pigment. By 15 min it had largely completed this movement (figure 45) although it is likely that the movement would be more complete in brighter light. In addition, as the eyeshine fades it changes colour from silvery white to reddish. In contrast to the eyeshine of the dark-adapted state (figure 47), the fully light-adapted eye shows a square black pseudopupil (figure 48).

7. Rhabdomeral membrane turnover in relation to light conditions and time of day

The rhabdoms of *Acetes* do not show large changes in size related to time of day such as have been described in the crabs *Leptograpsus* (Stowe 1980) and *Grapsus* (Nassel & Waterman 1979) so membrane turnover in *Acetes* may not be as extensive as in those species. However, membrane whorls were abundant near the basement membrane and multivesicular bodies were clearly more abundant at 08h10 than at any of the other times sampled in our light–dark adaptation experiments.

8. Optics

(*a*) *Type of eye*

As discussed above, and shown in figure 43 (which is still nearly fully dark-adapted), the dark-adapted *Acetes* eye has a wide pigment-free clear zone distal to the rhabdoms, and the eye shows a large patch of eyeshine when illuminated from the direction of observation (figure 47). These features mean that the eye is of the superposition type (Kunze 1969; Land 1981). The facets are square rather than hexagonal, and the crystalline cones have a nearly homogenous refractive index. With or without the presence of identifiable mirrors, these features indicate that the eye is of the reflecting rather than refracting superposition type (Vogt 1975, 1980; Land 1981). In the light-adapted state pigment cuts off oblique rays (see above and Discussion), so that each rhabdom probably receives light only from its 'own' facet, thus effectively converting the eye into the apposition type. In most respects the *Acetes* eye is optically very similar to the crayfish eye, described in detail by Vogt (1980).

(*b*) *Interommatidial angle: resolution*

The angle subtended by two adjacent receptors in outside space represents the smallest 'sampling' angle ($\Delta\phi$) with which the animal views the world. Because there is a one-to-one relation between facets and rhabdoms, the spherical geometry of the eye dictates that $\Delta\phi$ will be the angle subtended by each facet at the centre of curvature of the eye surface. This is thus D/r radians or 57.3 D/r degrees, where D is the shortest distance between ommatidial centres

along rows, and r is the radius of a circle best fitting the curvature of the eye. D had a maximum value of 30 μm in the centre of the eye, decreasing somewhat at the edges of the eye, and the corresponding range of $\Delta\phi$ was 3.8–2.8°. These determinations were made on both fixed sectioned eyes and on fresh eyes.

The finest grating that an eye can resolve has a spatial period of $2\Delta\phi$ (two receptors for each stripe pair). The reciprocal of this, the spatial sampling frequency, is in the range 7.5–10.2 cycles per radian in the eye of *Acetes*.

(*c*) *Properties of the crystalline cone*

A fresh *Acetes* eye was cut up in 2% formaldehyde (by volume) and the tissue was allowed to fix for 45 min. Crystalline cones were then isolated and examined with a Zeiss interference microscope. They gave straight interference fringes when lying on one face, indicating that they have a uniform refractive index radially (see Vogt 1980, figure 7). The refractive index, measured interferometrically in seawater, varied from 1.425 near the top to 1.418 two thirds of the way down the length of the cone. Cones of an animal that had been fixed for several years in formaldehyde gave a refractive index of 1.433. The homogeneity of the cone excludes the possibility of refracting superposition, which requires cones with a refractive index gradient (Exner 1891).

If we assume that the cones are surrounded by a fluid with the same refractive index as seawater (1.34) then we can calculate the critical angle for light to be retained inside the cone. This is given by arcsin (n_{out}/n_{in}), or arcsin 1.34/1.42, which is 70.7°. The complement of this angle (19.3°) will also be the maximum angle that rays can make with a normal to the surface of the eye and contribute to the ray-bundle reaching the image, *unless* the cones have a reflecting mechanism in addition to critical angle reflection.

(*d*) *The pupil of the dark-adapted eye: sensitivity*

In dark-adapted eyes fixed in liquid nitrogen and allowed to thaw it was possible to photograph the patch of eyeshine that results from axial illumination and to measure its size (see above and figure 47). This eyeshine patch represents the effective pupil of the eye because it is the area over which light reaching a single point on the retina both entered and left the eye. The widest patch of eyeshine seen was 9–10 facets across. Since the patch was roughly circular, this means that about 71 facets were contributing to the image at any one point. If in the light-adapted state this number reduces to 1, then the gain in image brightness due to the superposition mechanism alone should be a factor of 71; nearly 2 log units.

On the eye surface the maximum diameter of the glow patch was 0.327 times the diameter of the eye itself. This represents an angle at the centre of the eye of 2 arcsin 0.327, or 38.2° (figure 49). The marginal ray, which just contributes to the image, will make an angle with a normal to the eye surface which is half this, 19.1°. This angle, interestingly, is almost identical to the complement of the critical angle for the cones, given above (19.3°), which means that for a pupil of this diameter a total internal reflection mechanism would be adequate, and additional mirrors would not, strictly, be necessary.

(*e*) *Corneal lenses*

Bryceson (1981), studying crayfish eyes, found that each corneal facet acted as a weak converging lens, with a focal length roughly equal to the distance from the cornea to the

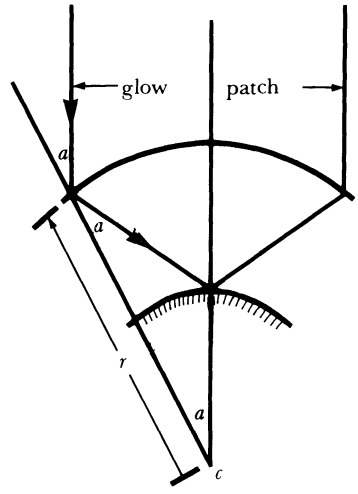

FIGURE 49. Showing that the semi-angle (a) subtended by the glow-patch at the eye centre is equal to the angle between the marginal ray of the pupil and a normal to the eye surface, if the cone faces are normal to the eye surface.

rhabdom layer. We looked for the same phenomenon in *Acetes* and found it. By using a fresh isolated cornea in seawater we were able to observe sharp images of distant objects at a real distance of 277 + 24 (s.d.) μm from the lens. The focal lengths of the same corneal lenslets were also measured from the magnification of the image of a pair of stripes, at the position of best focus. This gave a value of 300 μm, confirming the former estimate. In this eye (radius 375 μm, facet diameter 25 μm) the rhabdom layer would have been located around a sphere of radius about half that of the eye itself (187.5 μm). Thus the images formed by the corneal lenses on their own lie about 100 μm deeper than the rhabdom layer. There is an additional converging refracting surface at the proximal end of the cone, which will tend to reduce the overall focal length of the ommatidium, and there might thus be quite a well-focused image at the rhabdom tip. (The proximal part of the cone stalk may also behave to some extent as a light guide, but its strange shape and unknown refractive index make its contribution to the ommatidial optics unassessable.) One effect of the lens, as Bryceson (1981) pointed out, will be to taper slightly the beams contributing to the superposition image in the dark, which may improve its quality, and in the light, the lenses will ensure that the quality of the apposition image is good; better certainly than it would be without them.

9. DISCUSSION

Previous major papers on eye structure of species relatively closely related to *Acetes* include, within the Penaeidae, those of Ramadan (1952) on *Metapenaeus monoceros*, Zyznar (1970) and Zyznar & Nicol (1971) on *Penaeus setiferus* and Meyer-Rochow & Walsh (1977) on *Gennadas* sp. Within the Sergestidae Chun (1896) and Welsh & Chace (1938) have dealt particularly with the question of eye adaptations in relation to habitat but there are so many contradictions between the two papers that no pattern is apparent. It appears likely that Chun (1896) was working largely with immature specimens which are quite different from adults in their eye structure. He studied the eyes of *Sergestes longirostris* Kroyer (= *Sergestes corniculum* Kroyer, 1855),

S. longispinus Bate (= *S. cornutus* Kroyer, 1855), *S. magnificus* Chun (= *S. arcticus* Kroyer, 1855), and *S. armatus* Kroyer as well as those of many other species which he could not identify. Of the species listed by Chun only *S. armatus* is still considered a valid species: the other names have been synonymised with the names given in parentheses after each of Chun's species listed above (A. A. Fincham, personal communication). Chun deals in the greatest detail with the eye of *S. armatus* but some of his specimens were clearly immature because one of the facets is figured as hexagonal (plate XX, figure 4, in Chun 1896). The eyes of adults of this species are described quite differently by Welsh & Chace (1938). Chun's hypothesis with regard to the relation between habitat and eye structure in sergestids is invalid because it was based on a mixture of adult and immature material. This hypothesis was that shallow water species have round eyes on short eyestalks and a full complement of eye pigments while pelagic species mainly have asymmetrical eyes in which those ommatidia which point upward or upward and forward are elongate and the distal pigment has been lost.

Welsh & Chace (1938) attempted to relate the eye structure of sergestids to depth and bioluminescent capability. While their detailed conclusions need some modifications based on new information regarding photophore distribution, the now well-established bioluminescent function of the organs of Pesta and the depth distribution of certain species, their main conclusion that the largest eyes relative to body size are found in luminous species inhabiting the mesopelagic zone still appears to hold. There were, however, interesting variations in the pigmentation of the eyes of such species which could not be explained solely on the basis of habitat and luminescent capability.

The papers cited above indicate that there is a basic structural plan to which the eyes of members of the Penaeidea conform and where differences are described in the literature it is frequently difficult to decide whether these are real or due to differing interpretations of the different investigators. We will therefore here review our findings as they relate to those of previous workers.

The facets of adult Penaeidea are described by most investigators as square. However, Fincham (1980) and Nilsson (1983*a*) are in agreement that immature sergestids have hexagonal facets. Therefore, there seem to be two possible explanations for the hexagons (truncated squares?) found at the edge of the eye of adult *Acetes*. They may be neotenous features or they may result merely from the difficulty of packing perfect squares on a curved eyestalk.

The presence of two corneagenous cells surrounding the projecting tips of the four crystalline cone cells also appears to be a common feature (see, for example, Ramadan 1952; Zyznar 1970). The projection of these cells proximally surrounding the crystalline cone and cone stalk (figures 12 and 22), however, appears not to have been previously described in the Penaeidea, although it occurs in *Palaemonetes pugio* (Doughtie & Rao 1984) and in the crab *Macropipus* (D.-E. Nilsson, personal communication). In addition the morphology of the 'covering cell' described by Krebs & Lietz (1982) as surrounding the base of the cone stalk and the eighth retinula cell in the crayfish *Astacus fluviatilis* and *Astacus leptodactylus* bears a remarkable resemblance to the projections of the corneagenous cells described here in the same region (figures 20–24). It may therefore turn out that such projections of the corneagenous cells are common features of the decapod eye.

For most of their length the corneagenous cell extensions are compressed and ultrastructurally rather featureless. However, at their proximal ends, in the vicinity of the distal rhabdom, they swell and contain spheres or tubules of membrane covered with particles which are similar in

size to ribosomes (figures 23 and 24). Many possible roles could be postulated for these structures (on the assumption that the particles are ribosomes) but we have no concrete evidence as to their function.

The crystalline cone cells do not appear unusual, although the electron microscope reveals that they are packed with mitochondria (figures 11, 14 and 15) and that the cone itself is finer grained peripherally than centrally (figure 16). The crystalline tract has become almost cross-shaped before its junction with the distal rhabdom, but whether this will prevent it from acting as a light guide is not known. Fixation has almost certainly resulted in shrinkage, so in the intact animal the cone stalk may still be large enough to operate as a light guide in spite of its unusual shape.

The two-tiered arrangement of retinula cells in *Acetes* appears to be unusual, but not unique. Elofsson & Hallberg (1977) describe a similar arrangement in three species of deep sea mysids and Eguchi *et al.* (1982, figures 2 and 3) show an apparently identical retinula cell arrangement in the porcellanid crabs *Petrolisthes armatus* and *P. japonicus*. This is particularly interesting because *Petrolisthes* also has square facets and belongs to one of the groups of anomurans which Fincham (1980) has grouped, on the basis of eye structure, with the shrimps.

The occurrence of R8, a retinula cell which lacks proximal pigment and produces the distal portion of the rhabdom, is widespread among crustaceans (see Nassel (1976) for discussion). However, the distal rhabdom of *Acetes* appears to be unique with regard to the large amount of space between the individual microvilli. We have been unable to locate an axon projecting proximally from R8. However, there are clearly seven 'normal' retinula cells but eight axons per bundle below the basement membrane. For this reason, and because a small axon has been located leading proximally from R8 in such well-studied animals as the crayfish *Pacifastacus* (Nassel 1976) we believe that such an axon exists in *Acetes*. Except for the unusual nature of the distal rhabdom produced by R8 the rhabdom of *Acetes* fits within the general decapod pattern. Cummins & Goldsmith (1981) have established that R8 is a violet receptor in crayfish and given the structural and phylogenetic similarities the same may also be true in *Acetes*.

The role and movements of pigments in the crustacean compound eye have long been the topic of study and speculation (the reviews of Parker (1932), Kleinholz (1961), and Land (1981) summarize results and changing interpretations during this century). However, since the independent discovery of the principle of the reflecting superposition eye by Vogt (1975) and Land (1976) there has been no detailed investigation of such an eye except for the paper by Vogt (1980) on the eyes of several species of crayfish and that of Doughtie & Rao (1984) on the eye of *Palaemonetes*.

The basic complement of crustacean pigments appears to consist of a distal dark pigment which moves proximodistally and sometimes laterally to absorb stray light and in some cases to change the eye from an apposition to a superposition function; a proximal dark pigment within the retinula cells which moves up and down restricting light to a single rhabdom in the light-adapted state and allowing it to penetrate laterally in the dark-adapted state; and a light-coloured pigment located near the basement membrane which reflects any light that has passed through the eye back into the rhabdoms, thus increasing sensitivity. The pigment systems of the eye of *Acetes* are considerably more complex than this simple pattern and present us with some difficult but interesting problems of interpretation.

The difficulties of studying the pigment cells are multiplied by our inability to obtain simultaneously good fixation and assure ourselves that we are seeing the pigments in the position

that they actually occupied at a certain time of day under given light conditions. In addition to fixation artefacts there is the problem of inter-individual differences in the timing and degree of pigment movements. In general the differences between eyes that were boiled or quick-frozen, thus stopping the retinal pigment in place, and fixed material, were most pronounced for the proximal pigment, and involved movement of the pigments toward the light-adapted state. The probable explanation of this observation is that energy is required for maintenance of the dark-adapted state and anything that damages the cell causes a relaxation toward the resting state (Frixione *et al.* 1979).

As described in the Results, we remain uncertain as to how many types of distal pigment *cells* are actually present and of their shapes. Only for the DPC proper can we discern a regular pattern of cell arrangement and nuclear location.

Although we did not do chemical tests on the eye pigments sufficient information is available for related species to allow prediction of their composition in *Acetes* with a high probability of success based on the work of Elofsson & Hallberg (1973), E. Hallberg (unpublished), Struwe *et al.* (1975) and Zyznar & Nicol (1971). On the basis of these papers it appears likely that the DYP is a carotenoid, the DRP and TP are pteridines, and that the black pigments of DPCs and retinula cells are xanthommatins and ommins.

The recent ultrastructural study by Doughtie & Rao (1984) on the ultrastructure of the eye of *Palaemonetes* includes many relevant observations on the pigment cells. In *Palaemonetes* the distal pigment cells also contain a dark pigment and an electron-lucent pigment comparable to the MP in *Acetes*. Granules of the latter pigment take on a rectangular shape and become ordered against the sides of the cones in the dark-adapted state while they are polymorphic and not arranged in an orderly manner in the light-adapted state. This observation is consistent with what we have seen in *Acetes* in that we have only seen the mirror pigment in an ordered state in dark-adapted eyes. *Palaemonetes* is further similar to *Acetes* in having a thin cap of reflecting pigment distal to the distal pigment cells. In *Palaemonetes* this cap is clearly connected to the proximal reflecting pigment, at least in the light-adapted state (see figure 23 of the above paper). In *Acetes* the only connection we have seen between the two pigments (our DRP and TP) is at the edge of the eye. While we cannot rule out direct proximodistal connections in the eye of *Acetes* their presence there is problematical owing to our failure to see such connections in sections such as that shown in figure 19 and to the presence of nuclei in the DRP cells (figures 4 and 41).

Our optical studies demonstrate that internal reflection alone appears to be sufficient to account for the maximal eyeshine observed in *Acetes* so a question arises as to the function of some of the distal pigments. In dissected material the DYP is bright yellow in reflected light but when viewed on the animal the eyes appear a rather metallic golden brown. It therefore seems possible that the DYP serves as a reflective mirror helping to make the mostly transparent animal inconspicuous. The DRP forms such a thin layer that any functional role appears questionable. Had we not studied the eyeshine of the dark-adapted eye we would have assumed that the MP served to increase the reflectivity of the sides of the cones because Vogt (1980) has established that this is the function of a pigment of similar appearance in the crayfish (see his figure 3*b*). However, the patch of eyeshine shown in figure 47 is the largest we obtained from numerous eyes and if our assumptions about the refractive index of the material outside of the cone are correct this size can be accounted for by internal reflection alone. Therefore the function of the mirror pigment must remain in doubt. One possible explanation (D.-E.

Nilsson, personal communication) is that there is not enough space between the crystalline cones and the other pigments for an effective layer of low refractive index fluid; thus it is structurally and optically 'safer' to put in a modest multilayer. The function of the black distal pigment, on the other hand, is clearly the absorption of stray light. Although we were unable to quantify a convincing proximal movement of the distal pigment we feel that it probably does occur and would be revealed if a method could be worked out for observing such a movement in individual *Acetes* such as was done by Welsh (1930) using the relatively transparent eye of *Palaemonetes*. Even a small proximal movement of the distal pigment, combined with the distal movement of the proximal pigment, would go a considerable way toward making a superposition eye into an apposition eye (see Nilsson (1983*b*) for a discussion of the optics involved).

To evaluate adequately the selective pressures that may be operating on the visual system it is necessary to consider the ways in which vision is likely to be important to members of the genus *Acetes*. *Acetes* live mainly in shallow estuarine areas where visibility is frequently very poor, so vision at a distance of even 0.5 m would often be impossible. The species of *Acetes* for which dietary information is available are omnivorous, feeding on small zooplankton, phytoplankton and detritus (Le Reste 1970; Omori 1974; L. B. Quetin, R. M. Ross & E. E. Ball, unpublished). Judging from gut coloration, *A. sibogae* feeds more actively at night than during the day, so vision may not play a large role in feeding. During the day *A. sibogae* almost always occurs in schools and vision may play an important role in schooling. At night the schools appear to break up (L. B. Quetin, R. M. Ross & E. E. Ball, unpublished). *Acetes* is heavily preyed on by fish in many areas (Omori 1974; G. W. Henry, unpublished; E. E. Ball, R. M. Ross & L. B. Quetin, unpublished) and vision may play a role in predator avoidance. The extent to which *Acetes* uses its eyes at night is unknown although it seems likely that vision in very dim light will be less important in *Acetes* than in many mesopelagic sergestids which are luminous and live in much clearer water.

The eye of *Acetes* appears to be a general purpose eye without any of the regional specializations characteristic of the eyes of many deep-water Malacostraca (Chun 1896; Land *et al.* 1979; Hiller-Adams & Case 1984). The eyes of *Lucifer*, another sergestid found in the same sort of habitats as *Acetes*, are apparently quite similar to those of *A. sibogae*, having been characterized by Hanstrom (1933) as round and heavily pigmented. It is to be hoped that future studies combining anatomy, physiology, behaviour and natural history will lead us to a better understanding of the forces that have shaped the visual systems of many deep-sea species. It is clear from the dramatic anatomical changes in eye structure during development (compare the observations of Chun cited above and Nilsson (1983*a*)) that a satisfactory understanding of the structure and function of the eyes of individual species of sergestids in relation to natural history will only be available once eye structure has been described for all of the developmental stages in relation to their way of life. Such a study has now been done by Fincham (1984) for the prawn, *Palaemon serratus*. Also, the importance of *in situ* observation for meaningful analysis of anatomy is emphasized by the observation that different species of sergestids position themselves differently in the water column, some with their heads up and others nearly horizontal (Omori 1974, p. 263).

We are grateful to John Paxton for help in obtaining *Acetes*; to Bruce Hodgson and the Electricity Commission of New South Wales for permission to work and use the laboratory at the Tuggerah Lakes; to Langdon Quetin and Robin Ross for discussion, company in the field,

and for allowing use of unpublished material; to Ingeborg and Tammy Frank for use of their translation of Chun (1896); to George Weston and the staff of the RSBS EM Unit for technical assistance; to A. A. Fincham for help with sergestid taxonomy and nomenclature; and to Eric Hallberg, Page Hiller-Adams, Dan Nilsson, and Sally Stowe for helpful discussion during the work or for comments on the manuscript. We are especially grateful to Peter McIntyre for making the refractive index measurements, without which several aspects of the optics would have remained hypothetical.

References

Ball, E. E. 1977 Fine structure of the compound eyes of the midwater amphipod *Phronima* in relation to behavior and habitat. *Tissue Cell* **9**, 521–536.

Ball, E. E. & Cowan, A. N. 1977 Ultrastructure of the antennal sensilla of *Acetes* (Crustacea, Decapoda, Natantia, Sergestidae). *Phil. Trans. R. Soc. Lond.* B **277**, 429–457.

Bryceson, K. P. 1981 Focusing of light by corneal lenses in a reflecting superposition eye. *J. exp. Biol.* **90**, 347–350.

Chun, C. 1896 Atlantis, Biologische Studien über pelagische Organismen. Leuchtorgane und Facettenaugen. Ein Beitrag zur Theorie des Sehens in grossen Meerestiefen. *Bibliotheca zool., Stuttg.* **7**, 193–262.

Cummins, D. & Goldsmith, T. H. 1981 Cellular identification of the violet receptor in the crayfish eye. *J. comp. Physiol.* **142**, 199–202.

Denys, C. J. & Brown, P. K. 1982 Euphausiid visual pigments: the rhodopsins of *Euphausia superba* and *Meganyctiphanes norvegica* (Crustacea, Euphausiacea). *J. gen. Physiol.* **80**, 451–472.

Denys, C. J., Adamian, M. & Brown, P. K. 1983 Ultrastructure of the eye of a euphausiid crustacean. *Tissue Cell* **15**, 77–95.

Doughtie, D. G. & Rao, K. R. 1984 Ultrastructure of the eyes of the grass shrimp, *Palaemonetes pugio*. General morphology, and light and dark adaptation at noon. *Cell Tissue Res.* **238**, 271–288.

Eguchi, E., Goto, T. & Waterman, T. H. 1982 Unorthodox pattern of microvilli and intercellular junctions in regular retinular cells of the porcellanid crab *Petrolisthes*. *Cell Tissue Res.* **222**, 493–513.

Elofsson, R. & Hallberg, E. 1973 Correlation of ultrastructure and chemical composition of crustacean chromatophore pigment. *J. ultrastruct. Res.* **44**, 421–429.

Elofsson, R. & Hallberg, E. 1977 Compound eyes of some deep-sea and fiord mysid crustaceans. *Acta Zool.* **58**, 169–177.

Exner, S. 1891 *Die Physiologie der facettirten Augen von Krebsen und Insecten*. Leipzig und Wien: Deuticke.

Fincham, A. A. 1980 Eyes and classification of malacostracan crustaceans. *Nature, Lond.* **287**, 729–731.

Fincham, A. A. 1984 Ontogeny and optics of the eyes of the common prawn *Palaemon* (*Palaemon*) *serratus* (Pennant, 1777). *Zool. J. Linnean Soc.* **81**, 89–113.

Foxton, P. 1969 The morphology of the antennal flagellum of certain of the Penaeidea (Decapoda, Natantia). *Crustaceana* **16**, 33–42.

Frixione, E., Arechiga, H. & Tsutsumi, V. 1979 Photomechanical migrations of pigment granules along the retinula cells of the crayfish. *J. Neurobiol.* **10**, 573–590.

Hallberg, E. 1977 The fine structure of the compound eyes of mysids. (Crustacea: Mysidacea). *Cell Tissue Res.* **184**, 45–66.

Hallberg, E., Nilsson, H. L. & Elofsson, R. 1980 Classification of amphipod compound eyes – the fine structure of the ommatidial units (Crustacea, Amphipoda). *Zoomorphology* **94**, 297–306.

Hanstrom, B. 1933 Neue Untersuchungen uber Sinnesorgane und Nervensystem der Crustaceen. II. *Zool. Jahrb. abt. Anat. Ontog. Tiere* **56**, 349–558.

Hanstrom, B. 1934 Neue Untersuchungen uber Sinnesorgane und Nervensystem der Crustaceen. III. *Zool. Jahrb. abt. Anat. Ontog. Tiere* **58**, 1–170.

Hiller-Adams, P. & Case, J. F. 1984 Optical parameters of euphausiid eyes as a function of habitat depth. *J. comp. Physiol.* A **154**, 307–318.

Kleinholz, L. H. 1961 Pigmentary effectors. In *The physiology of Crustacea*, vol. II (ed. T. H. Waterman), pp. 133–169. New York: Academic Press.

Krebs, W. & Lietz, R. 1982 Apical region of the crayfish retinula. *Cell Tissue Res.* **222**, 409–415.

Kunze, P. 1969 Eye glow in the moth and superposition theory. *Nature, Lond.* **223**, 1172–1174.

Land, M. F. 1976 Superposition images are formed by reflection in the eyes of some oceanic decapod Crustacea. *Nature, Lond.* **263**, 764–765.

Land, M. F. 1980 Eye movements and the mechanism of vertical steering in euphausiid Crustacea. *J. comp. Physiol.* A **137**, 255–265.

Land, M. F. 1981 Optics and vision in invertebrates. In *Handbook of sensory physiology*, vol. VII/6B (ed. H. Autrum), pp. 471–592. Berlin: Springer.

Land, M. F., Burton, F. A. & Meyer-Rochow, V. B. 1979 The optical geometry of euphausiid eyes. *J. comp. Physiol.* **130**, 49–62.

Le Reste, L. 1970 Biologie de *Acetes erythraeus* (Sergestidae) dans une baie du N.W. de Madagascar (Baie d' Ambaro). *Cah. O.R.S.T.O.M. Ser. Ocean.* **8**, 35–56.

Meyer-Rochow, V. B. 1978 The eyes of mesopelagic crustaceans. II. *Streetsia challengeri* (Amphipoda). *Cell Tissue Res.* **186**, 337–346.

Meyer-Rochow, V. B. & Walsh, S. 1977 The eyes of mesopelagic crustaceans. I. *Gennadas* sp. (Penaeidae). *Cell Tissue Res.* **184**, 87–101.

Meyer-Rochow, V. B. & Walsh, S. 1978 The eyes of mesopelagic crustaceans. III. *Thysanopoda tricuspidata* (Euphausiacea). *Cell Tissue Res.* **195**, 59–79.

Nassel, D. R. 1976 The retina and retinal projection on the lamina ganglionaris of the crayfish *Pacifastacus leniusculus* Dana. *J. comp. Neurol.* **167**, 341–360.

Nassel, D. R. & Waterman, T. H. 1979 Massive diurnally modulated photoreceptor membrane turnover in crab light–dark adaptation. *J. comp. Physiol.* **131**, 205–216.

Nilsson, D.-E. 1982 The transparent compound eye of *Hyperia* (Crustacea): Examination with a new method for analysis of refractive index gradients. *J. comp. Physiol.* **147**, 339–349.

Nilsson, D.-E. 1983*a* Evolutionary links between apposition and superposition optics in crustacean eyes. *Nature, Lond.* **302**, 818–821.

Nilsson, D.-E. 1983*b* Refractive index gradients subserve optical isolation in a light-adapted reflecting superposition eye. *J. exp. Zool.* **225**, 161–165.

Omori, M. 1974 The biology of pelagic shrimps in the ocean. *Adv. mar. Biol.* **12**, 233–324.

Omori, M. 1975 The systematics, biogeography, and fishery of epipelagic shrimps of the genus *Acetes* (Crustacea, Decapoda, Sergestidae). *Bull. Ocean Res. Ins.*, University of Tokyo, no. 7, pp. 1–91.

Parker, G. H. 1932 The movements of the retinal pigment. *Ergeb. Biol.* **9**, 239–291.

Ramadan, M. M. 1952 Contribution to our knowledge of the structure of the compound eyes of Decapoda Crustacea. *Lunds Univ. Arsskrift* N.F. **48**, 1–20.

Ribi, W. A. 1976 The first optic ganglion of the bee. II. Topographical relationships of the monopolar cells within and between cartridges. *Cell Tissue Res.* **171**, 359–373.

Stowe, S. 1977 The retina-lamina projection in the crab *Leptograpsus variegatus*. *Cell Tissue Res.* **185**, 515–525.

Stowe, S. 1980 Rapid synthesis of photoreceptor membrane and assembly of new microvilli in a crab at dusk. *Cell Tissue Res.* **211**, 419–440.

Struwe, G., Hallberg, E. & Elofsson, R. 1975 The physical and morphological properties of the pigment screen in the compound eye of a shrimp (Crustacea). *J. comp. Physiol.* **97**, 257–270.

Vogt, K. 1975 Zur Optik des Flusskrebsauges. *Z. Naturforsch.* **30**c, 691.

Vogt, K. 1980 Die Spiegeloptik des Flusskrebsauges. *J. comp. Physiol.* **135**, 1–19.

Welsh, J. H. 1930 The mechanics of migration of the distal pigment cells in the eyes of *Palaemonetes*. *J. exp. Zool.* **56**, 459–494.

Welsh, J. H. & Chace, F. A. Jr 1938 Eyes of deep-sea crustaceans. II. Sergestidae. *Biol. Bull.* **74**, 364–375.

Zyznar, E. S. 1970 The eyes of white shrimp, *Penaeus setiferus* (Linnaeus) with a note on the rock shrimp, *Sicyonia brevirostris* Stimpson. Contributions in Marine Science, University of Texas. **15**, 87–102.

Zyznar, E. S. & Nicol, J. A. C. 1971 Ocular reflecting pigments of some Malacostraca. *J. exp. mar. Biol. Ecol.* **6**, 235–248.

1

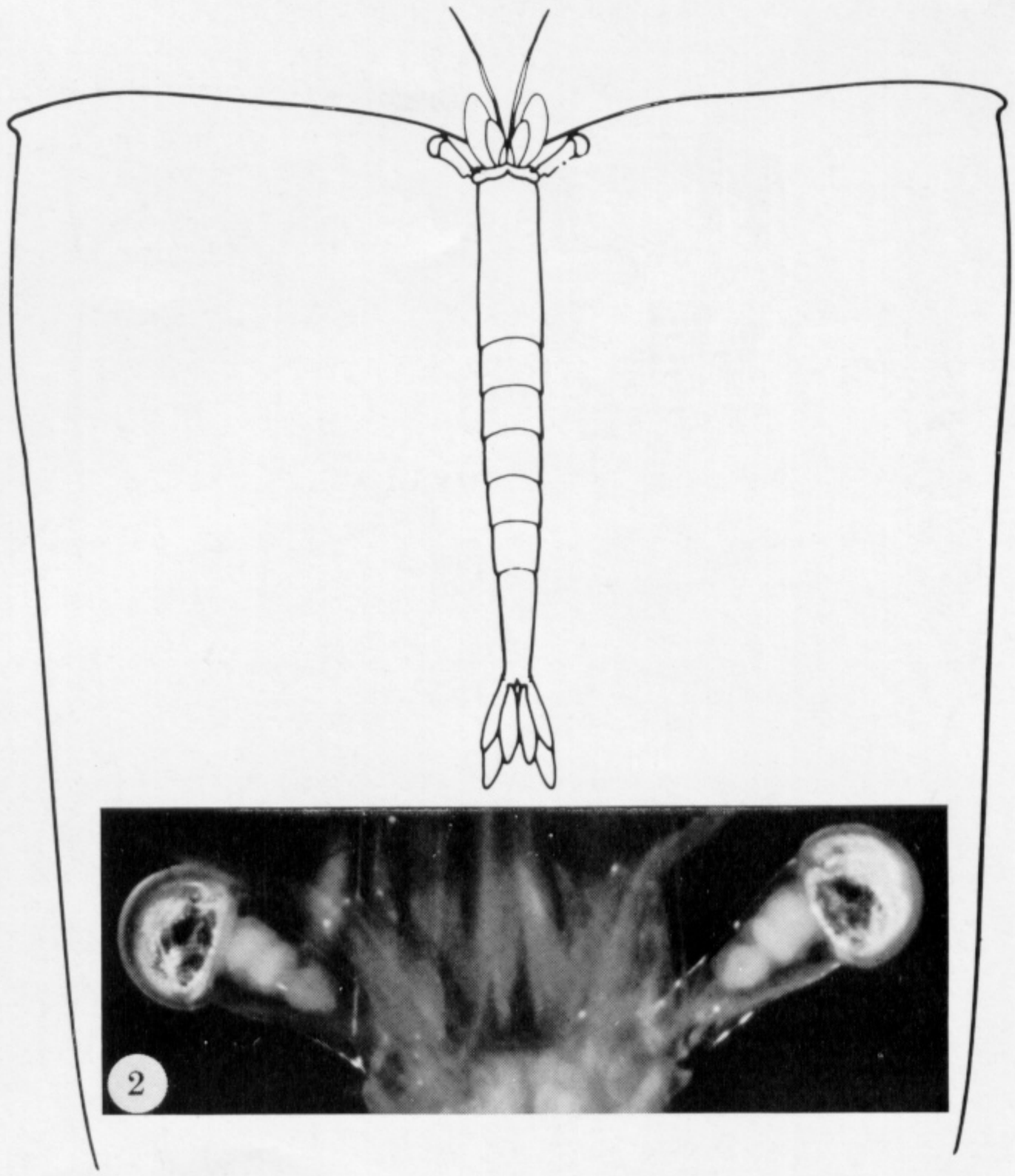

2

3

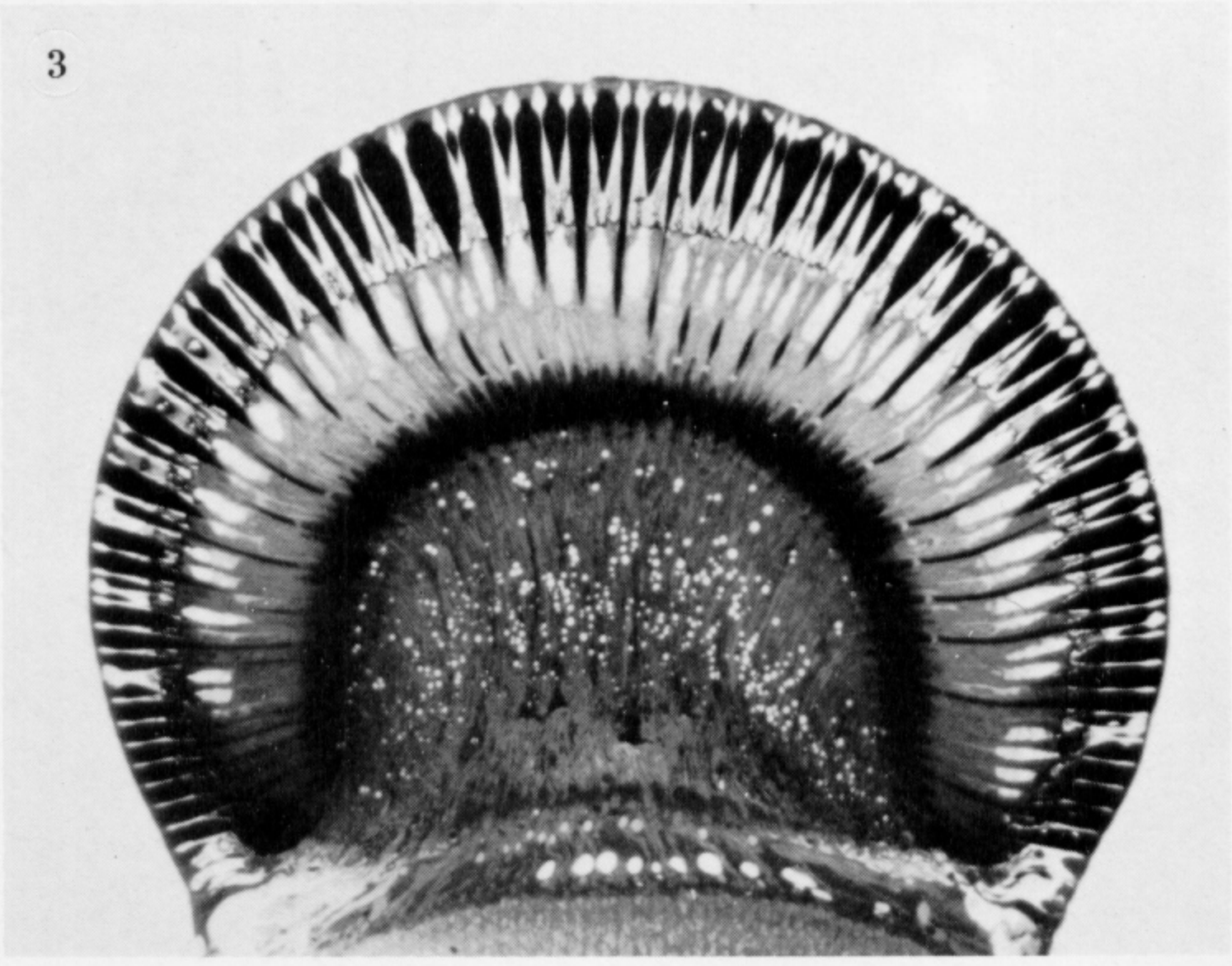

PLATE 1. *Acetes* and the gross morphology of its visual system.

FIGURE 1. Schematic drawing of a swimming *Acetes* with the long antennae trailing back parallel to the body from the elbow. Magn. × 2.5.

FIGURE 2. The stalked eyes of *Acetes* as seen in the living animal. The optic ganglia are visible through each of the transparent eyestalks. Scale bar 500 μm.

FIGURE 3. Section through the eye of *Acetes* to show its overall organization. The eye is nearly spherical and has an obvious clear zone. Scale bar 100 μm.

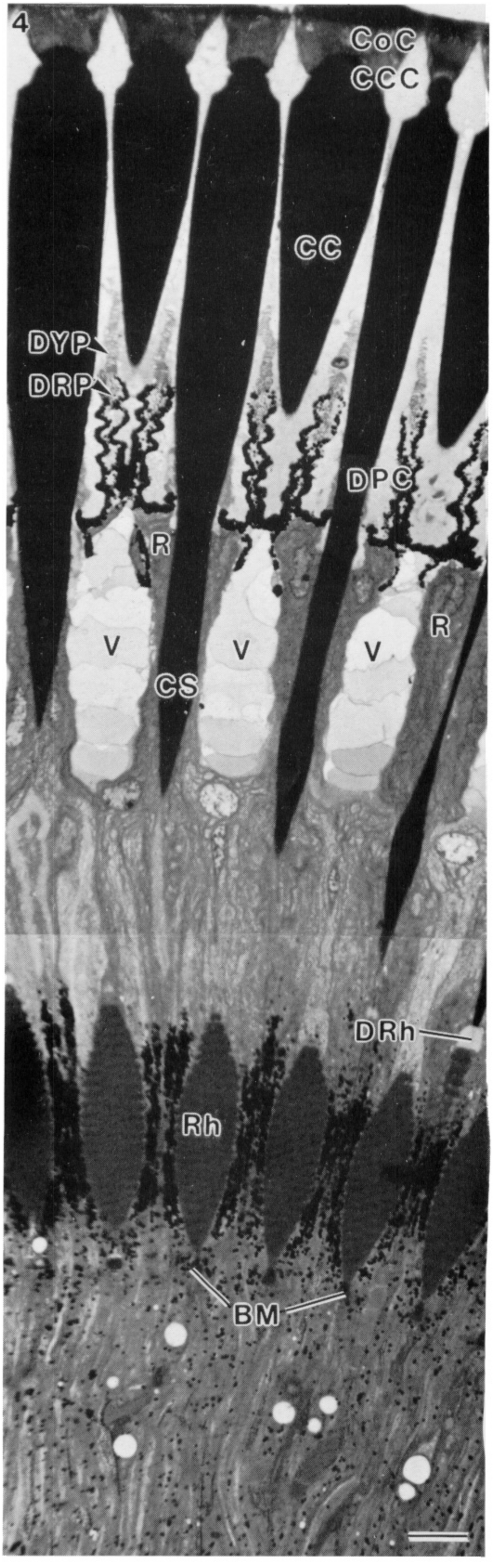

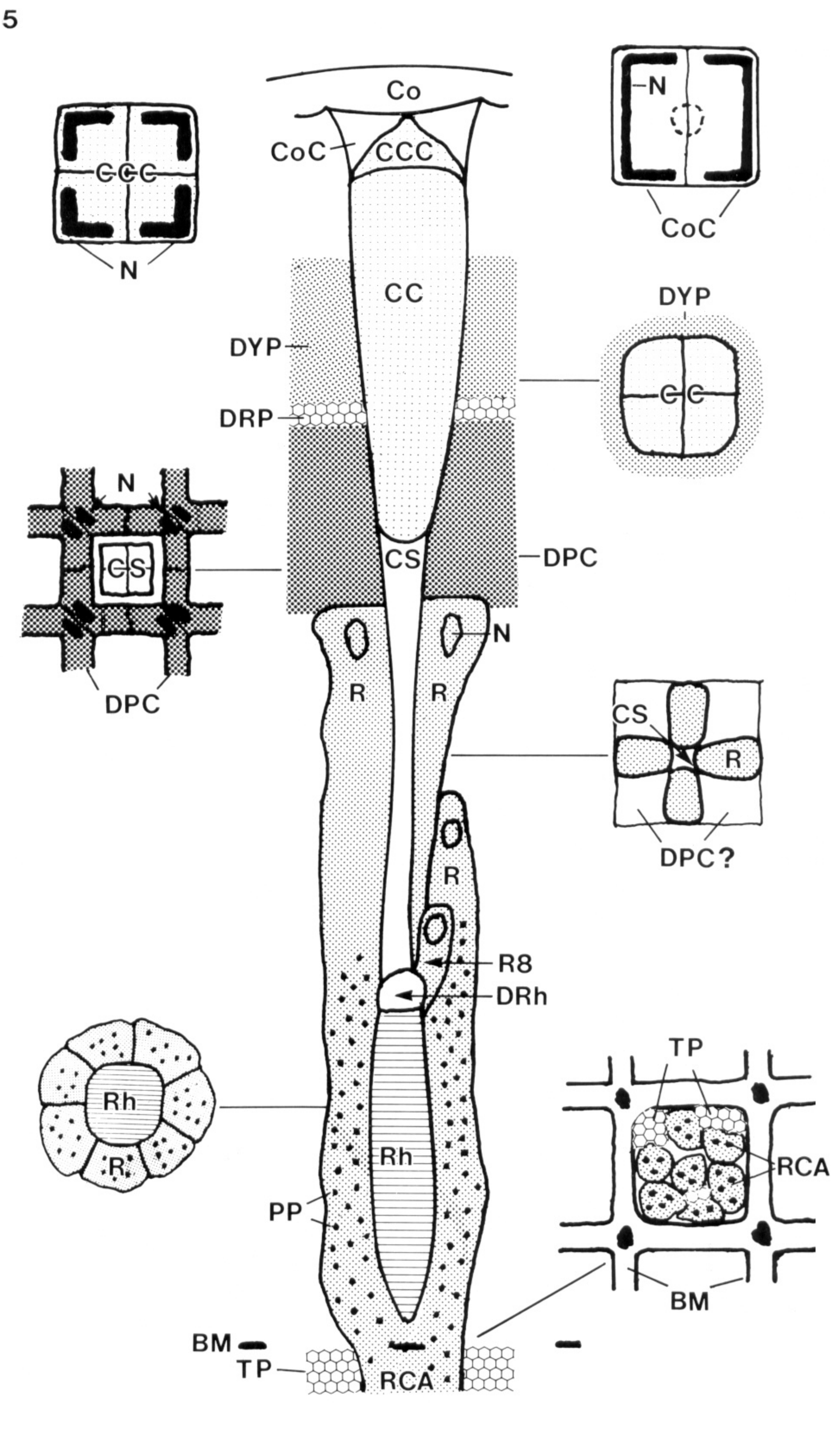

FIGURES 4 AND 5. For description see p. 254.

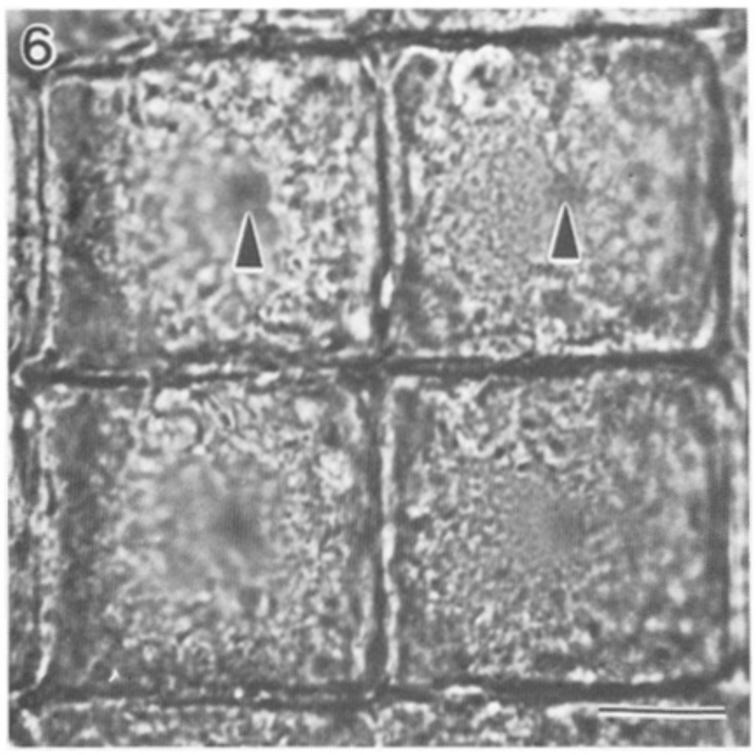

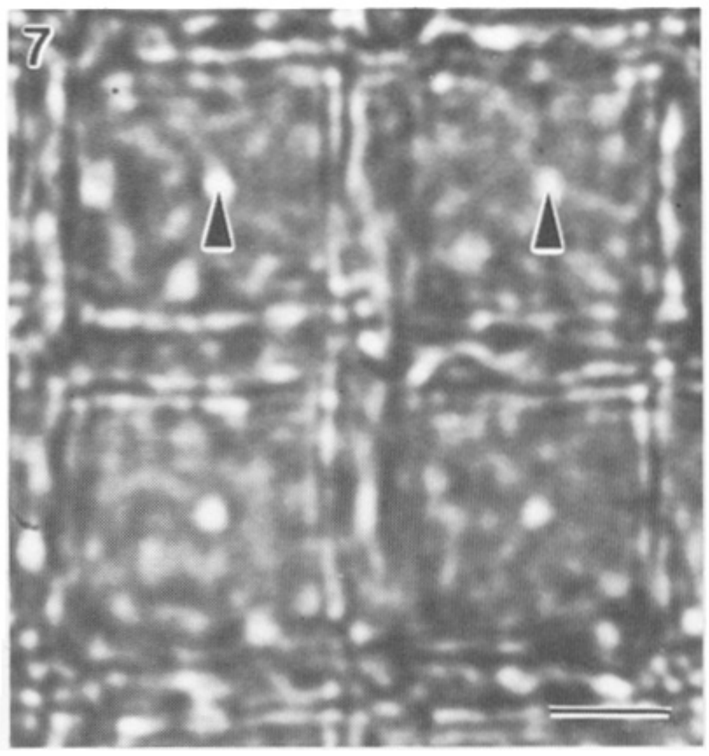

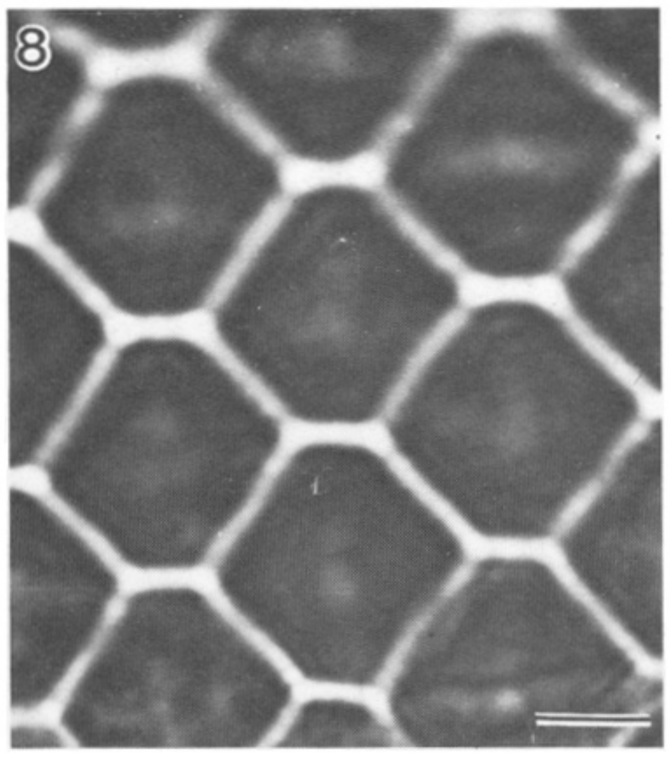

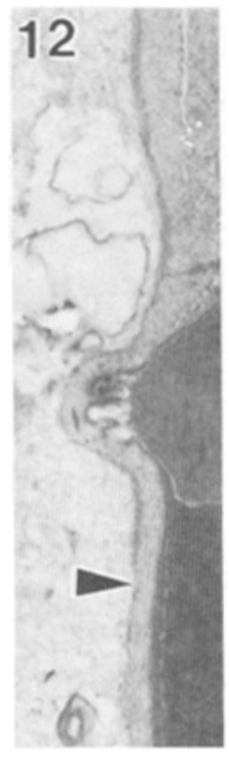

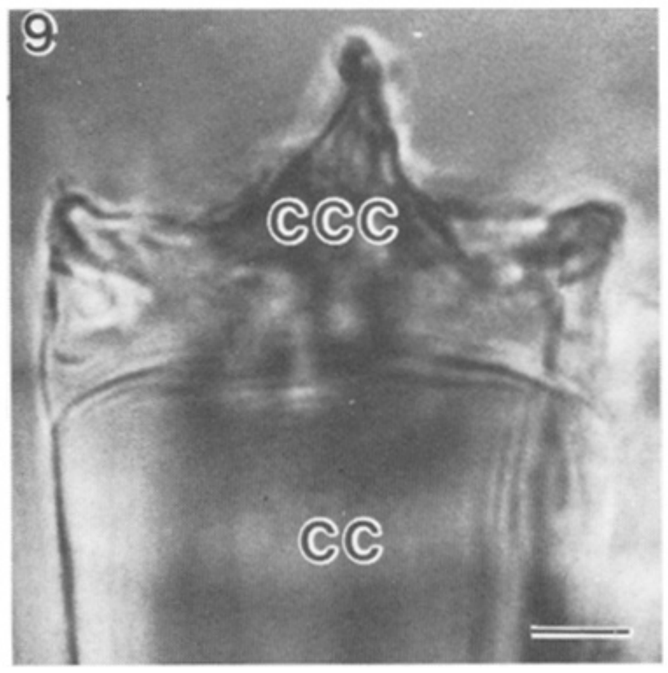

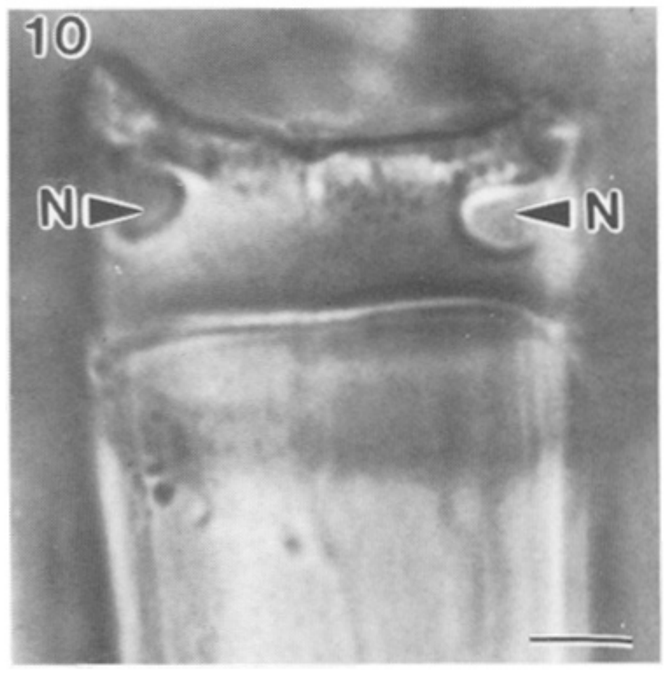

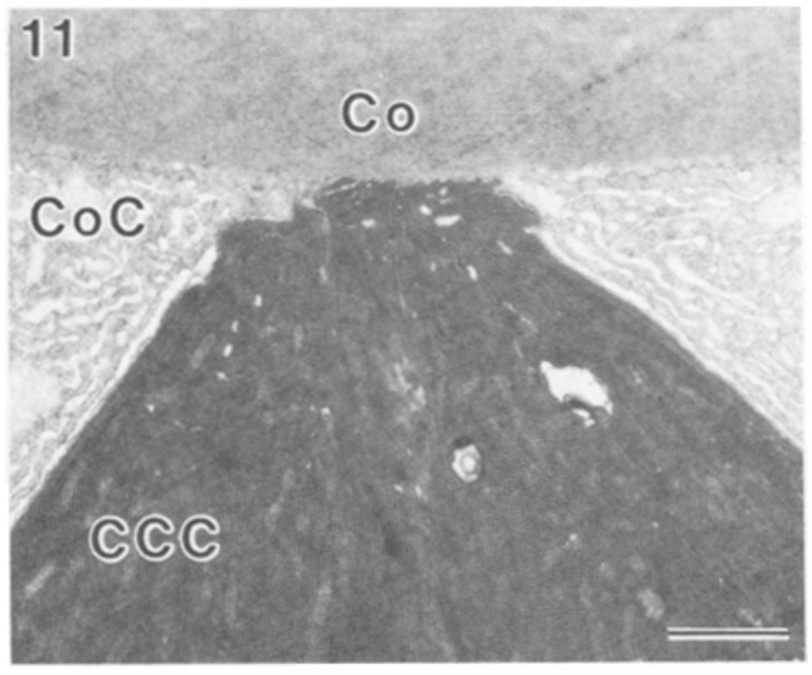

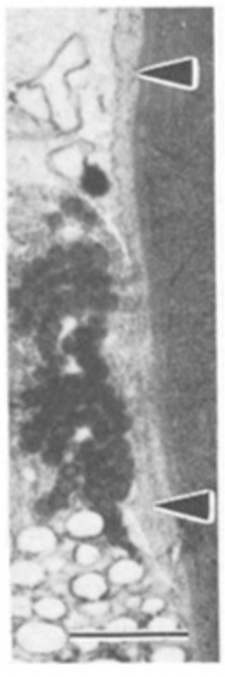

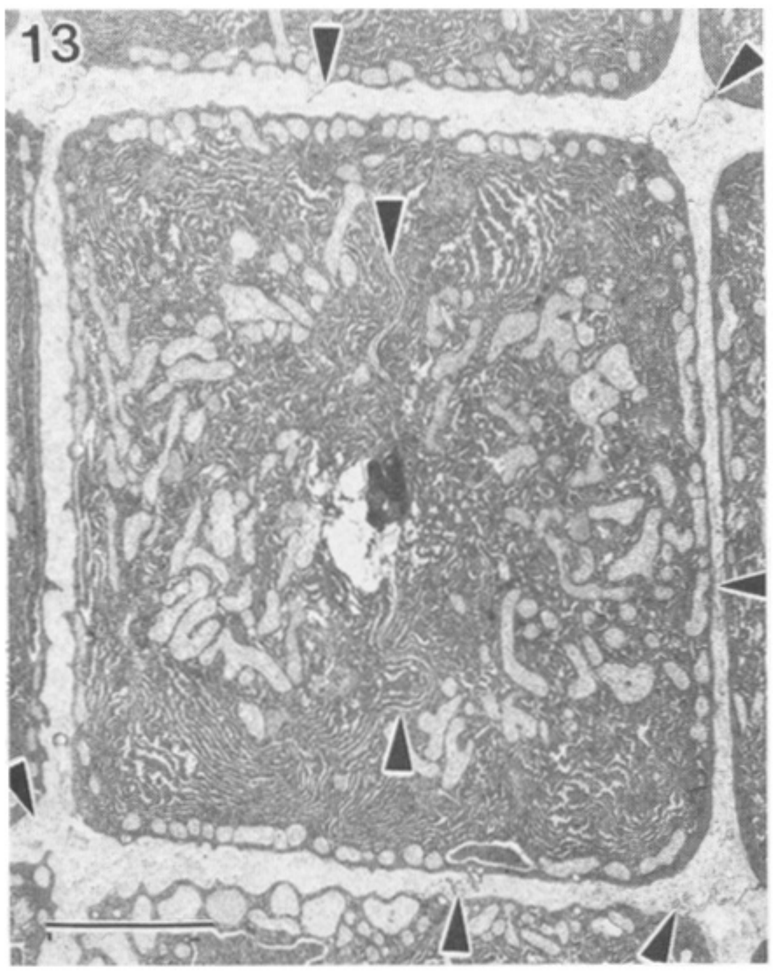

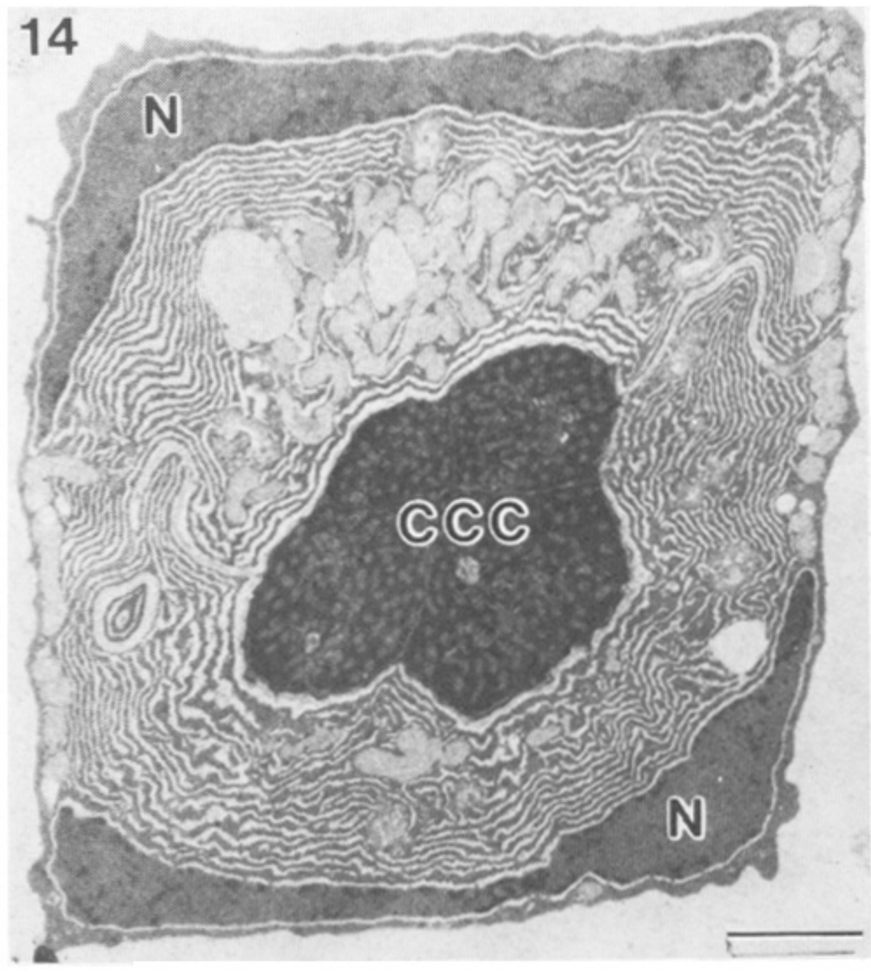

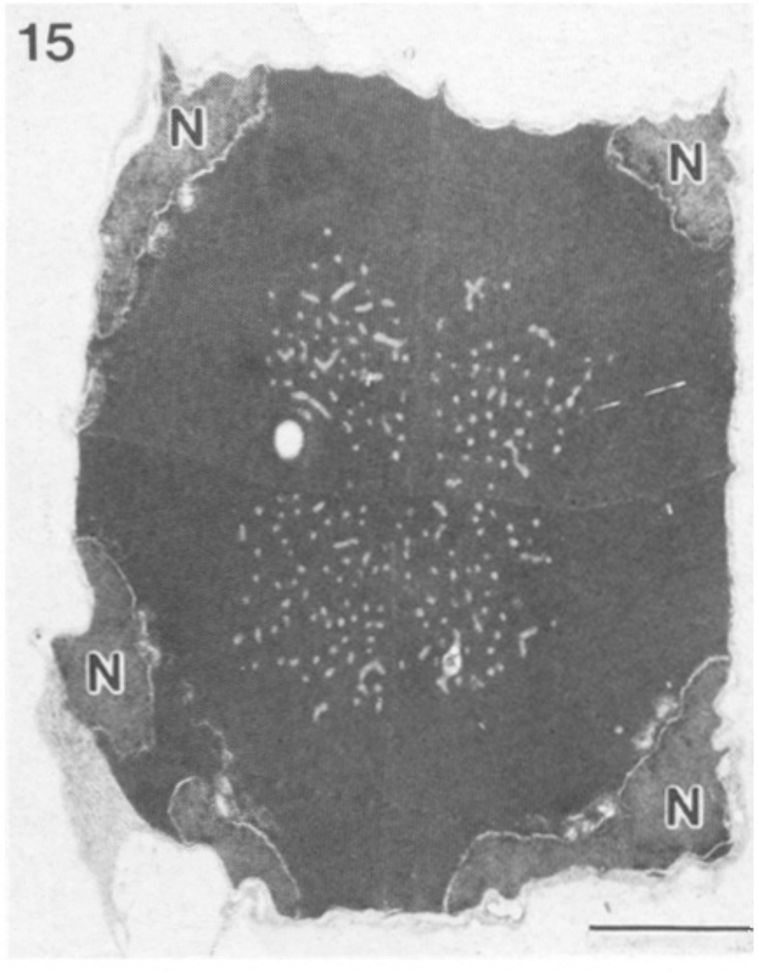

FIGURES 6–18. For description see p. 255.

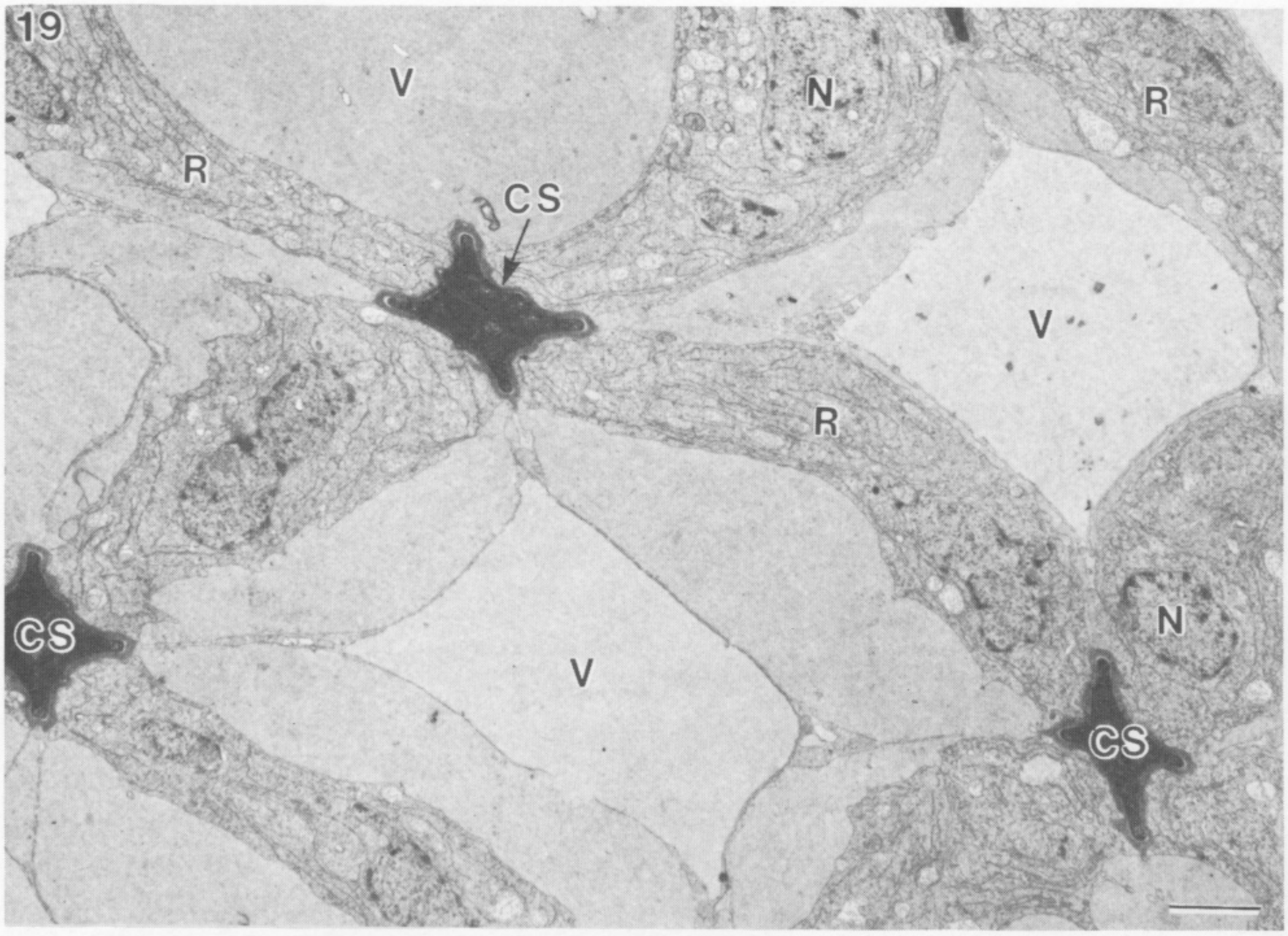

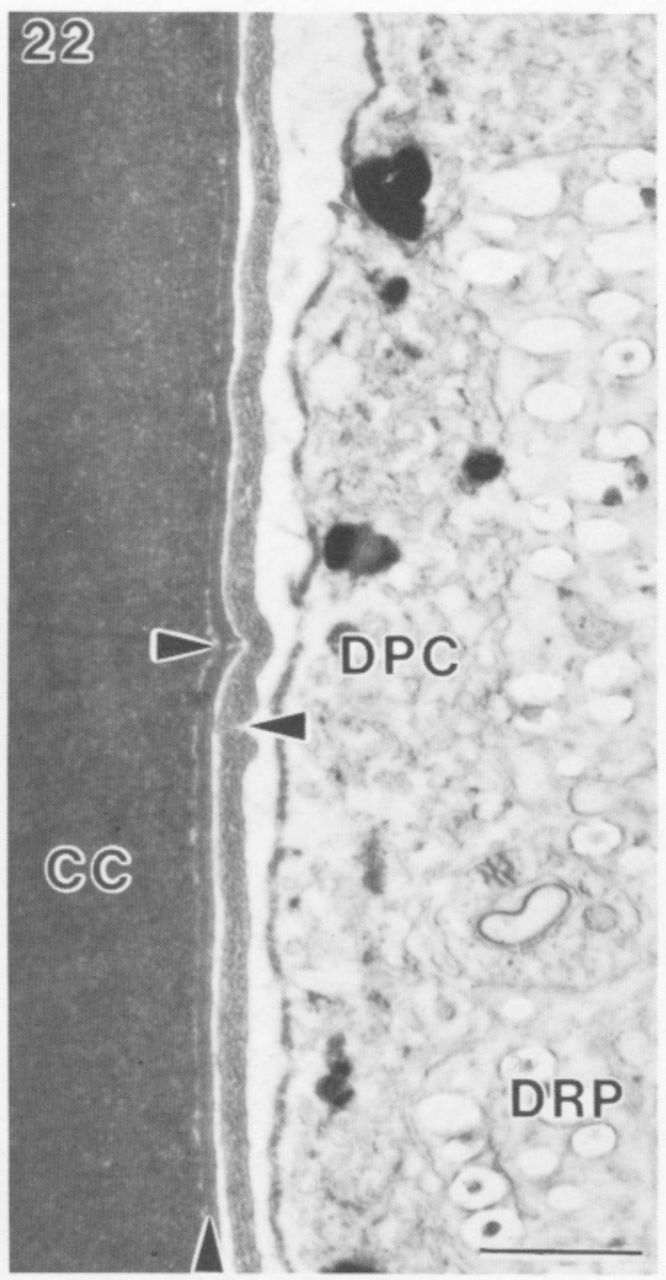

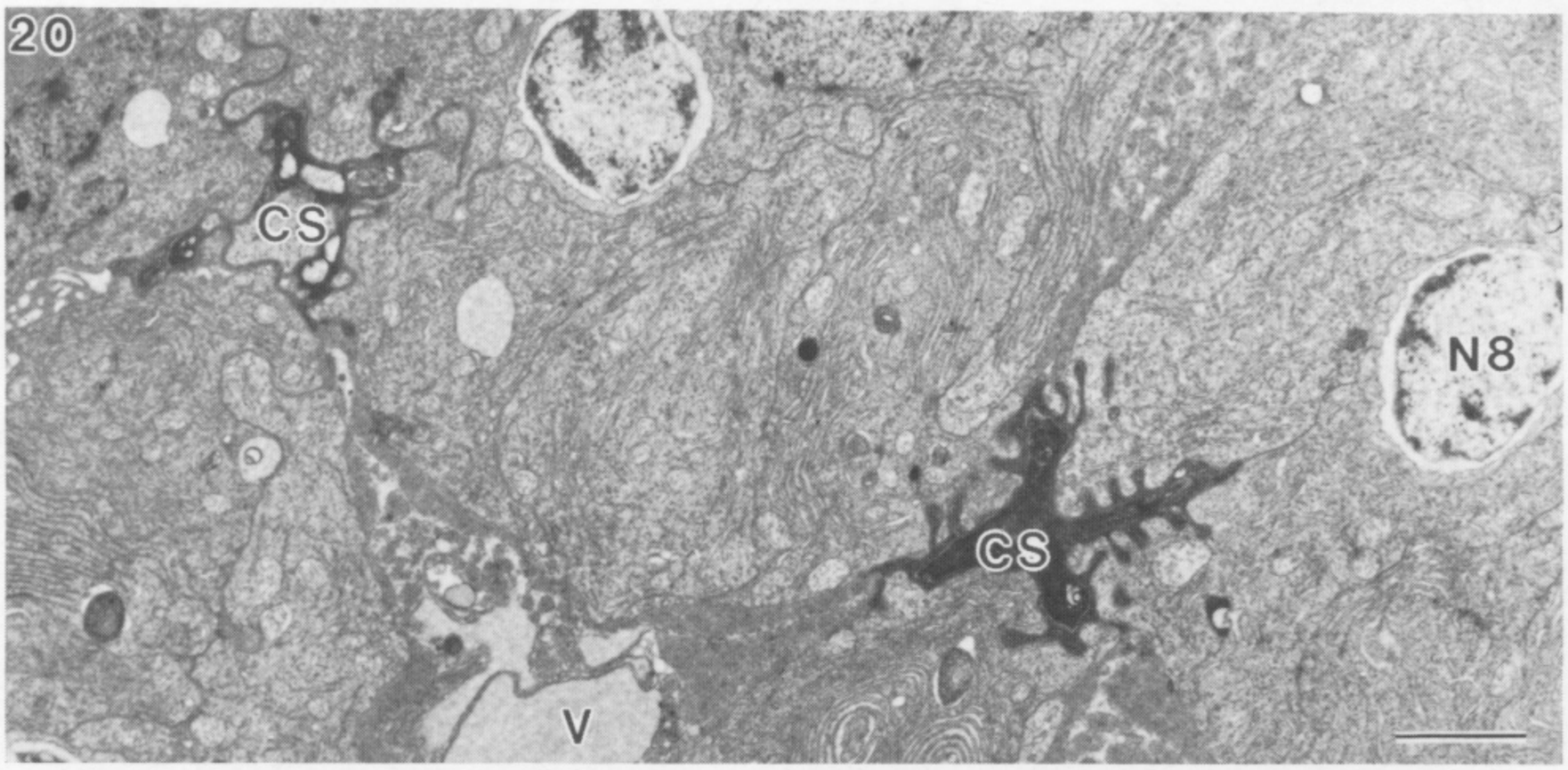

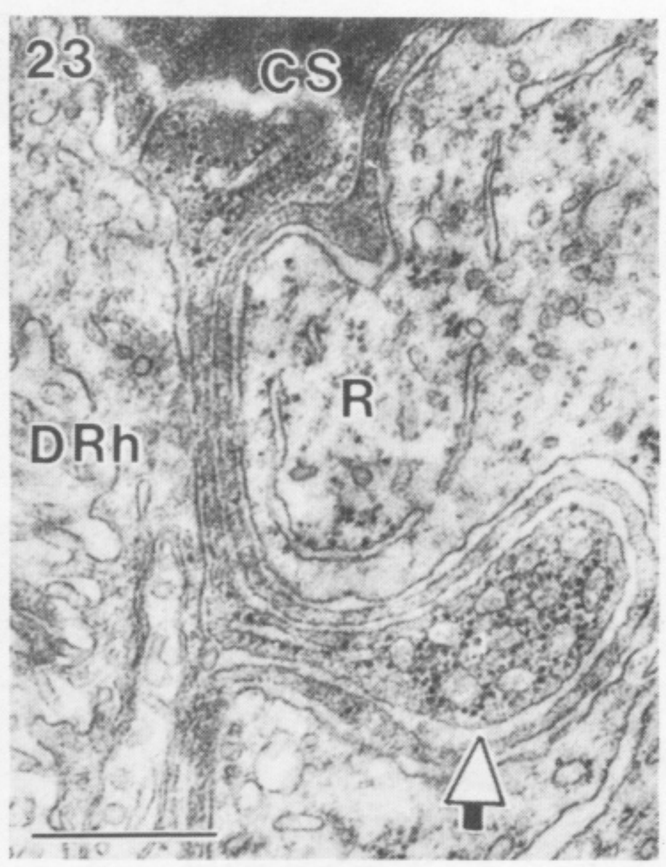

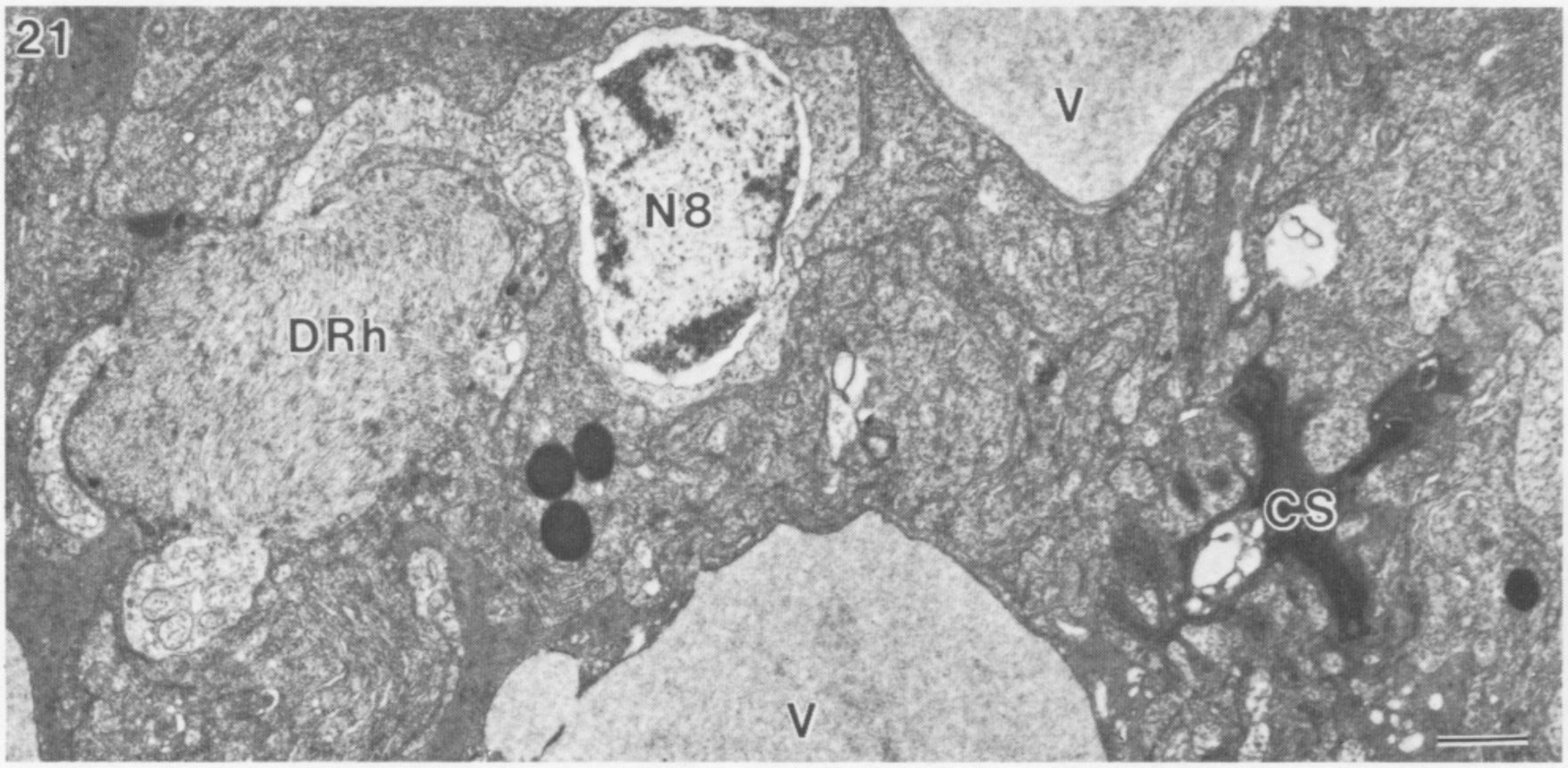

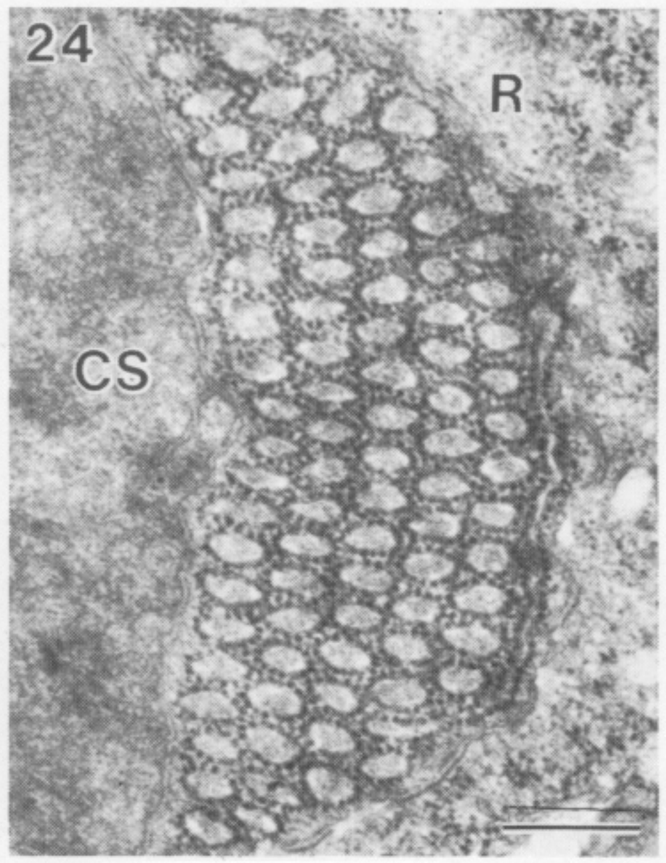

FIGURES 19–24. For description see opposite.

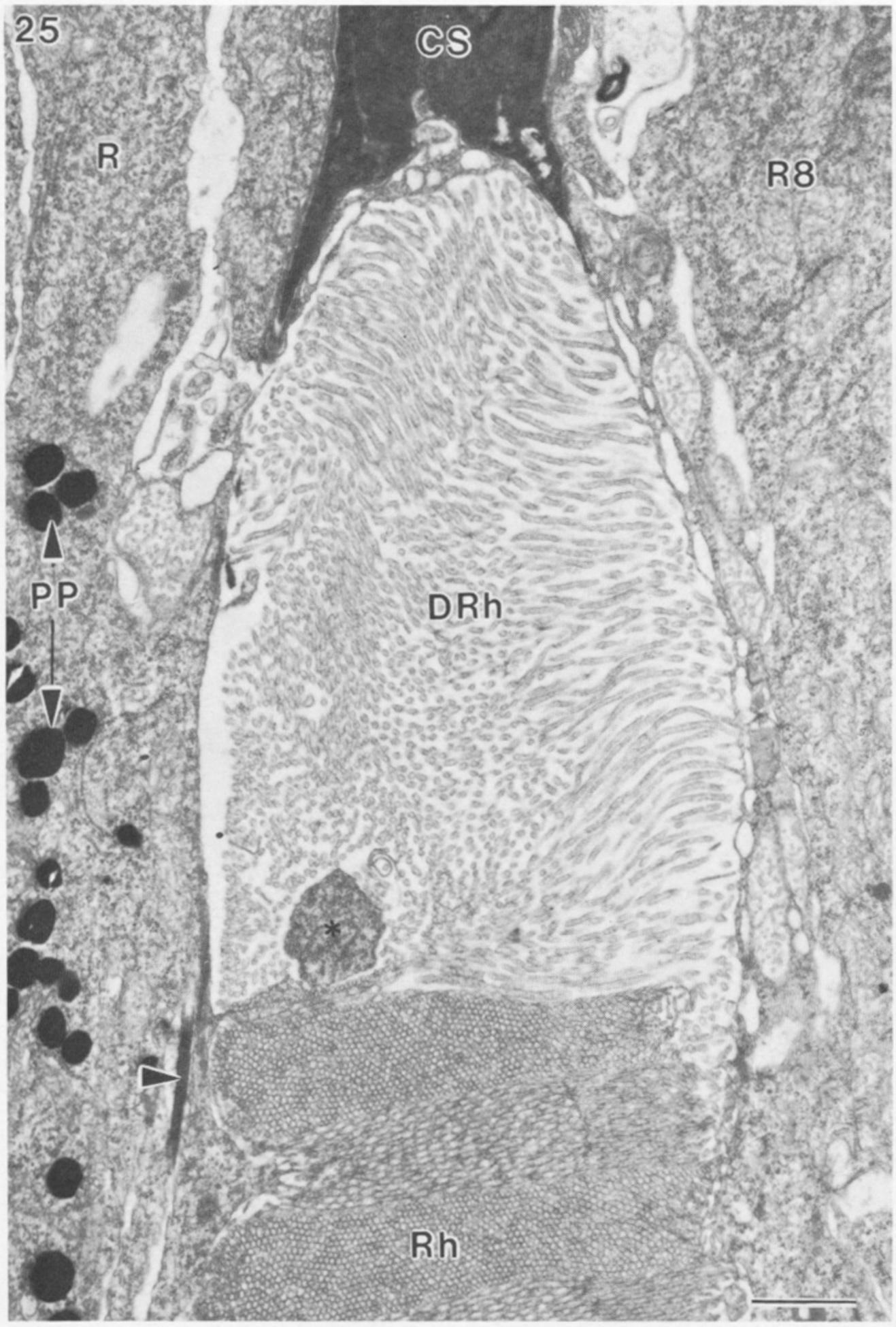

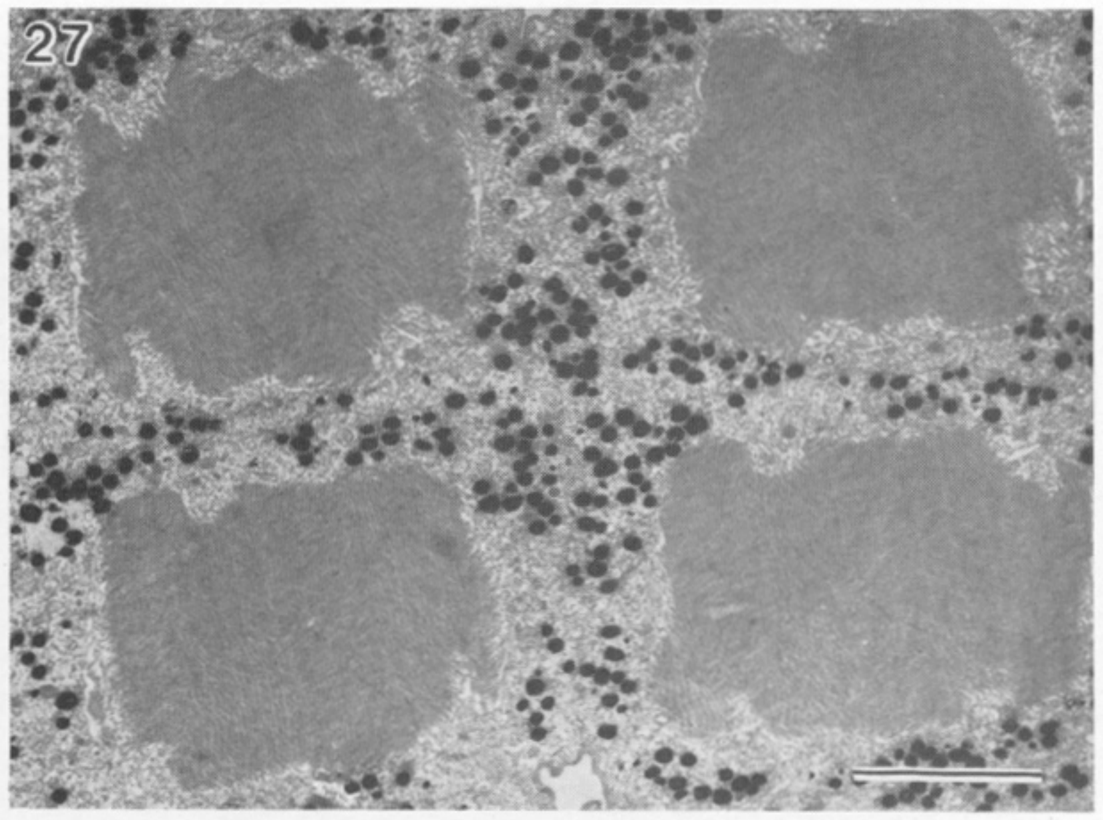

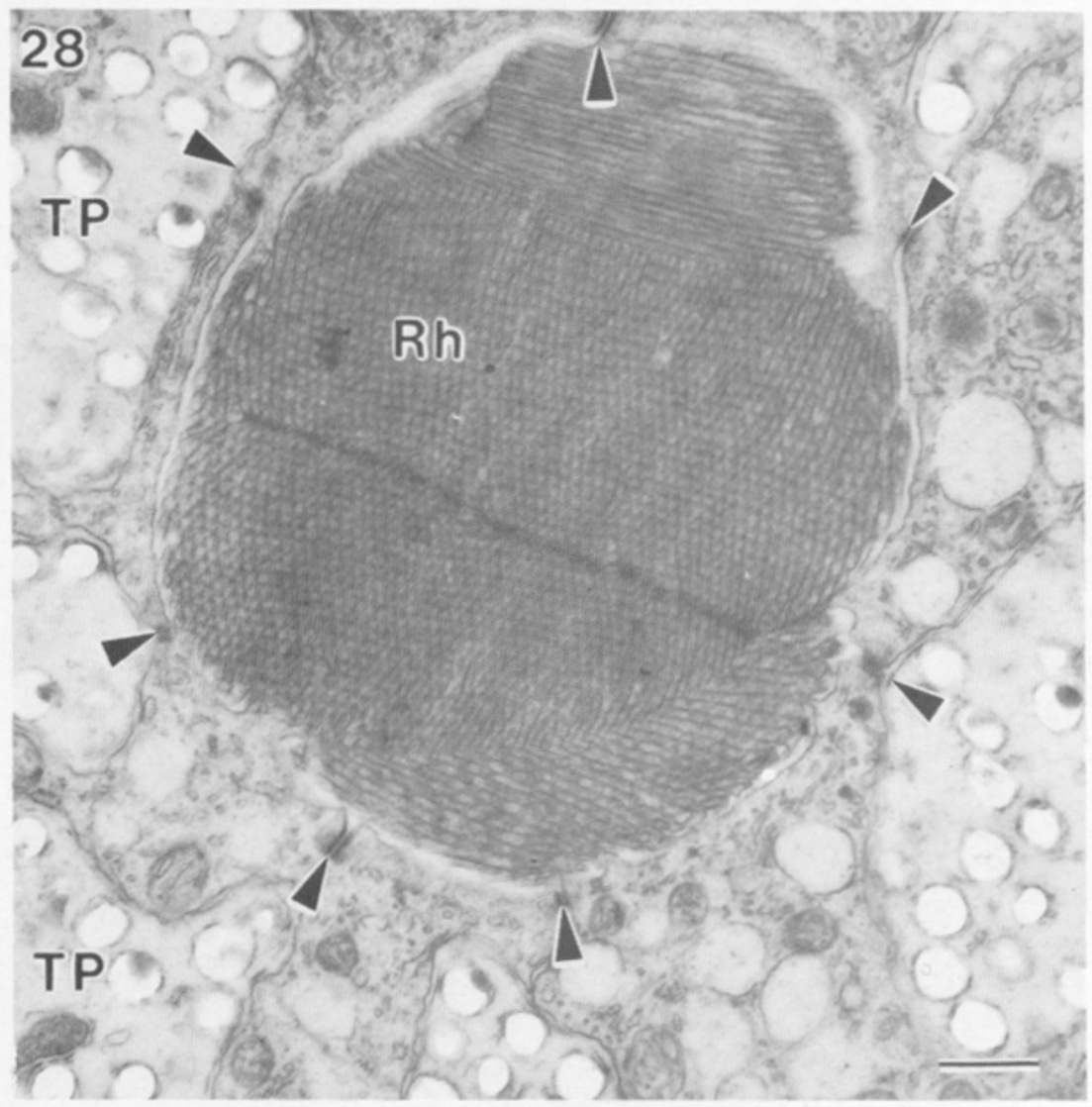

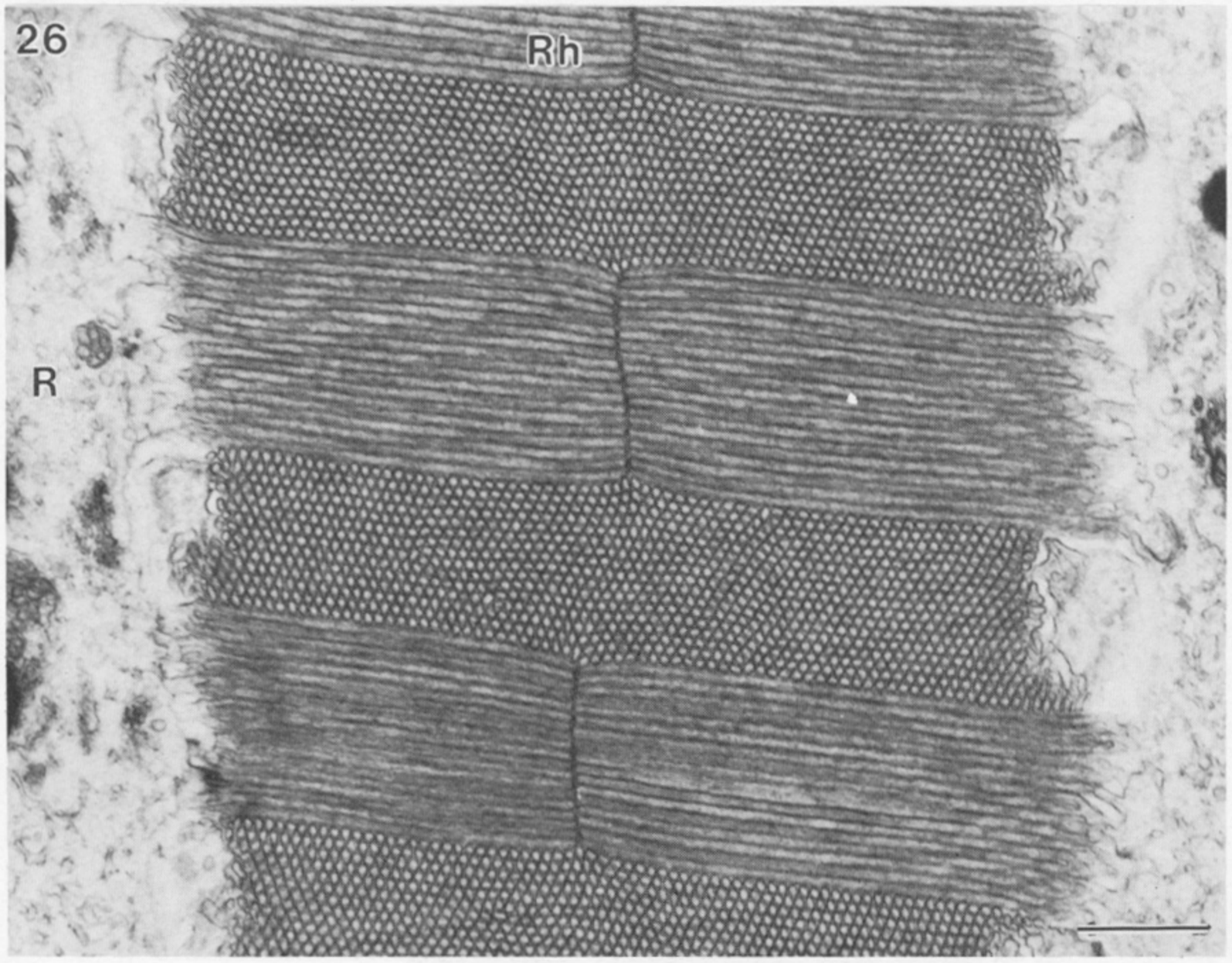

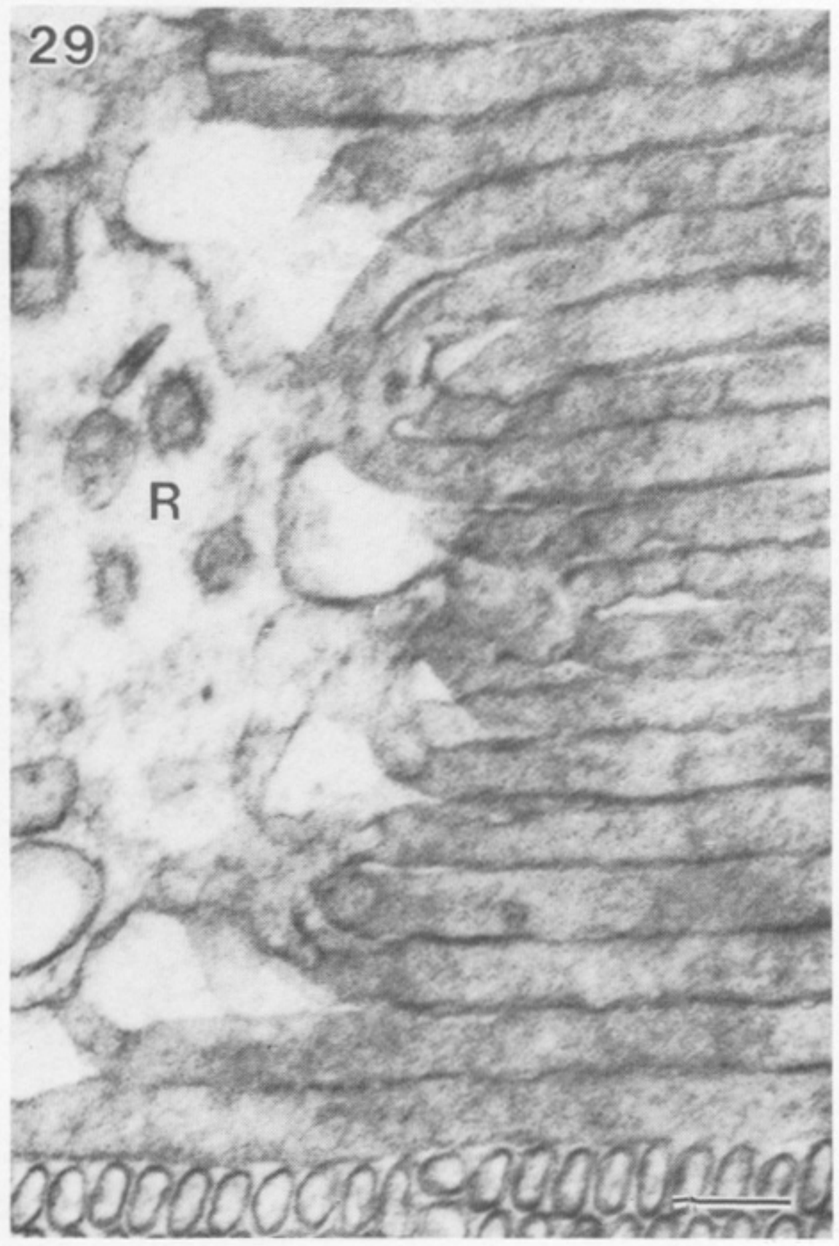

FIGURES 25–29. For description see opposite.

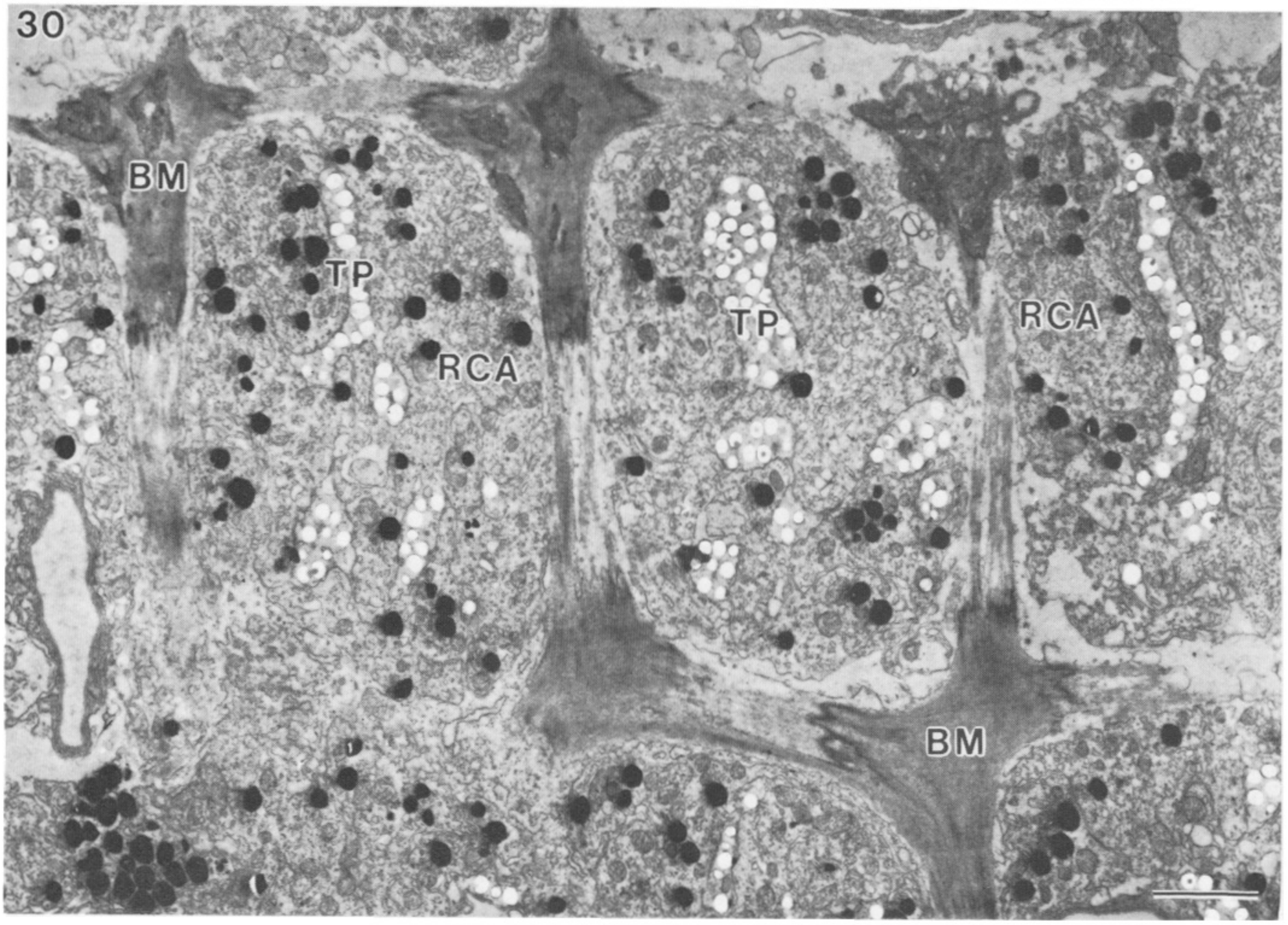

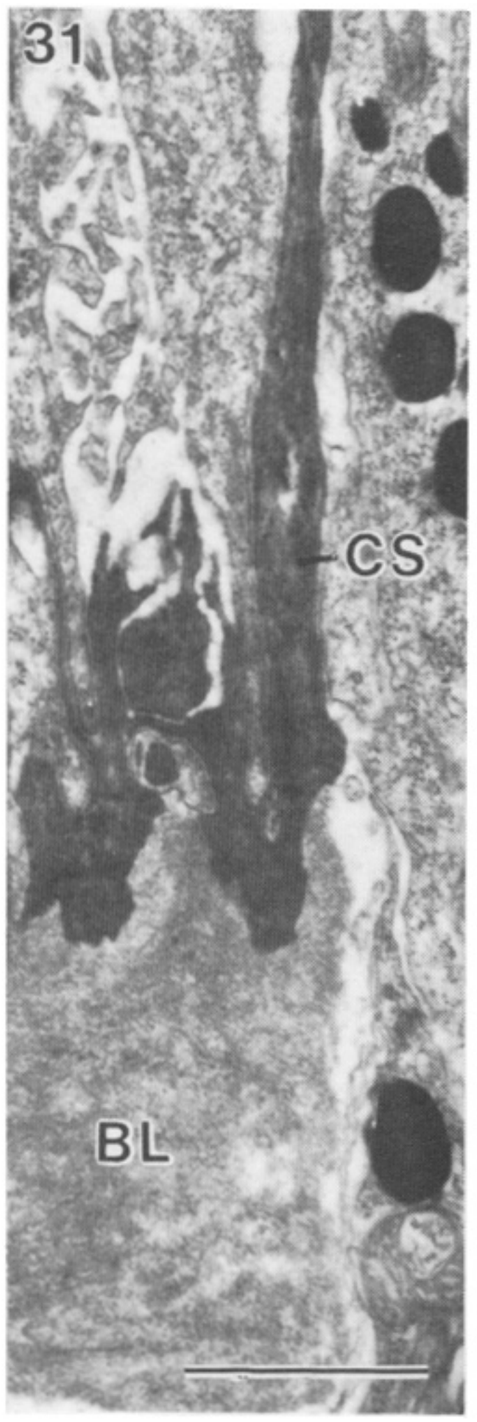

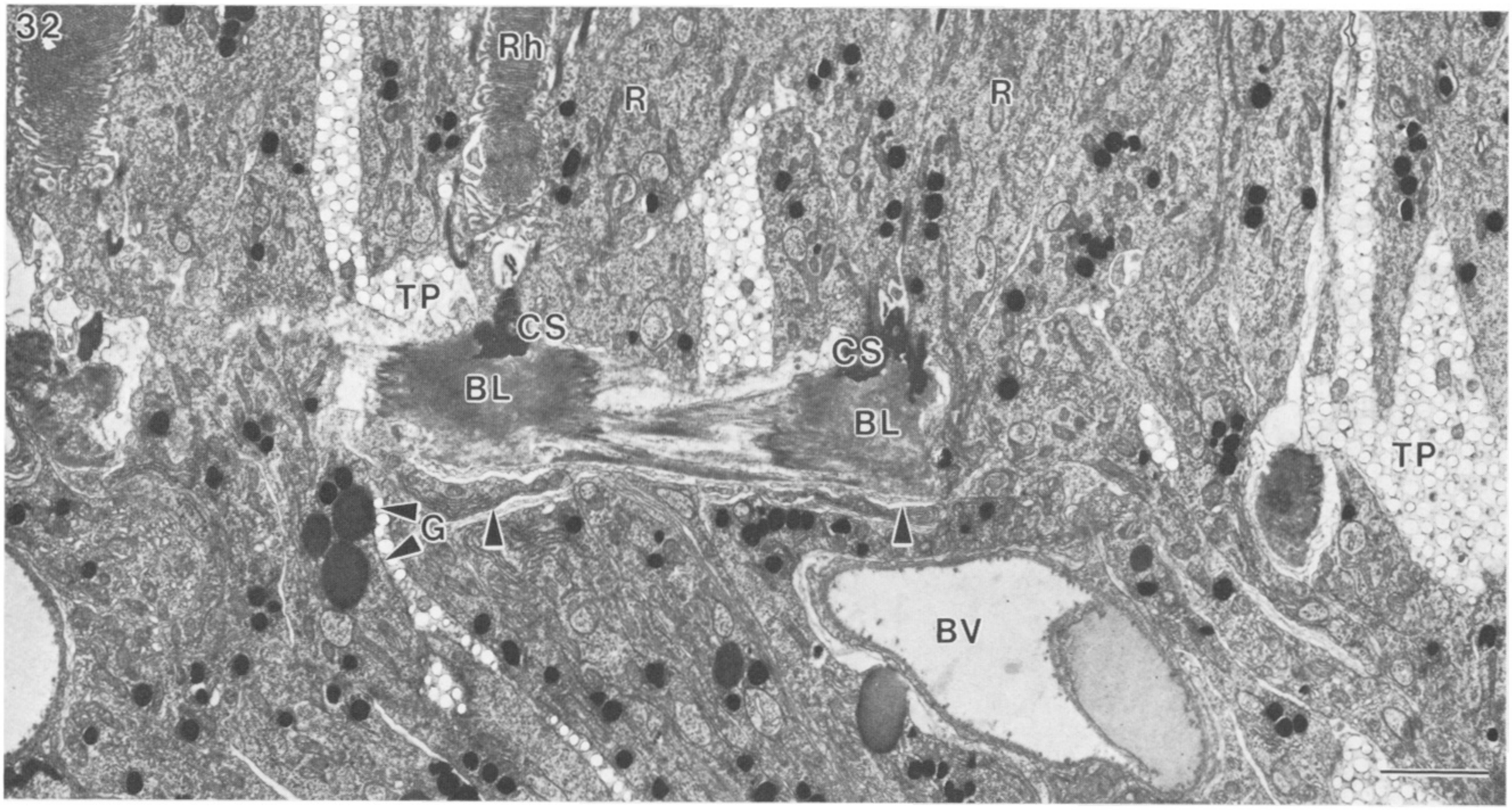

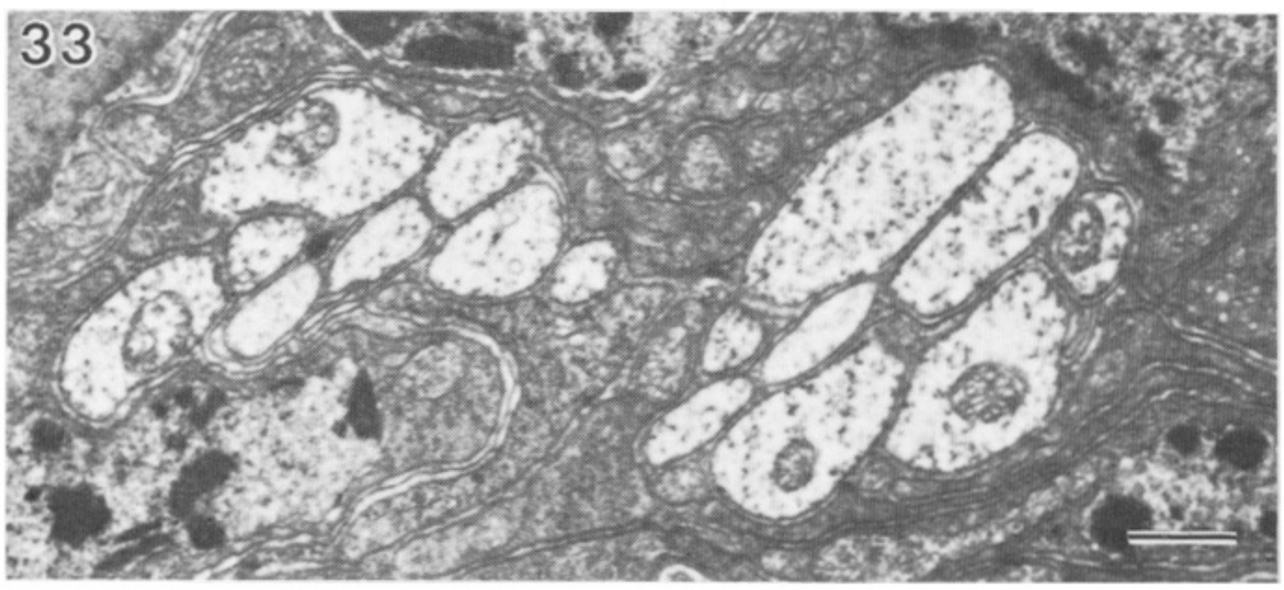

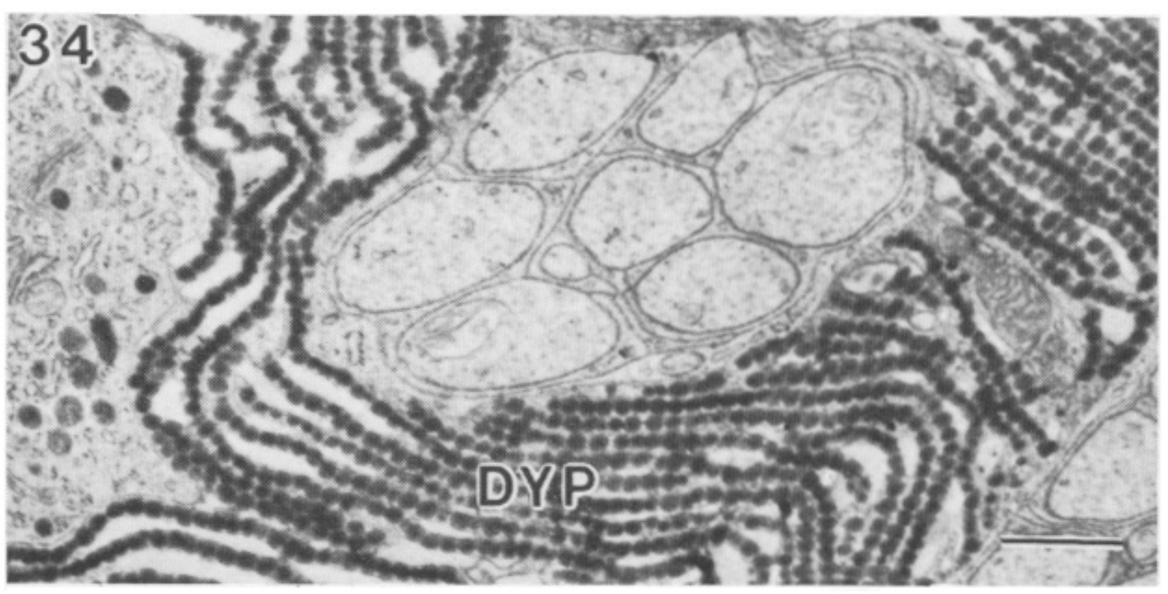

FIGURES 30–34. For description see p. 258.

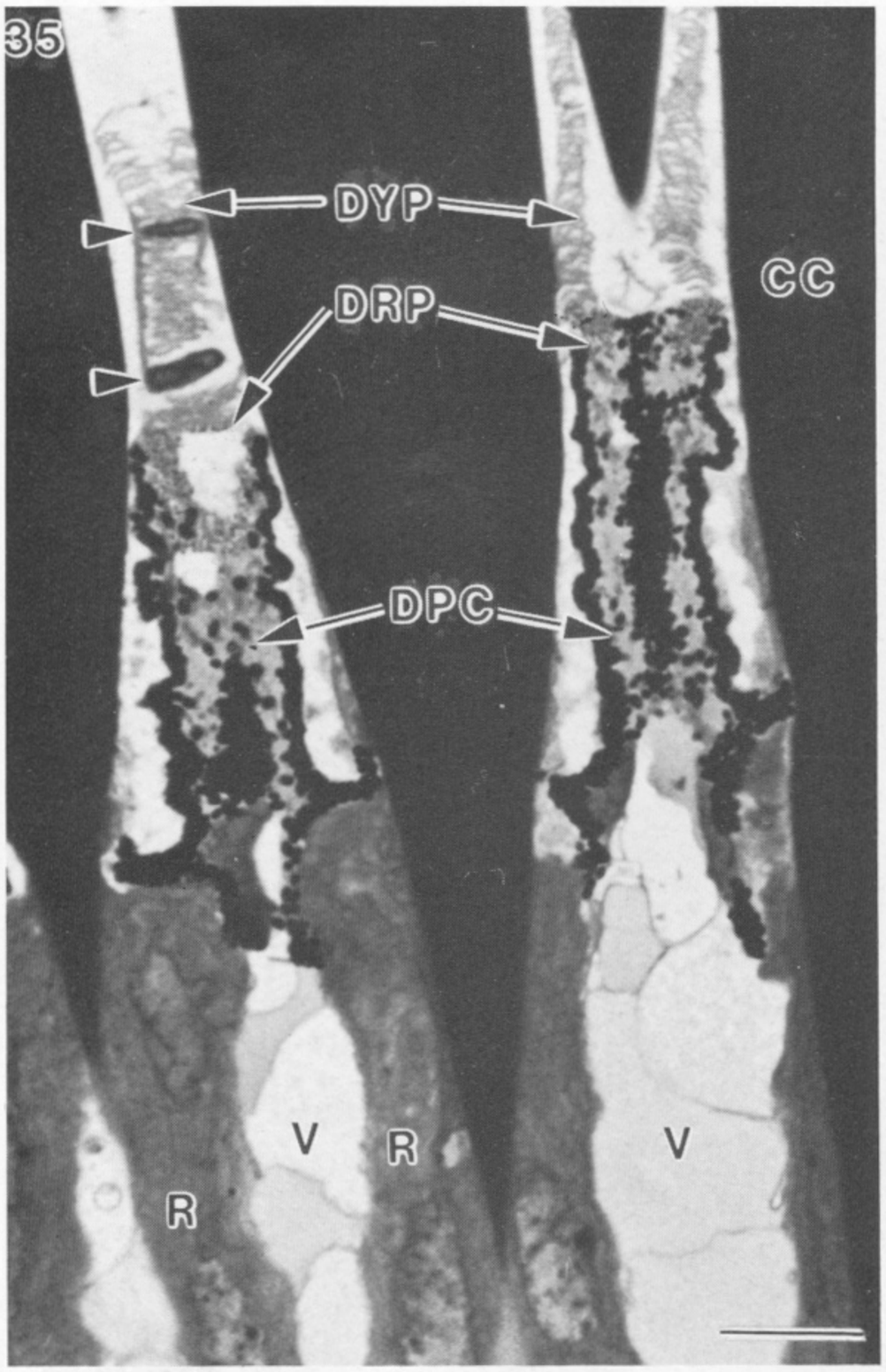

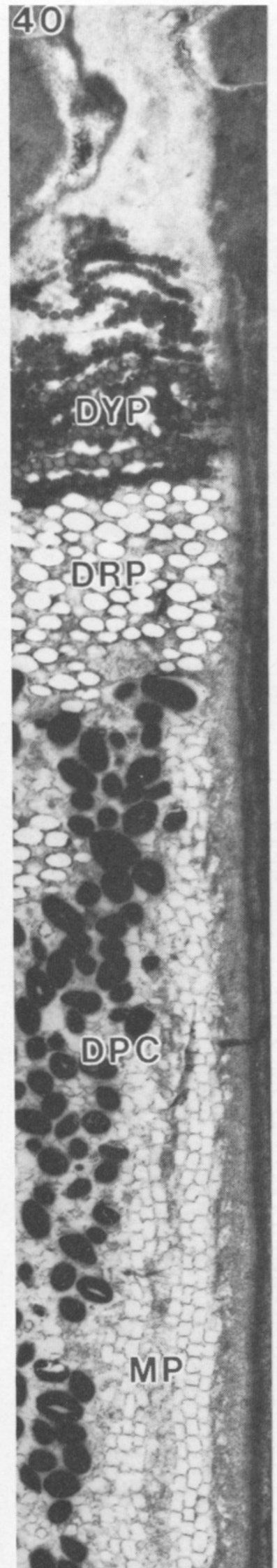

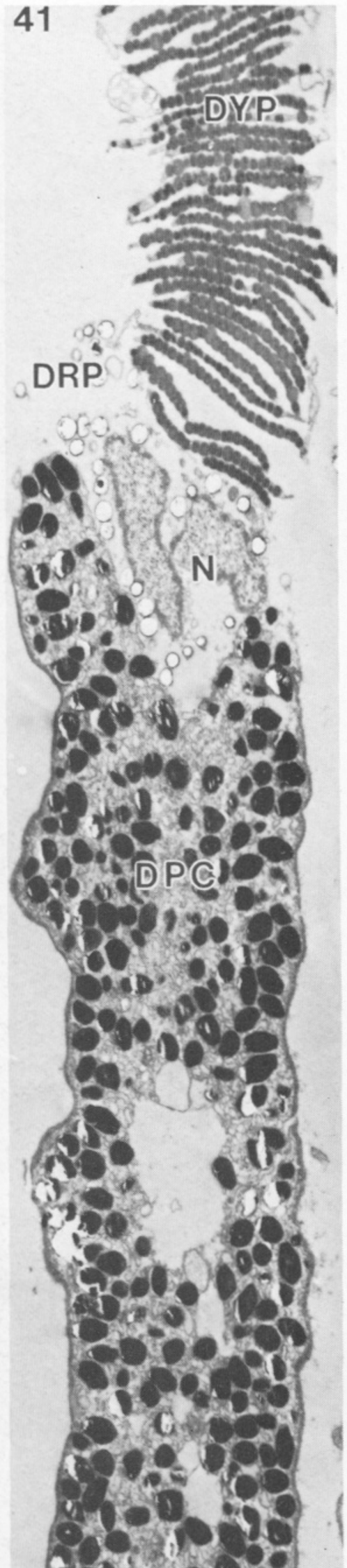

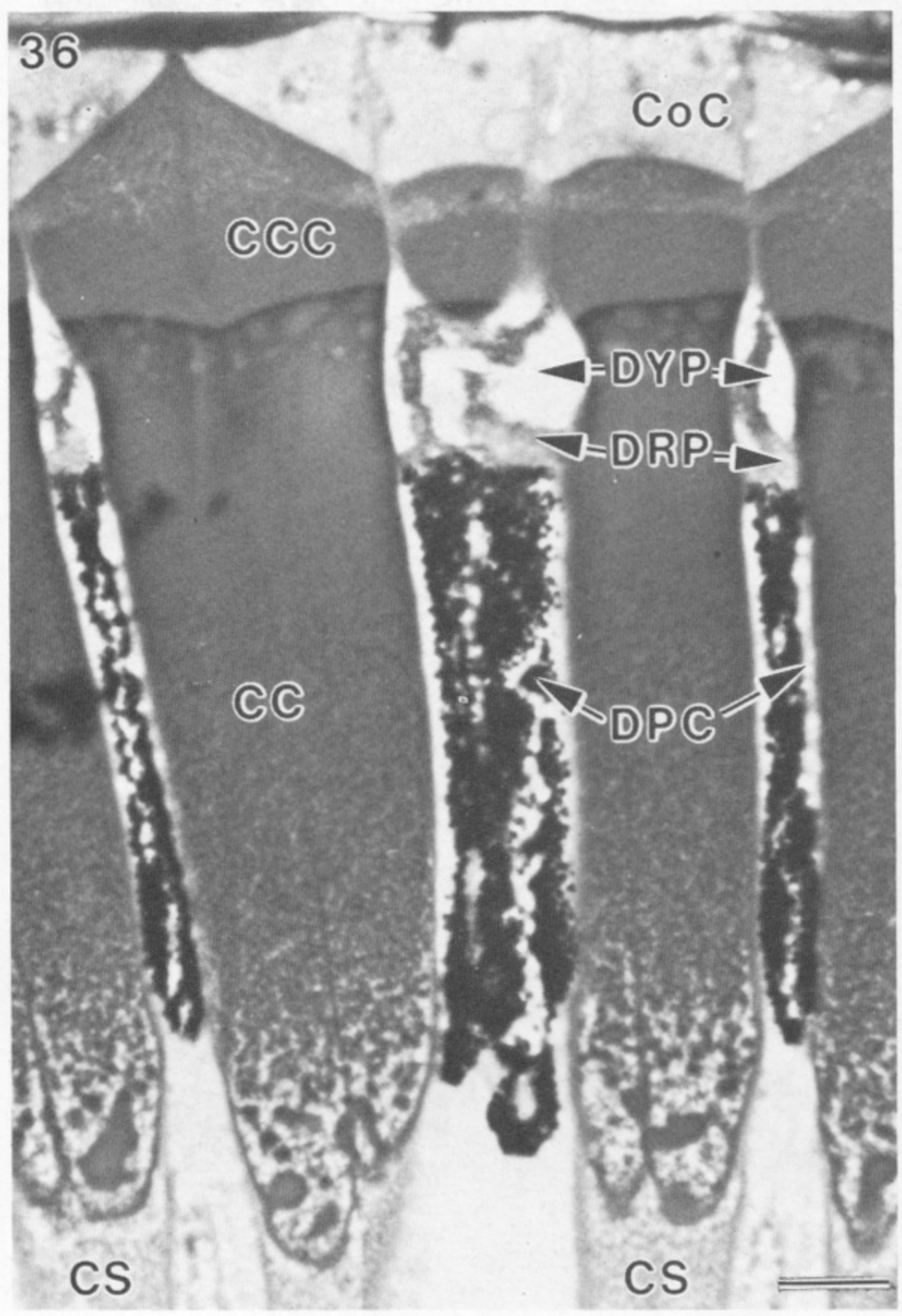

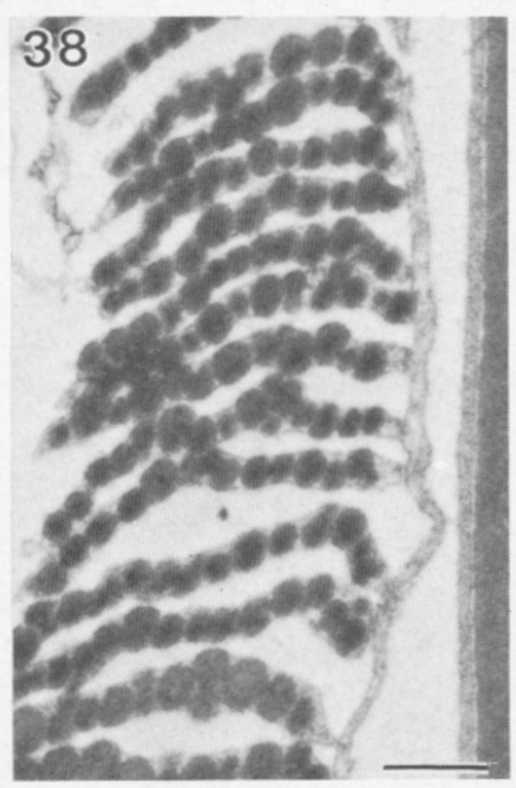

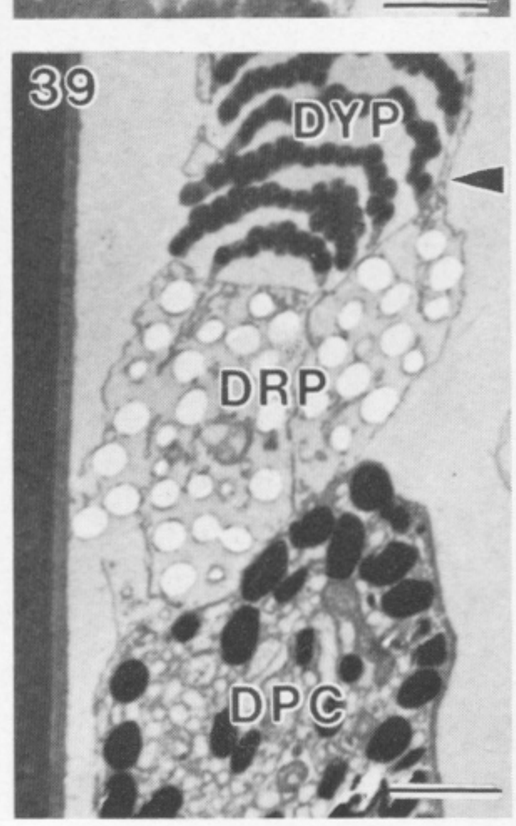

FIGURES 35–41. For description see p. 259.

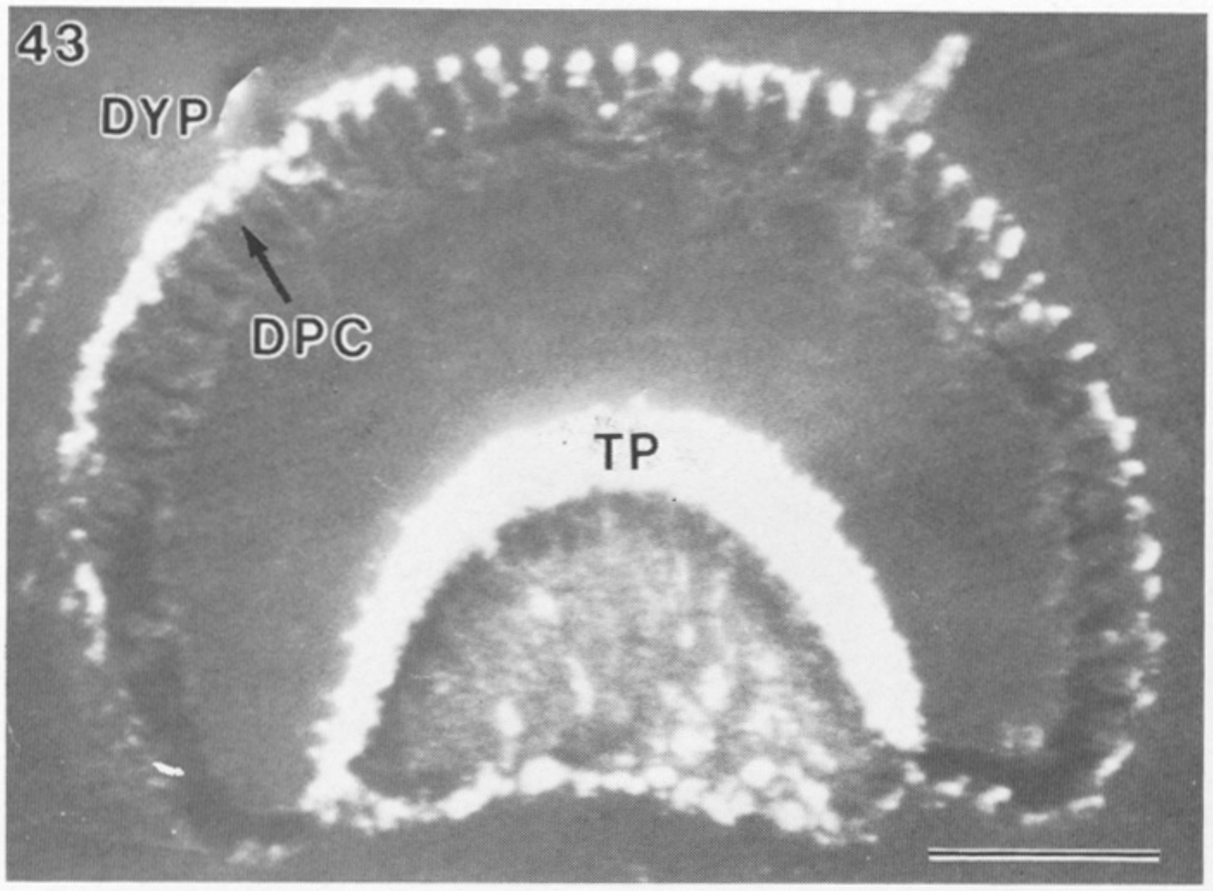

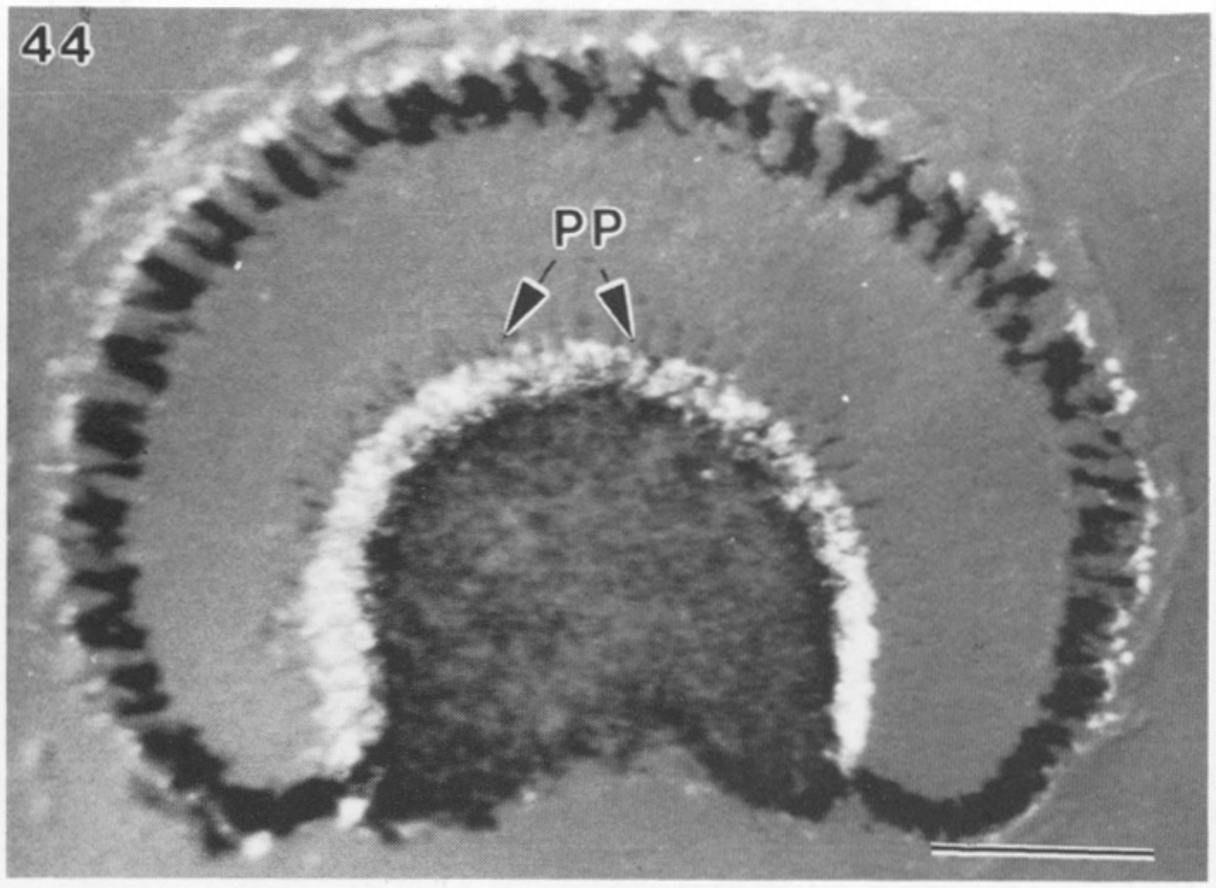

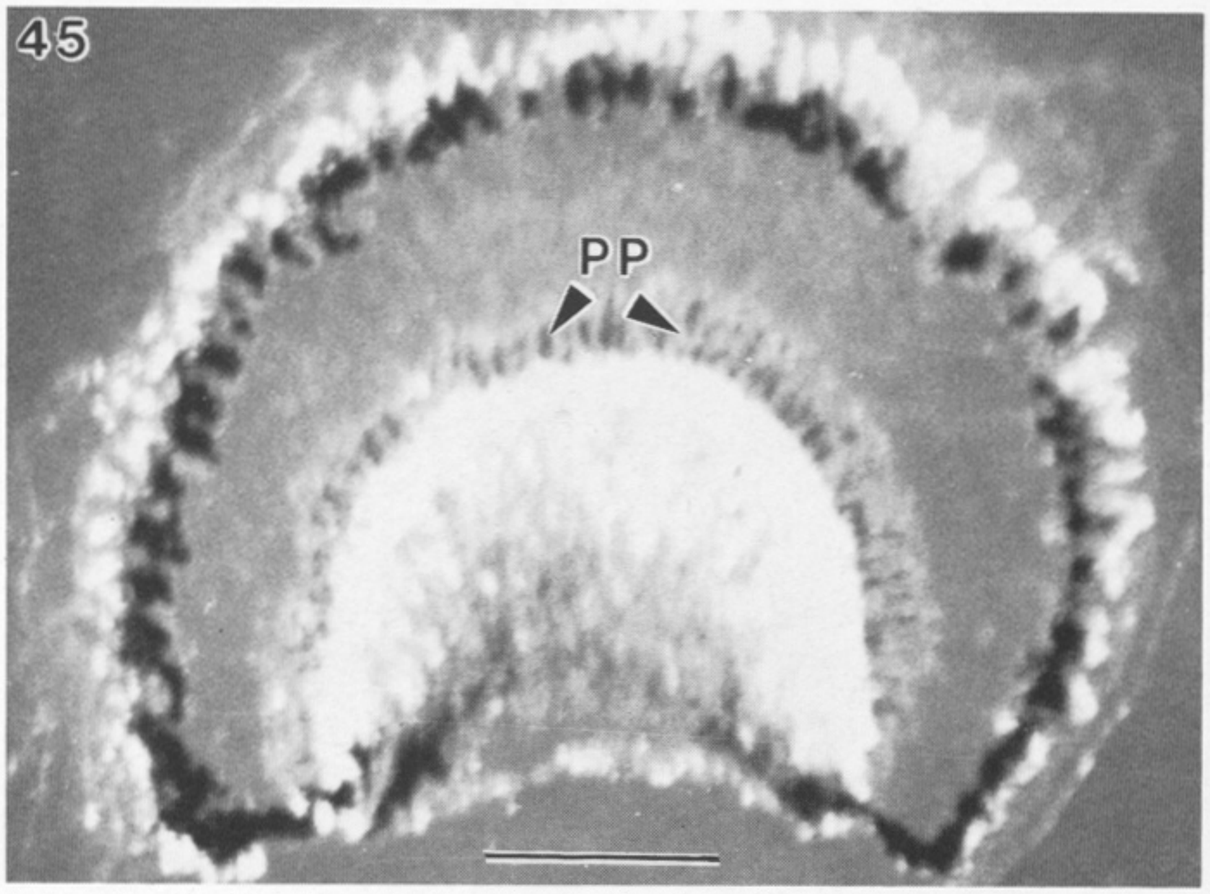

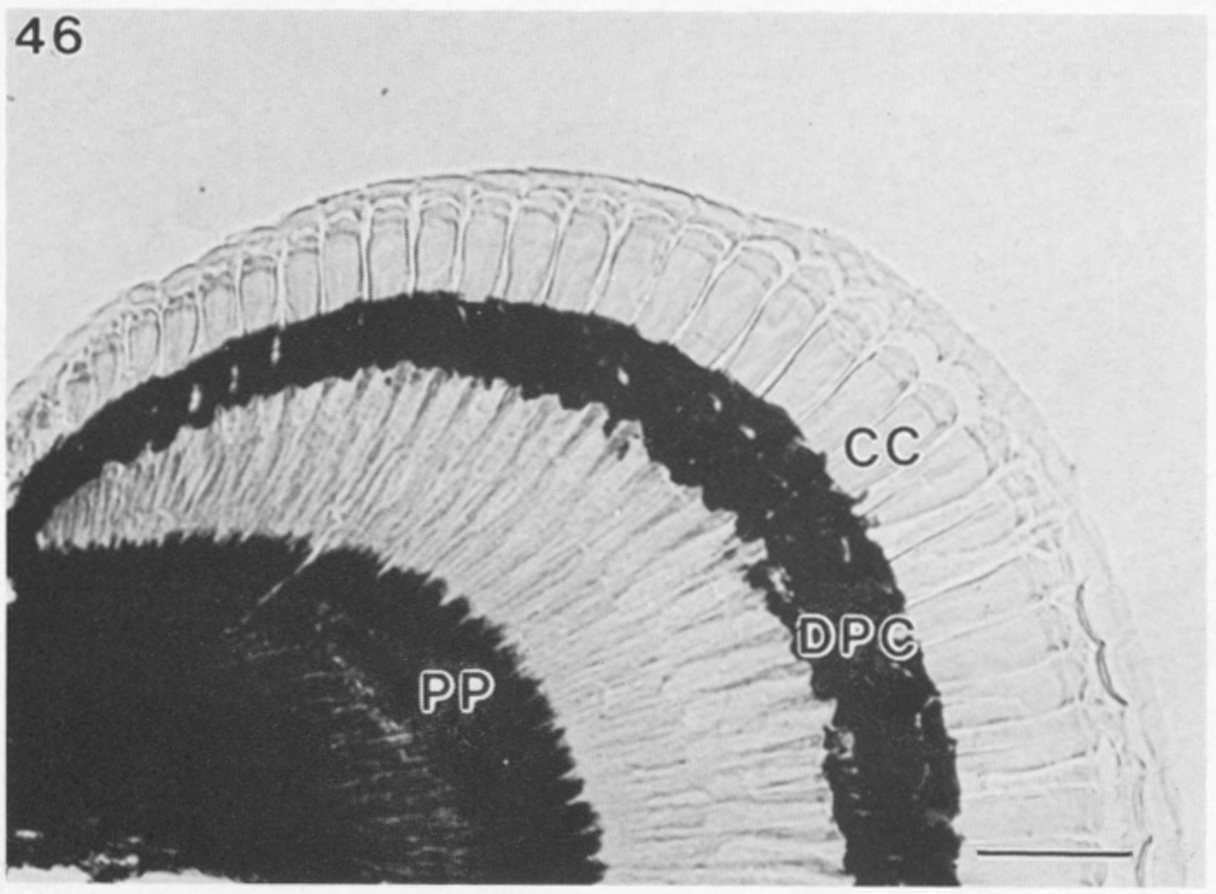

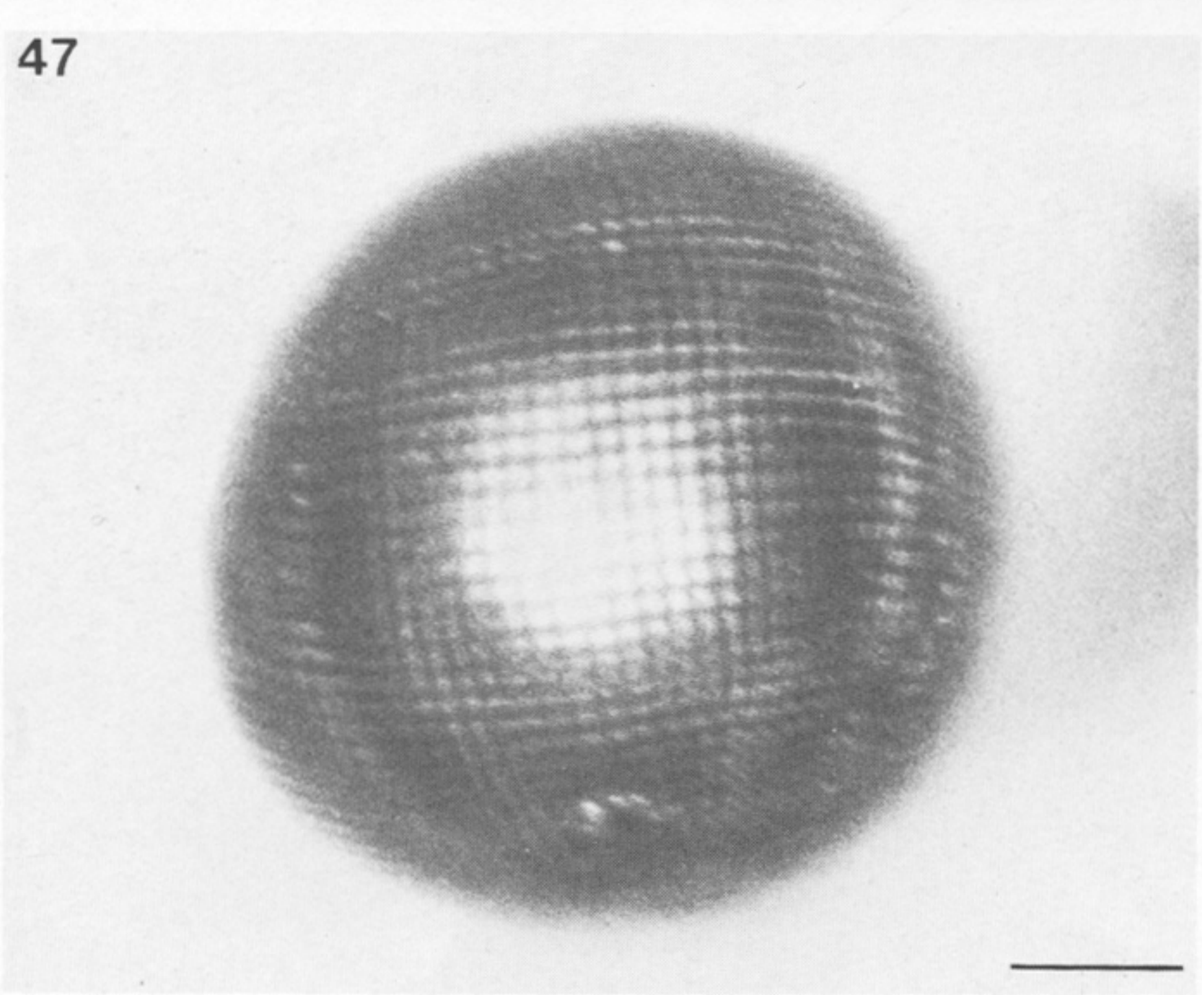

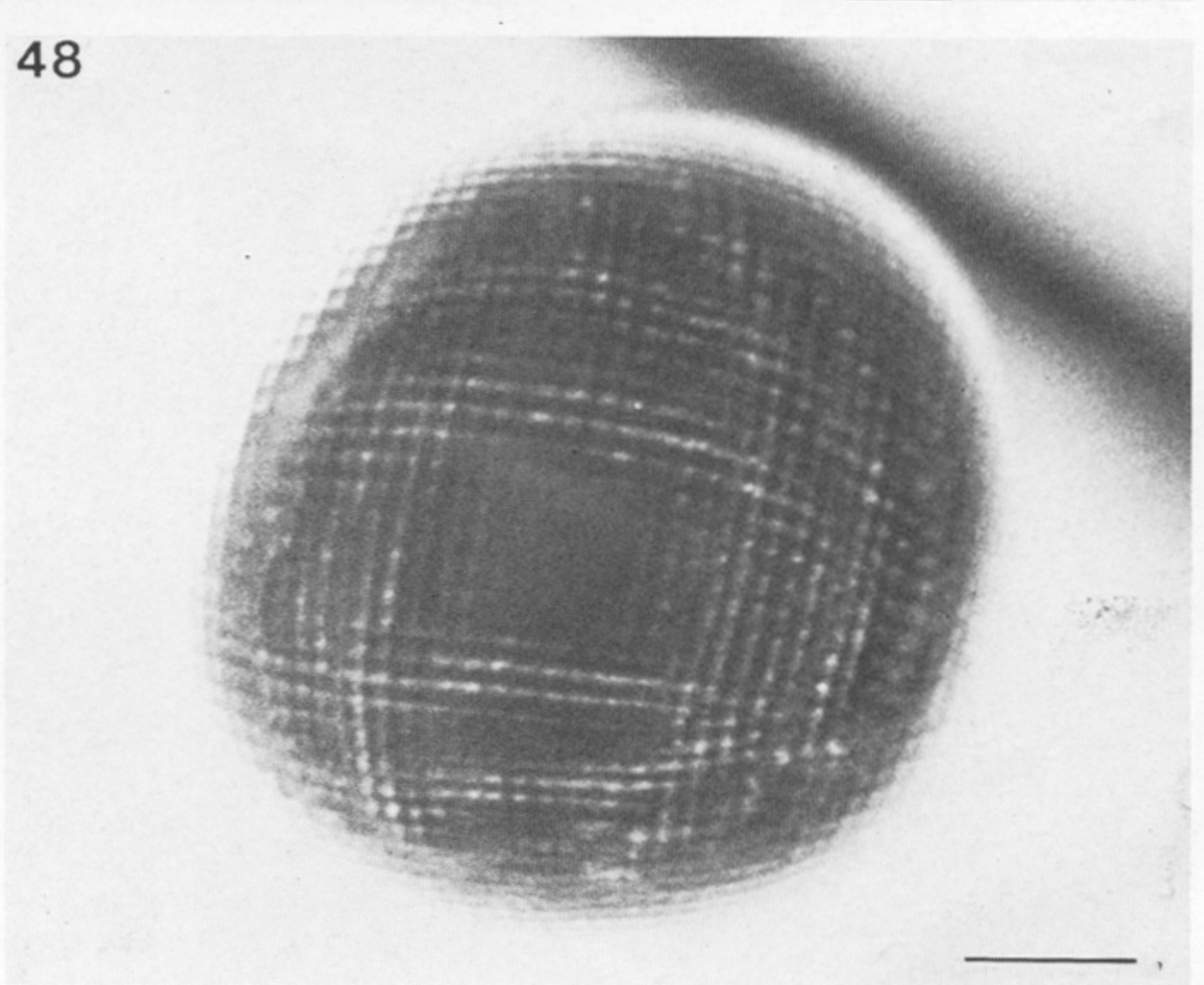

FIGURES 43–48. For description see opposite.